Spectacularly Binocular:
Exploiting Binocular Luster Effects
for HCI Applications

Haimo Zhang

B.Comp.Eng(Hons), NUS

A THESIS SUBMITTED
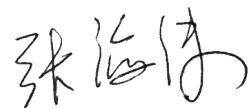
FOR THE DEGREE OF DOCTOR OF PHILOSOPHY
DEPARTMENT OF COMPUTER SCIENCE
SCHOOL OF COMPUTING
NATIONAL UNIVERSITY OF SINGAPORE

2014

Declaration

I hereby declare that this thesis is my original work and it has been written by me in its entirety. I have duly acknowledged all the sources of information which have been used in the thesis.

This thesis has also not been submitted for any degree in any university previously.

_____

Haimo Zhang

30 July, 2014

Acknowledgments

I thank my parents, Nan Zhang and Wendong Yang, for their encouragement for me to pursue the PhD course. I thank my wife, Judy, for her support and sacrifice during my PhD course, volunteering for user studies, and encouraging comments on my projects. Sincere appreciation goes to my PhD advisor, Dr. Shengdong Zhao, who introduced me to the fascinating field of human-computer interaction, for his immense patience and kind guidance while I learn about HCI from zero background, critical suggestions and comments for my projects, and, above all, great encouragement for me to pursue various crazy ideas. I am grateful to my collaborators of the various projects I am involved in: Xiang Cao, Seokhwan Kim, Desney Tan, Michael McGuffin, Xiaole Kuang, Soon Hau Chua, Hammad Mohammad, Sahil Goyal, Karan Singh, Yang Li, and Hao Lü. It has been enjoyable working with them, not only to learn from their knowledge, but also their passion towards science. I would like to thank Dr. Fook Kee Chua for his invaluable input without which the psychophysics study in this thesis is not possible. I would also like to thank Dr. Ravin Balakrishnan, for his intriguing ideas regarding the use of binocular rivalry in advertising. I thank all participants of the user studies for their time and feedback. Last but not least, I am most fortunate to have spent 5 profound years of my life with colleagues in NUS-HCI lab, a big family which I always identify myself as part of.

Contents

iii

Summary

The human eyes enable binocular vision, allowing the perception of depth from the two slightly different retinal images seen through the two eyes. However, when the two images seen by the two eyes are not stereo image pairs, the depth perception would break and instigate a visual phenomenon called binocular rivalry.

Although known for a long time in psychology and vision sciences, binocular rivalry has rarely been exploited in HCI (human-computer interaction) applications. Contrary to the conventional view of binocular rivalry as an image defect to be avoided, we feel that binocular rivalry could serve as a unique visual artifact that supplements the visual experience of the users. Among the various types of binocular rivalry, we are specifically interested in binocular luster, in which the light presented to each eye differs only in brightness, but not in color.

This thesis reports our research to characterize and utilize binocular luster in HCI context. First a psychophysics study is presented that uncovers characteristics of the viewing experience of binocular luster. Then the design and evaluation of an application of binocular luster is presented, which helps color blind users distinguish colors, by adding binocular luster to confusing colors. Lastly, an exploration of some novel visual effects involving binocular rivalry in general is presented, and their potential applications in HCI are suggested.

The contribution of this thesis is three-fold: to advance the fundamental understanding of the psychological experiences of binocular luster effect, to design and evaluate a novel approach to color blind relief using binocular luster effect, and to propose several novel visual effects with binocular rivalry that suggest potential

applications in HCI.

List of Tables

List of Figures

Chapter 1

Introduction

In this chapter, a brief overview of the motivation behind our research is given, followed by a proposal of the research questions. Then the background and previous research on related topics are presented, based on which the knowledge gap is identified. Finally the research scope and methodology are introduced, and contributions of our research are summarized.

1.1 Motivation

Being placed at slightly different locations, the two human eyes look at the world from slightly different points of view. As a result, two slightly different images are perceived by each eye. Human stereo vision is able to generate depth sensation by processing these differences. First explained by Sir Charles Wheatstone [116], this mechanism is known as stereopsis, which is illustrated in figure 1.1[1].

Leveraging on this mechanism, stereoscopic display technologies are invented to digitally recreate the human depth sensation [51, 94, 82]. Regardless of their spe-

---

[1]Image courtesy of http://www.vision3d.com/stereo.html
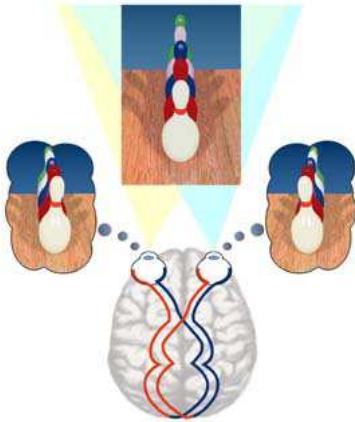
Figure 1.1: Illustration of human stereoscopic vision.

cific implementations, stereoscopic display systems deliver two separate images to each of the human eyes. As long as the two images are proper stereo pairs either captured or synthesized, the human viewer is able to experience the depth sensation.

Interestingly, stereoscopic display technologies are capable of presenting not only stereo image pairs, but also two images that are arbitrarily different. For these arbitrarily different images, the depth perception would fail, and a visual phenomenon termed "binocular rivalry" would be instigated in the human observer [15]. Interest in this phenomenon has rarely gone beyond the research domain of psychology, vision, and cognitive sciences, mostly as a research tool to understand neural processes in the brain [32, 73, 86, 100].

From an HCI (Human-Computer Interactions) standpoint, it is a curious question whether binocular rivalry offers unique and novel affordances in the HCI field, such as the design of graphical user interfaces, and special effects in media production. This thesis reports our research trying to address the above intriguing questions.

1.2 High-Level Research Questions

This research is interested in the following general questions:

1. What are the characteristics of binocular rivalry?

2. What are the product areas in HCI that could benefit from binocular rivalry?

3. How to design and evaluate an HCI application that uses binocular rivalry?

1.3 Background and Knowledge Gap

There are three main domains of work that are relevant to this research: stereoscopic display technologies, discoveries about binocular rivalry in the vision and cognitive sciences, and their applications in HCI. State-of-the-art technologies and research in each of these domains are introduced in the following subsections, and the knowledge gap is identified for the research presented in this dissertation.

1.3.1 Stereoscopic Display Technologies

From a user experience point of view, according to how a human viewer experiences a stereoscopic 3D effect, the mainstream stereoscopic display technologies are divided into two categories: those that require wearing a pair of goggles, referred to as "glass-based stereoscopic" displays, and those without the need of the goggles, referred to as "autostereoscopic", or, more colloquially, "glass-free" displays. Additionally, most head-mounted displays support stereoscopic viewing, although they are designed with other primary focuses, such as visual immersion.

Figure 1.2: NVidia 3D Vision active shutter glasses.

Glass-Based Stereo

Glass-based stereoscopic displays use a pair of glasses to demultiplex the two views for each separate eye. There are three mainstream commercialized approaches to glass-based stereoscopic display systems: active shutters [46], polarized filters [95], and spectral filters [57].

Preceded by a classic implementation of active shutter technology on CRT display [46], the NVidia 3D Vision technology[2] is one example of a commercialized active shutter 3D (figure 1.2). The active shutter glass encapsulates liquid crystal molecules between the dual-layer panels in front of each eye. Electric field between the two layers of panels controls the orientation of the liquid crystal molecules, which in turn makes the glass in front of each eye either transparent or opaque. The transparency of each eye's glass is synchronized with the refreshing of the display (normally as high as 120Hz), so that the odd-numbered frames are only seen by one eye, and the even-numbered frames by the other. By presenting one eye's view in the odd-numbered frames and the other eye's view in the even-numbered frames, the user's two eyes see separate images specifically designed for that eye, and a stereoscopic viewing experience is created. The essence of the active shutter approach is the use of shutter glasses to allow only one eye to see the screen at any instance of time, and by quickly interleaving the

---

[2]http://www.nvidia.com/object/3d-vision-main.html

two eyes' views, a stereoscopic experience is created. This mechanism is referred to as "time-multiplexed" stereo. The major drawback of the active shutter approach is cross-talk, where view for one eye might still be partially visible to the other eye, due to imprecise synchronization between the display and the active shutter glasses. Another drawback is a degradation in image brightness, since each eye is blocked 50% of the time.

The RealD technology [25] is an example of the polarization-based approach [95] to 3D stereoscopic display. The pair of glasses in RealD technology consists of two lenses with opposite polarization for each eye (figure 1.3). When an image is polarized with the same direction as the left-eye filter, it can only transmit through the left-eye filter, and no light can pass the right-eye filter. The left-eye view is thus delivered specifically to the left-eye. By the same principle, the right-eye view is delivered to the right eye by the same polarization direction as the right-eye filter. Being projection-based, the RealD technology requires the use of a metallic screen to preserve the polarization of the reflected light, since normal screens would lose the polarization. Owing to the polarization filter, in the polarization-based approach, there is a decrease in the brightness of the scene, and only 35% of the original brightness is preserved [25]. The requirement of a metallic screen in projected stereo 3D settings is another factor affecting its cost. RealD is usually used in cinemas to present stereoscopic views on a large screen. There also exist other polarization-based stereo 3D technologies, such as the HP 2311gt 3D LCD monitor [4], that are implemented for an LCD screen. However, it suffers from reduced resolution, since each horizontal line is only presented to one eye in the 3D mode, halving the effective resolution.

The Dolby 3D technology [2, 8] exemplifies the use of spectral filters for stereo-

Figure 1.3: RealD polarization glasses, demonstrating the opposite polarization between the two eyes' filters.

scopic display on a large screen projection [57]. The two views are displayed using primary spectral colors that are slightly different in spectral wavelengths (figure 1.4). The filter lenses in the Dolby 3D glass then transmit only the primary colors corresponding to the individual eye, thus reconstructing the view designed only for that eye. This technique is also referred to as the "wavelength multiplex visualization". Its benefit is that no special projection screen is needed.

---

[4]Image from `http://en.wikipedia.org/wiki/Dolby_3D`
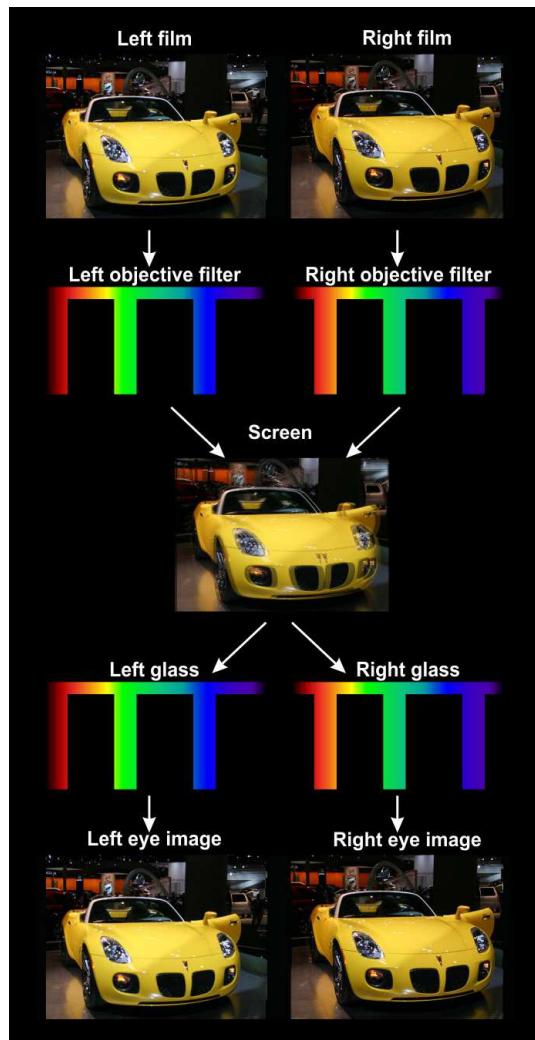
Figure 1.4: Dolby 3D technology [4], showing the different spectral wavelengths as primary colors used in each eye's view.

Glass-Free Stereo

Stereoscopic display technologies without the need of glasses are called autostereo-scopic displays [30]. Common autostereoscopic display technologies include par-allax barrier, lenticular lenses, volumetric displays, and light-field displays.

Parallax barrier [93, 83, 67], in its simplest form, is a sheet of uniformly placed pinholes. When a parallax barrier is carefully placed a certain tiny distance from the underlying display, the two eyes see different pixels of the screen through a same pinhole (figure 1.5). By controlling the value of each pixel, a separate view is seen by each individual eye. The major drawback of parallax barriers is that this approach severely reduces brightness and spatial resolution of the stereoscopic scene.

The lenticular stereo 3D technology uses a sheet of tiny optic lenses ("lenslets") [106, 117] to direct light from each pixel of the underlying screen towards a specific direction in space, and the underlying pixel is therefore only seen in that direction (figure 1.6). However, the lenticular approach also reduces the resolution of the scene, since no pixels are shared between each view. An example of a commercialized product using the lenticular lenses technology is the EyeFly 3D film, which is essentially a lenticular sheet used with smart phone screens [3]. The lenticular and parallax barrier stereo 3D technologies are called "space-multiplexed" stereo.

Volumetric displays present pixels in actual 3D space [24, 34]. This can be achieved by mechanically spinning a display in space, which shows the cross section of the volume it "sweeps" through, at its instantaneous orientation, hence the name "swept-volume display" (figure 1.7).

8
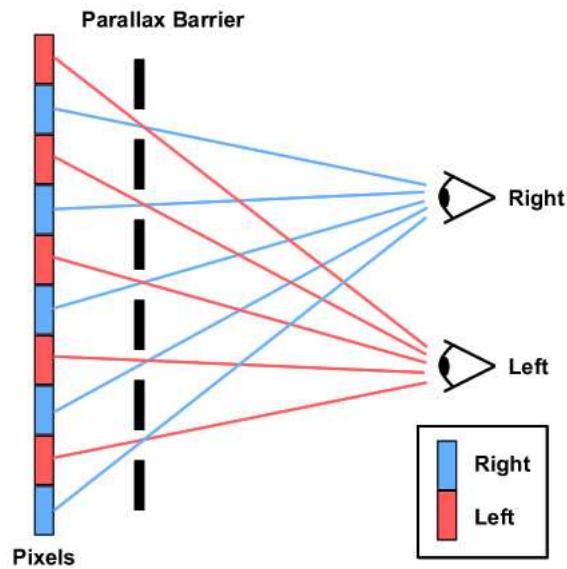
Figure 1.5: Parallax barrier shows different pixels to each eye through the same pinhole.
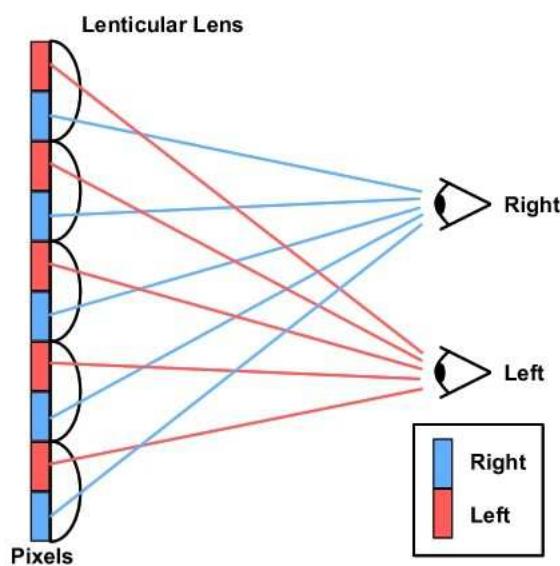
Figure 1.6: Tiny lenses on a lenticular sheet direct light from each pixel to a specific eye.
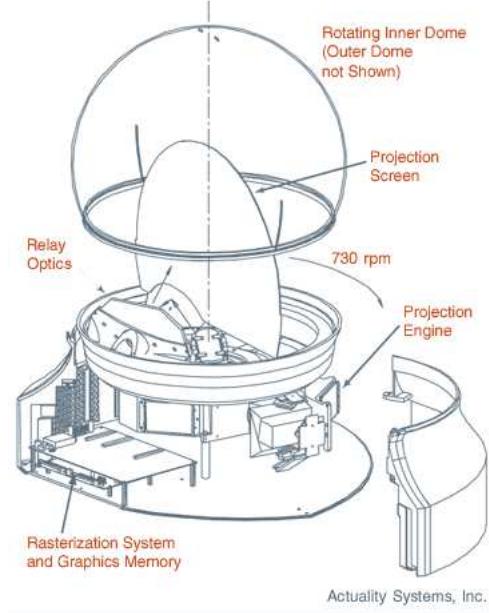
Figure 1.7: Schematic of a "swept-volume display", showing a planar screen attached to a rotating mechanism.
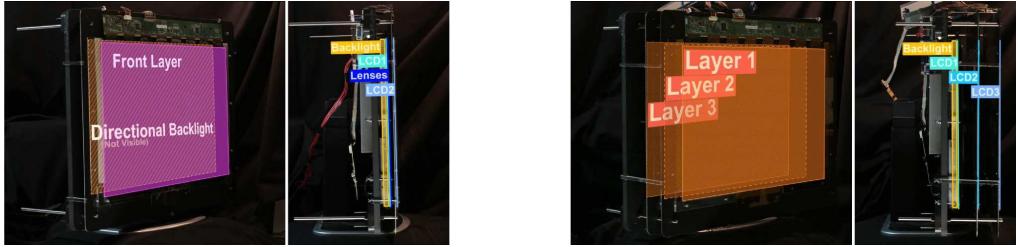
Figure 1.8: Two prototypes of light-field display built in MIT [115]. Left: a directional backlighting setting. Right: a multi-layer setting.

Light-field displays [115] use multiple LCD panels and directional backlighting to recreate the light field of the scene (figure 1.8). It is an active field of research and has shown promising applicability in future commercialization.

Other Stereoscopic Technologies

In addition to the above two categories of technologies, some head-mounted displays (HMDs) are designed to have separate screens for each eye, thus capable of achieving the stereoscopic effect. The Vuzix VR920 HMD (figure 1.9) is one such example [5]. It is equipped with two separate screens, and a program has explicit

Figure 1.9: Vuzix VR920 head mounted display.

Figure 1.10: Oculus Rift head mounted display. Left: front view. Center: back view. Right: control box.

control of which screen the current frame buffer is rendered for. Other HMDs, such as the Oculus Rift (figure 1.10) [6] and SONY HMZ-T3W (figure 1.11) [7] are also capable of producing the stereoscopic effect.

1.3.2 Binocular Rivalry

When the human vision system fails to interpret the difference between the two eyes' views as depth of objects, a phenomenon called "binocular rivalry" arises. This phenomenon was first described by Porta in 1593 [87] and subsequently acknowledged in [108]. During binocular rivalry, the two eyes' views compete for perceptual dominance. In other words, since the visual message from each eye is conflicting, telling the brain that different objects are occupying the same spatial location, the brain alternates between seeing the left view and the right view [15].

Figure 1.11: SONY HMZ-T3W head mounted display

Characteristics

Binocular rivalry is characterized by both temporal and spatial fluctuation between the two eyes' views. The perception of a single eye's view usually only last for a brief period of time, after which the perception of the other eye's view dominates [70, 39, 18, 69]. Apart from this temporal characteristic, binocular rivalry also manifests as "piecemeal" rivalry [78, 52], a spatial fluctuation in which part of the perception is dominated by the left view, and some other part of the perception is dominated by the right view.

Factors Affecting Binocular Rivalry

In binocular rivalry, the dominance and suppression of each eye's view is affected by various factors, such as eye dominance, size of visual stimuli, transient changes in stimuli, and high-level semantics of the visual stimuli.

A user could have a dominant eye, whose visual input is preferred over the other, non-dominant eye's input. During binocular rivalry, the dominant eye's view is more likely to dominate the visual perception. It is also likely that a user does

not demonstrate any apparent eye dominance, and the visual perception is not apparently biased towards any of the two eyes' views. Eye dominance has a large effect on binocular rivalry and can be caused by several reasons such as visual acuity [19], direction of gaze [61, 88], clinical conditions [11, 107], etc.

When the rivaling region in the retina is small, the entire view from one eye could dominate the perception, whereas for large rivaling region, piecemeal rivalry is more likely to happen [16].

Human eyes and brain are more sensitive to a dynamic stimuli than to a static stimuli. As a result, if a change in motion or brightness is present in only one eye during rivalry, that eye's view is more likely to dominate [38, 110, 111].

The dominance and suppression of the two eyes' views are also affected by the high-level semantics of the rivaling visual information. For example, emotional pictures are found to dominate over neutral pictures [9].

Types of Binocular Rivalry

If the two eyes' views only differ in their contours, contour rivalry arises [70, 20]. If they differ only in color, color rivalry arises [55, 58]. And if they differ only in brightness, binocular luster arises [84, 36]. In practice, when a pair of complex images is shown, the effect on the user is much more complex than simply combining single types of binocular rivalry, and little is known that could be potentially usable in HCI applications.

Binocular Luster

The binocular luster effect is characterized by the perception of a metallic shininess on an object in our binocular vision [53]. The luster can be seen when there are enough differences in brightness on the same object between two eyes relative to the background. When the binocular brightness disparity is larger than the binocular fusion limit [55, 58], noticeable alternation between the left and right image would take place in human vision and the object would appear shiny and shimmering to the viewers [70]. In natural scenes, this effect can be usually seen on the surface of metallic objects when highlights reflecting off the object are only visible to one eye [105]. Human eyes are capable of perceiving the luster effect rapidly, making the effect intensely salient [13] and uncomfortable at times [62].

Binocular luster has been studied in the context of visual perception [37, 85, 123]. One characteristic of luster effect that is of practical interest to the HCI community is the perceived level of shininess. The perceived shininess intensity of the binocular luster effect is influenced by several factors. The primary factor is the object's brightness disparity between the two eyes [74]. As the binocular brightness difference of an object becomes larger, the luster effect appears shinier and more salient. The second factor is the contrast polarities of both monocular images between the luster region and its background [10]. According to previous work, luster effect is more perceivable and shiny in binocular images with opposite contrast polarity, in which the luster region is brighter than the background in one eye's view, and darker than the same background in the other eye's view. The third factor is the size of the luster object, where bigger size has been associated with more shininess [84].

Modern stereoscopic technology has enabled such effects to be presented to the normal household via TVs, gaming devices (Nintendo 3DS), and personal computer. Despite this, the application of the binocular luster effect in 3D has been very limited in the HCI domain. Zhang et al. recently proposed the use of luster for highlighting, which makes objects in 3D images more noticeable to the viewer [124]. In this paper, we investigate the viability of using this effect as a post-publication color blind aid that augments color information for color blind users.

1.3.3   Application of Binocular Rivalry in HCI

Being of interest only in the fields of psychology, neural science, and vision and cognition sciences as a tool to understand human visual processing, binocular rivalry has hardly received any interest in HCI research and applications. Instead, they are merely treated as negative effects that need to be eliminated in the design and evaluation of stereoscopic display systems [54]. One hint on its potential application has been proposed by Wolfe and Franzel in 1988 [119], who suggested that binocular luster effect is useful in visual search tasks. In their research, Wolfe and Franzel found that targets with binocular luster in a visual search task are easier to find. Binocular luster has also been mentioned in Healey et al. [47] as a preattentive visual property in information visualization, but without concrete examples of it being used in actual applications.

1.3.4   Summary of Knowledge Gap

Although binocular rivalry has been extensively studied for decades in cognitive and vision sciences, it remains nearly unnoticed in the HCI field, the reasons for
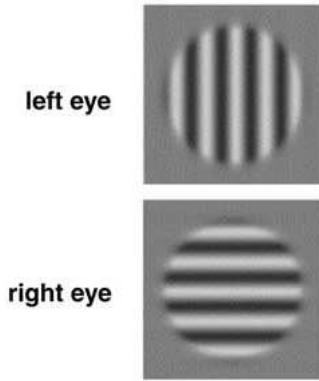
Figure 1.12: Typical simple and abstract grating patterns used in most research on binocular rivalry. From [17].

which are enumerated below.

First is the lack of connection between binocular rivalry as a visual phenomenon and its specific implementation guidelines for HCI applications. Research on binocular rivalry in psychology, and vision and cognitive sciences domain concerns only abstract stimuli, such as simple gratings and color patches (figure 1.12). However, in practical HCI applications such as graphical user interfaces and information visualization diagrams, visual entities appear with a combination of simple graphical properties such as shape, color, and size. As a result, conclusions about binocular rivalry in vision sciences may not be directly applicable to HCI applications.

Second is the lack of concrete implementation and evaluation of binocular rivalry effects in actual HCI applications. Different applications serve different purposes, and have different measures of performance and efficiency. Binocular rivalry in HCI cannot be studied without actual application scenarios.

To bridge these knowledge gaps, practical scopes have to be defined, and appropriate methods have to be employed, which is discussed in the next section.

1.4 Scope and Methodology

Exploring the whole application space of binocular rivalry in HCI is a huge task demanding years of research and collaborative effort. To inspire future research, this thesis provides a certain extent of both breadth and depth, by carefully controlling each study within some operable scope. Of the various aspects of binocular rivalry, binocular luster is of primary interest for this PhD research, since it has been shown to be an important factor in visual search, which is a fundamental task in graphical user interfaces. Therefore, this PhD research provides depth about binocular luster to articulate detailed discoveries. The breadth is provided by profiling various effects of binocular rivalry in general, with images in practical context, which suggest potential applications in HCI context.

Three studies are presented in this thesis. First, a psychophysics study is introduced that characterizes perception of binocular luster and empirically establishes the relationship between its physical parameters and psychological experience of the user. Next, an application of binocular luster to help color blind users is developed and evaluated. Finally, a number of novel visual effects using binocular rivalry in practical contexts are created, which are studied in a user interview.

The first study focuses on the fundamental knowledge about binocular luster. Psychophysics methods are adapted to measure users' perceptual thresholds to binocular luster. An experiment was carried out to measure detection and discrimination thresholds for various stimuli in the binocular luster space. An empirical model is fitted with the experiment data, to describe and predict perceptual responses to binocular luster and brightness perception without luster. It is fur-

ther used to calculate approximate perceptual difference between two binocular stimuli. With this model, we developed a generic approach to create binocular images that can appear differently in monocular views, binocular view, and merged view, which is the average of the two monocular views. We also developed computationally tractable methods to create dual-view images in special cases. We believe that the study presented is a solid contribution to psychology and vision research, as a first-time quantitative result specifically for perceptual characteristics of binocular luster, and its relationship to brightness perception without luster. Although the results in this study are only empirical, we hope that it could become an inspiration for future research that aim to explain these results from psychological and physiological perspectives.

The second study focuses on a specific application of binocular luster to help color blind people distinguish between colors that look confusing to them, by annotating the confusing colors with different luster effects. A user study was conducted to show that users are able to process color information with less effort using this technique than other previous techniques that mostly focused on color substitution. In addition, our technique preserves color information for users with normal color vision, due to the choice of stereoscopic display technology that blends the left and right views when viewing without stereo glasses. This work contributes to the human-computer interaction field through the design and evaluation of a novel approach to color blind relief. It also implies the potential of binocular luster to supplement the visual vocabulary that can be used in visual interfaces and communication.

The third study focuses on exploring other potential applications in HCI of not only binocular luster, but binocular rivalry in general. Several novel visual effects

with binocular rivalry are created, which are loosely grouped into four categories: highlighting, compositing, hiding, and wowing, suggesting different HCI application scenarios. A user interview was conducted to find out how users perceive and interpret these effects.

1.5 Contribution

The output of this research includes:

1. Psychophysical characterizations of the perception of the binocular luster effect, which relates the presentation of a stimuli to the corresponding user experience it induces.

2. A quantitative empirical model that unifies perception of binocular luster and brightness perception without luster. The model can describe and predict perceptual differences between achromatic (i.e., colorless) stimuli presented binocularly.

3. Design and evaluation of a specific application of binocular luster in color blind relief.

4. A set of novel binocular visual experiences, created by various stimuli instigating binocular rivalry effect, and their potential application scenarios in HCI field.

The impact of this research is bidirectional. For downstream applications, this research provides knowledge on the relationship between the physical parameters of binocular presentations and the psychological experience of the users. This is extremely useful in designing desired user experience in target application do-

main. For upstream sciences in psychology, vision, cognitive, and neural sciences, this research collects psychophysics data and performs initial analysis that might suggest possible directions for investigation into binocular luster, or binocular rivalry in general.

Overall, we believe that binocular luster and binocular rivalry in general have great potential in HCI applications. Due to the conventional view of them as image defects, they are largely underutilized or overlooked in HCI research. We hope that this thesis will articulate the alternative view of binocular luster and binocular rivalry as a unique visual artifact that could be utilized positively in HCI applications, and inspire future research in this subject from various perspectives, including psychology, vision sciences, cognition, arts, and communication.

Chapter 2

Perception of Binocular Luster

This chapter describes how psychophysics methods are adapted to investigate the perceptual responses of binocular luster, how the result is processed to build a numeric empirical model, and how this model is used to exploit binocular luster as a new perception channel in HCI context.

2.1   Introduction

It is impractical to apply binocular luster in HCI without knowledge about its quantitative perceptual characteristics. To address this problem, we investigated into the perceptual aspects of binocular rivalry using psychophysics methods, and are able to learn an empirical model that numerically predicts the perceptual response of binocular luster.

2.1.1 Motivations

This investigation is motivated by the lack of quantitative data to demonstrate perceptual characteristics of binocular luster, and a numeric model that directly implies applications of binocular luster in HCI.

Thus, we set out to study the perceptual characteristics of binocular luster, and to uncover findings with direct implications for HCI applications. It is a significant addition to the visual vocabulary in designing visual human-computer interfaces.

2.1.2 Scope

As introduced in the previous chapter, binocular luster, where only the brightnesses in the two eyes' views are different, has been found to be a more dominant effect in visual search [119], a fundamental task in interactions with visual interfaces. In addition, considering chroma into our research exponentially increases the control space of binocular rivalry effects, making experimentation too long and too complex to be practical. Therefore, we focus on investigating the perception of binocular luster, without any color information. To separate brightness from color, YUV color space is used [27, pp. 470–471], with zero U and V components.

2.1.3 Research Questions

There are two research questions in this investigation. One queries the intrinsic characteristics of binocular luster, and the other its relationship with conventional 'monocular' brightness perception (i.e., without luster).

Characteristics of Binocular Luster Perception

The first question is, whether it is possible to quantize the perception of binocular luster? Quantization of the perception of binocular luster allows for interesting analysis and processing of binocular images, such as calculating which part of the binocular image is most salient to the user due to binocular luster, and how to transform a monocular image into a binocular image to create salient regions with binocular luster sensation. Quantization of binocular luster also facilitates derivation of at least an empirical model that might shed light on the perceptual nature of binocular luster.

Interaction between Binocular Luster and Monocular Brightness Perception

The second question is, what is the relationship between the perception of binocular luster and brightness perception without rivalry? Knowing their relationship would help determine whether binocular luster could be used as an independent channel in HCI applications, or as an auxiliary channel to augment monocular perception of colors.

If binocular rivalry is shown to be completely independent, applications relying on separate identification of rivaling and non-rivaling brightness are possible. For example, heat and noise level of an engine, both continuous real values, could be simultaneously encoded on the screen, one with monocular brightness, and the other with binocular luster.

If binocular rivalry is somehow correlated with monocular brightness perception, applications could still leverage binocular rivalry to extend the presentation space

of monocular colors, such as annotating anomalous portions (i.e., binary label) in a pie chart.

2.1.4 Physical Dimensions of Binocular Luster

Due to the existence of three types of cone cells in the human eye, each corresponding to scalar responses to long, medium, and short wave-length lights [26], most color spaces are three-dimensional, such as the CIE XYZ color space [97]. From the point of view of most display devices, it can be safely assumed that the control space for physically presenting a color is three-dimensional as well. It further follows that in order to create binocular rivalry, another, different, color needs to be presented to the user. As a result, the control space for binocular rivalry has six degrees of freedom, three for each eye's view. With the research scope of binocular luster, which only concerns the difference in brightness, the six degrees of freedom could be further reduced to two brightness values in each eye, which we equate with the Y value of the YUV color space [27, pp. 470–471].

Creation of the binocular rivalry effect is thus equivalent to assigning points belonging to the six-dimensional 'binocular rivalry space' to each object in the image. As far as only binocular luster is concerned, the 'binocular luster space' is a 2D sub-space of the full 6D 'binocular color space'.

Intuitively, the two eyes' brightness values (noted L and R) could be used as two basis vectors to construct a 2D space that encompasses all possible combinations of left- and right-eye brightness presented to the user. We refer to this naive construct as the 'raw' binocular luster space. Denoting the brightness range presentable by a display device to each eye as $[0, 1]$, figure 2.1 shows the range of all presentable binocular luster stimuli in the plane defined by the L and R axes.
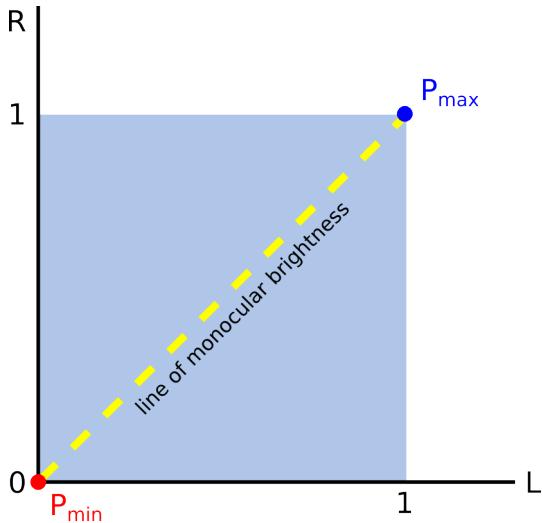
Figure 2.1: Display range in LR space

Also shown in the figure is the *line of monocular brightness*, where no luster effect is present, since both the eyes are presented with the same brightness. The points of minimum and maximum brightness presentable by the device are marked in the figure as P_{min} and P_{max} respectively.

Several issues with the above formulation limit its expressiveness.

Firstly, the physical strength of the presented binocular luster (i.e., the brightness difference) is not directly expressed as a single value, but rather as the difference between the two coordinate values in the raw binocular luster space (i.e., $L - R$). This extra level of indirection is undesirable in our research.

Secondly, in the special case of both eyes having a same brightness value, the raw binocular luster space reduces to a diagonal line of $L = R$. This line of monocular brightness has only one degree of freedom, but involves both bases in the raw binocular luster space. To enable simpler representation, the ideal binocular luster space should have the line of monocular brightness aligned with one of its axes.
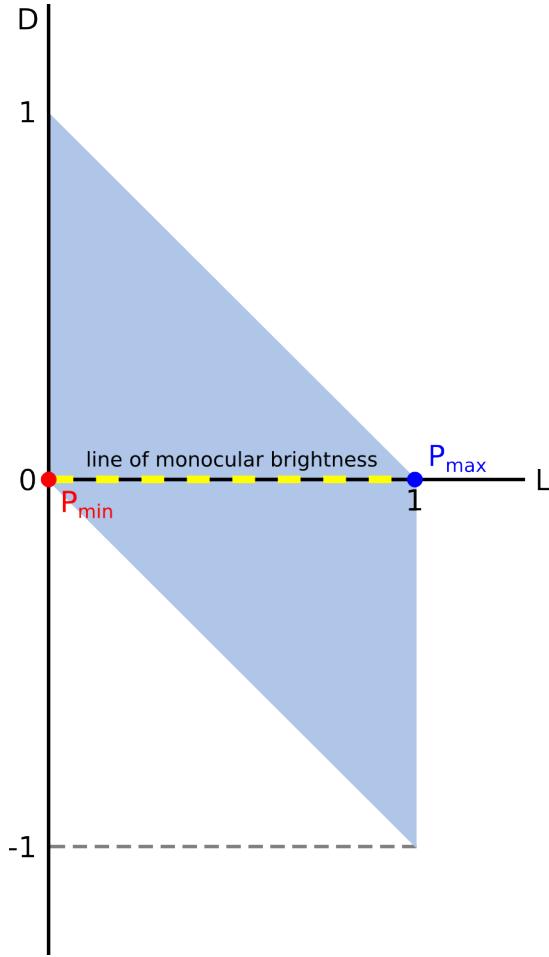
Figure 2.2: Display range in LD space

Thirdly, since users have different eye dominance, swapping the left- and right-eye brightness values should be convenient. For a point in the raw binocular luster space, swapping is done by finding its reflected point about the line of monocular brightness. Mathematically, this swapping operation involves transformation through the matrix of

$$\begin{bmatrix} 0 & 1 \\ 1 & 0 \end{bmatrix}.$$

Both values of the coordinates in the raw binocular luster space change after the swapping operation, which is not efficient enough.

To address these limitations of the raw binocular luster space, we can use the

26

line of monocular brightness as one axis, and define another 'binocular' axis that captures the brightness difference between the two eyes. Figure 2.2 illustrates the range of presentable binocular luster stimuli of a device in the binocular luster space using brightness value in the left eye as the horizontal axis (L), and brightness change from left to right eye as the vertical axis $(D = R - L)$. It is worth noting that the raw binocular luster space (LR space) is associated with this space (LD space) through a shear transformation of

$$\begin{bmatrix} L \\ D \end{bmatrix} = \begin{bmatrix} 1 & 0 \\ -1 & 1 \end{bmatrix} \cdot \begin{bmatrix} L \\ R \end{bmatrix},$$ (2.1)

and as a result, this space occupies a part of the first quadrant and a part of the fourth quadrant of the entire 2D space. Although the LD space addresses the first two limitations of the raw binocular luster space, it fails to simplify the swapping operation, which still requires a transformation of

$$\begin{bmatrix} 1 & 1 \\ 0 & -1 \end{bmatrix}.$$

To also address the third limitation of the raw binocular luster space, we define two axes, B and T, as follows, to construct the binocular luster space that addresses all three limitations of the raw binocular luster space.

B is defined as the average brightness values in the left and right eye:

$$B = \frac{L + R}{2}.$$ (2.2)

This dimension reflects the total amount of energy presented to both eyes.

T is defined as half the inter-ocular brightness difference from the left to the right eye:

$$T = \frac{R - L}{2}.$$ (2.3)

27
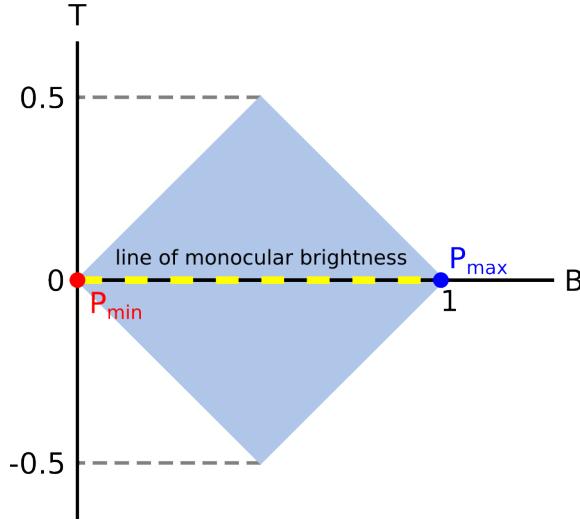
Figure 2.3: Display range in BT space

This expression reflects the physical intensity of binocular luster, with the sign indicating which eye is presented with higher brightness.

As illustrated in figure 2.3, the BT space is scaled and rotated from the LR space. The line of monocular brightness aligns with the horizontal axis, where the inter-ocular difference is zero. The BT space is symmetric about the horizontal axis, and the left- and right-eye brightness can be swapped by simply inverting the sign of the T coordinate value.

Hypothesized Findings

With the BT space defined, we hypothesize that, first, along the horizontal axis, where no luster effect is present, knowledge about monocular brightness perception would still apply. Second, the perceptual characteristics for $T > 0$ and $T < 0$ would be qualitatively similar, since they differ only by a swap of brightness values in the dominant and non-dominant eyes.

2.2 Methodology

This section introduces the fundamentals of the psychophysical methods used for the investigation, the specific adaptation of the selected methods for our study, and the detailed design and procedure of the experiment we conducted.

2.2.1 Psychophysical Methods

Psychophysics is the study of the relationship between the strength of a physical stimulus that elicits a sensation, and the human response to that stimulus [42]. This subsection introduces fundamentals of psychophysics. Being a well-established prior knowledge closely related to our subject of binocular rivalry, the study of brightness perception is taken as an example where applicable.

Fundamental Questions in Psychophysics

Unlike physical properties of the stimuli, such as weight of a mass, energy of a light source, and length of a line segment, the human perceptual experience cannot be directly measured. The early psychophysicist Gustav Fechner proposed three fundamental questions in psychophysics: detection, discrimination, and scaling [35].

The question of detection concerns with how much the minimum strength of a stimulus must be, for an observer to detect its presence. The perception process inevitably involves various noises, arising from external environment and neurons in the internal nervous systems. As a result, an external stimulus must be significantly stronger than these noises, for an observer to reliably detect its presence. The minimum stimulus strength that can be reliably detected is termed as

29
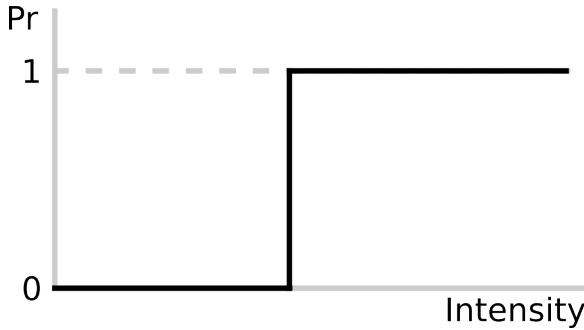
Figure 2.4: Ideal detection threshold in psychophysics. Horizontal axis is the intensity of stimuli. Vertical axis is the probability of correct detection of the stimuli. The relation between probability of detection/discrimination and stimuli intenstiy is a step function.

'absolute threshold' in psychophysics literature [63, pp. 2.3–2.4].

The question of discrimination concerns with how much the minimum difference between two stimuli must be, for an observer to acknowledge their difference [22, pp. 25]. Due to the variance in perception, two stimuli must be sufficiently different, so that they consistently appear different to an observer. The minimum stimulus strength difference between two stimuli that can be reliably differentiated is termed as 'difference threshold' in psychophysics literature.

The question of scaling concerns with how the physical intensity of the stimuli is related to the strength of the sensation perceived by the observer [41]. Answering this question provides a way to describe the experience for a perception channel.

Model of Perception

Ideally, if a stimulus is stronger than a threshold, an observer should always detect its presence, and vice versa (figure 2.4). However, this is rarely the case in practice. As illustrated in figure 2.5, the probability of an observer responding 'yes' to a psychophysics question such as 'Do you see the stimulus?', or 'Do you think the two stimuli are different?' demonstrates a gradual change as the
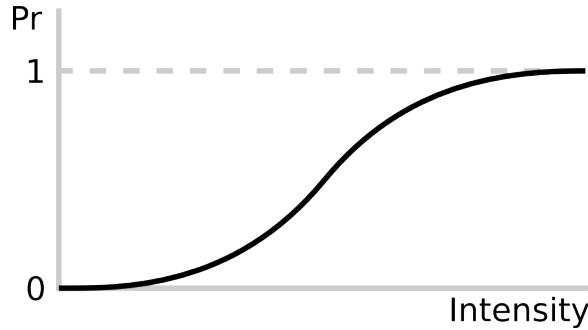
Figure 2.5: Practical detection threshold in psychophysics. Horizontal axis is the intensity of stimuli. Vertical axis is the probability of correct detection of the stimuli. Probability of detection gradually increases from 0 to 1 with increasing stimuli intensity.

intensity of the stimulus, or difference between two stimuli increases. This S-shaped curve is a fundamental characteristic curve in psychophysics, termed as the 'psychometric curve' [68, 103].

Many psychophysics studies query the properties of psychometric curves specific to their experiment setup, to approach the questions of detection and discrimination. For example, to measure the detection threshold of brightness perception, psychophysicists could present stimuli of various strengths, and record the proportion of positive responses (i.e., 'Yes, I see the stimulus.') by the observer [120, pp. 519–525]. The proportions are plotted against the respective stimuli strengths, and a psychometric curve could be fitted to these data points, reflecting the perceptual response of the observer in this experiment.

As there is no abrupt change in practical psychometric curves, the definition of the absolute threshold is somewhat arbitrary, and a commonly accepted definition is the stimuli strength for which the observer responds positively 50% of the time [63].

The model of discrimination follows a similar characterization. When presented with a fixed-intensity stimulus as the baseline for comparison, termed the 'stan-
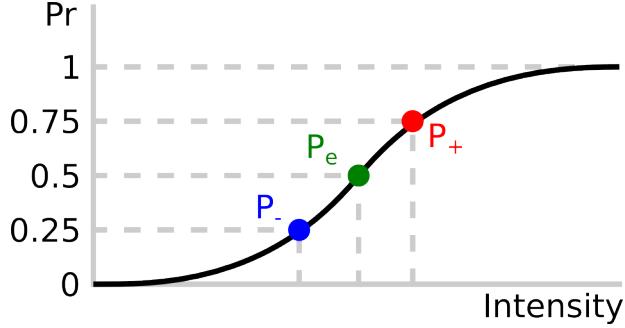
Figure 2.6: Psychometric curve for bi-directional difference threshold. Horizontal axis represents the intensity of the stimuli. Vertical axis represents the probability of the comparison stimulus feeling stronger. Showing point of subjective equality (P_e), point of positive difference threshold (P_+), and point of negative difference threshold (P_-).

dard' stimulus, and another stimulus differing by a certain amount, termed the 'comparison' stimulus, the probability of an observer reporting the comparison stimulus being stronger also follows the psychometric curve. However, the point of 50% response of the comparison stimulus being stronger is not a good choice of the difference threshold. Since at this point, the other half of the time, the observer would feel that the comparison stimulus is weaker than the standard, this point merely indicates 'subjective equality', which is perceptually most similar to the standard stimulus. A commonly accepted definition of the difference threshold is when the observer reports the difference 75% of the time, half-way between the point of subjective equality and perfect discrimination rate of 100% [22, pp. 28]. Since the difference from the comparison stimulus to the standard could be perceived as either weaker or stronger, the difference threshold is usually calculated as the average of the detection thresholds in both directions, as illustrated in figure 2.6. The difference threshold is also known as 'just noticeable difference' (JND).

Early psychophysicists have found that, instead of being a constant value, difference threshold is proportional to the intensity of the standard stimulus [113].

This finding is known as the Weber's Law, named after the psychophysicist who discovered it. Mathematically Weber's Law states that:

$$\Delta I = k\,I, \tag{2.4}$$

where ΔI is the difference threshold, I is the intensity of the standard stimulus, and k, known as the Weber fraction, is an empirical coefficient dependent upon the perception modality and unit of measurement used in the experiment. An often debated topic in psychophysics, Weber's Law seems to find support from recent findings in the neurology domain [29, 81].

Weber's Law does not apply to detection thresholds. With its form as a line through the origin, Weber's Law predicts an infinite detection sensitivity by predicting a zero detection threshold, which would never be the case, due to internal noise of the perceptual system, and noise in the environment.

Fechner further extended Weber's Law to describe the relationship between the physical intensity of stimuli and the intensity of perceptual response [35]. This law, known as the Fechner's Law, describes a logarithmic relationship between them:

$$S = \frac{1}{k}\,\ln\frac{I}{I_0} \tag{2.5}$$

where k and I are defined as before, S is the intensity of the perceptual response, and I_0 is the intensity of the absolute threshold.

Methods for Threshold Search

Over the century of psychophysics research, detection and discrimination remain central questions, and various methods have been proposed.

Method of Constant Stimuli One straightforward method is to directly profile the psychometric curve of the perceptual modality being tested [66]. For example, when testing the absolute threshold of brightness perception, the experimenter could repeatedly present stimuli whose intensities are determined before the experiment, and count the number of times the observer reported detection, for each intensity level. In this way, the psychometric curve for brightness detection is profiled at these predetermined intensities. A psychometric curve could then be fitted, and the respective threshold point could be found.

Since the tested intensity levels are determined prior to the experiment, this method is referred to as the method of constant stimuli. It can happen that the tested levels are far from the threshold level, producing a nearly perfect detection performance or a complete inability of detection, and useless if the main focus of the experiment is the threshold, instead of the shape of the psychometric curve. Therefore, this method often involves pre-testing, in which intensity levels with a more coarse scale are tested. A finer scale on a subregion of the intensity range could then be determined for the actual test, which focuses on the threshold with greater granularity.

Overall, the method of constant stimuli is time consuming and tiring for the participants of the experiment, which would introduce additional factors such as lapse of attention and fatigue, making the results less conclusive [56, 71].

Method of Limits The method of limits [50] improves on the method of constant stimuli. It starts by presenting a stimulus clearly detectable, or a pair of stimuli clearly distinguishable, and reduces the stimulus intensity or the difference between stimuli, until the observer no longer detects or differentiates.

This sequence is termed as a descending sequence. An ascending sequence is conducted by starting from a trial clearly undetectable or indistinguishable.

The experiment consists of many ascending and descending sequences, and the threshold value is calculated as the average of the intensities of the reversal points, where the observer stops detection or differentiation in a descending sequence, or detects or differentiates for the first time in an ascending sequence.

Since the ascending and descending sequences always start at intensities far away from the threshold intensity, there are still lots of wasted trials. This becomes the main motivation of adaptive methods, as introduced next.

Adaptive Methods   In threshold search, adaptive methods is a family of methods which select the intensity of the next trial based on the observer's responses to all or some previous trials [68, 103].

Staircase Methods   Staircase methods [23] are developed, starting from a simple alteration to the method of limits. Instead of terminating the sequence and starting another sequence with opposite direction at an intensity level far from the threshold, staircase methods reverse the direction of intensity change at the reversal point, as illustrated in figure 2.7. This simplest staircase method is called 1-up-1-down staircase, since the direction of search is reversed immediately after the reversal of the response.

It is found that the simple staircase can only target the 50% point on a psychometric curve. Often, some other points on the psychometric curve are of higher interest, such as the 75% point in a discrimination experiment. Levitt [72] developed the method of transformed staircase that can target several other
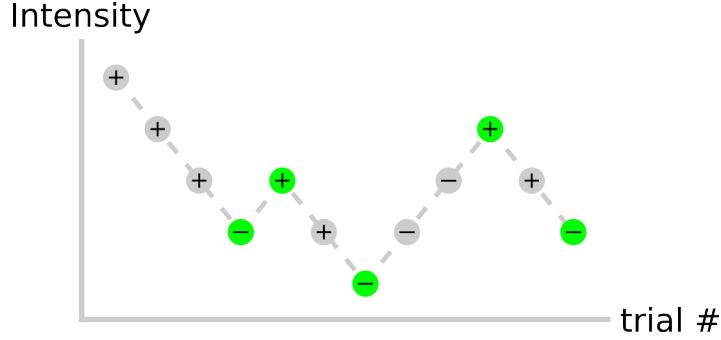
Figure 2.7: Records of Trials in a Staircase Threshold Search. Horizontal axis represents the trial number. Vertical axis represents the intensity tested in that trial. Plus sign indicates positive response. Minus sign indicates negative response. Trials in green background are reversal points where search direction is reversed.

fixed positions in the psychometric curve, such as 70.7% and 29.3% points. It is achieved by changing the conditions for the reversal of direction. For example, if the tested intensity level is decreased only after two consecutive responses of non-detection, and increased immediately after one response of detection, the final result would be the 70.7% point on the psychometric curve.

To be able to target arbitrary points on a psychometric curve, methods with adaptive step size are developed [31, 59, 60, 92]. These methods use different step sizes for different search directions, or change the step size after a certain number of reversals, to narrow the range of threshold search and increase the resolution of result.

Maximum-Likelihood Methods   The maximum-likelihood method is an efficient process to target arbitrary point on a psychometric curve, leveraging on the known properties of its shape, which are essentially parameters of the function characterizing the psychometric curves [76].

Denote the psychometric curve as a function of the form:

$$f(\vec{x}, I),$$

36

where $\vec{x}$ is the vector of parameters, and I is the intensity tested. This function is essentially the probability of a positive response, acknowledging the detection or discrimination.

The result of a trial is denoted as the event tuple:

$$\langle I, z \rangle,$$

where z is the observer's response to intensity level I, 1 meaning detectable/differentiable, and 0 otherwise.

The likelihood of such an event is essentially the probability of the response at the tested intensity level, given the parameters of the underlying psychometric curve. This probability is expressed as:

$$P(I, z|\vec{x}) = z\,f(\vec{x}, I) + (1 - z)\,(1 - f(\vec{x}, I)) = h(\vec{x}). \tag{2.6}$$

The notation of $h(\vec{x})$ is used to indicate the fact that I and z are constant for a given result of a trial, so the likelihood of this result is a function of $\vec{x}$.

Assuming the results of each trial are independent of each other, the collective likelihood of all previous trials can be calculated as the product of all individual results. In mathematical terms:

$$H(\vec{x}) = \prod h_i(\vec{x}) = \prod P(I_i, z_i|\vec{x}), \tag{2.7}$$

where h_i is the likelihood of each individual result.

x is thus estimated as the parameter that maximizes the likelihood for all previous results:

$$x = \arg\max_x H(\vec{x}). \tag{2.8}$$

It means that the psychometric curve with the parameter $\vec{x}$ is the most probable explanation for all previous results. And the estimated threshold could be

calculated as the intensity level with the target detection/discrimination rate, as predicted by the fitted psychometric curve, and this threshold estimate could then be tested in the next trial.

2.2.2 Experimental Design

Due to the scarce literature regarding the quantitative characteristics of binocular luster, we set out to conduct psychophysics studies to investigate the properties of binocular luster.

To address the question of detection, discrimination, and scaling, we adapted similar designs of experiments in other psychophysics studies, with a few changes specific to the unique characteristics of binocular luster.

Testing Paradigm, Testable Range, and Method

To address the question of detection, it is required to first identify what constitutes a binocular luster stimulus and the background for its detection.

A binocular luster stimulus is presented to an observer with two separate brightness for the two eyes, which we refer to as 'binocular brightness'. A binocular color can be expressed in any of the valid binocular color spaces described in the previous section. It can be presented with any stereoscopic display technologies described in chapter 1.

In conventional psychophysics study, the ideal background for detection is usually the complete absence of external signal of the perceptual modality, such as the complete absence of light in studying brightness detection. In our study, the modality of interest is the *difference* between the brightness in the two eyes, and

it follows that the absence of such *difference* does not necessarily imply absence of light in either eye: as long as the light presented to each eye is the same, the signal of binocular luster is considered absent, making this condition a valid background for detection experiment.

For discrimination, the definition of the standard and comparison stimuli follows the convention, which are two stimuli of different inter-ocular brightness difference.

Usually, the question an observer is asked in a psychophysics experiment is either 'Do you detect the presence of the stimulus?', for detection, or 'Do you think the two stimuli are different?', for discrimination. However, these questions ask for subjective response of the observer, without verifying that the observer is actually able to detect/discriminate. To cope with this issue, we present a 3-by-3 grid of stimuli (figure 2.8, among which one contains the target stimulus to be detected/discriminated, and ask the observer to select the stimulus that he/she thinks is the target. In this way, instead of measuring the observer's *subjective feelings* of ability to detect/discriminate, we are able to directly measure the observer's *objective ability* to do that.

It is worth noticing that just by guessing randomly, the observer has 1 in 9 chance (11.1%) of selecting the target stimulus correctly, even if he/she is unable to detect/discriminate. Therefore, following conventional definitions of just-noticeable difference [101, pp. 144], we define the detection/discrimination threshold as half-way between random performance of 11.1% and perfect performance of 100%, which is the 55.5% point on the underlying psychometric curve.

This paradigm is used for measuring both detection and discrimination thresh-
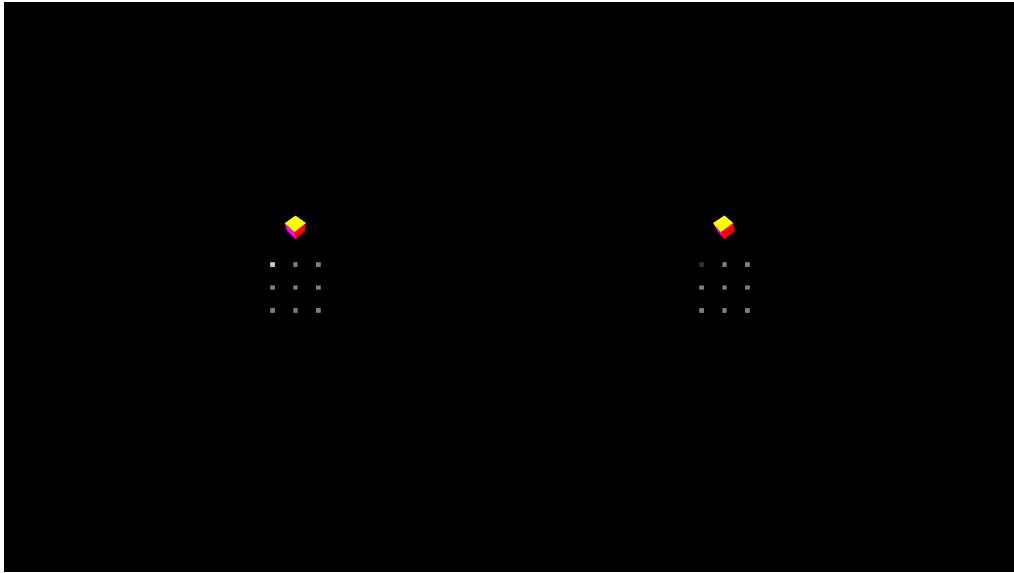
Figure 2.8: Structure of a Trial in the Experiment. The left half of the image is shown to the left eye, and the right half to the right eye, through the Oculus Rift device. The target is the top left square, which the participant has to explicitly select, as an objective proof of detectability/discriminability. The colored rotating cube is meant as a stereo cue to facilitate stereoscopic viewing of the stimulus.

olds, since the task in both cases is the same: to select the square that appears most different from the remaining 8 squares.

For most stereoscopic display devices, the presentable brightness range is limited. For example, for backlit displays, the darkest possible light still contains certain amount of light from the illuminator, and the brightest presentable light is also limited by the maximum energy of the illuminator.

As previously shown in figure 2.3, due to limited output energy of the device, it is impossible to present stimuli outside the diamond region in the BT space. To search for detection or discrimination threshold for a binocular luster stimulus, the space around it must also be presentable. Thus, we are not able to search for detection and discrimination thresholds for standard stimuli on the boundary of the presentable range. We thus confine the standard stimuli to the central quarter of the full presentable range of the display device, as shown in figure 2.9.
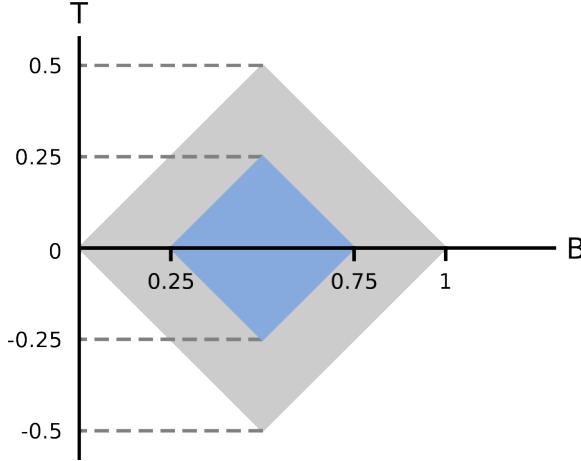
Figure 2.9: Tested Range in BT space. It covers a quarter of the full range presentable by the device, to allow room for threshold search.

Initially, the staircase method was used for threshold search, but was later found to be very sensitive to step size. If the step size is too large, the result might be inaccurate, and might require testing at a level outside the presentable range (figure 2.10). If it is too small, due to the nature of our experiment paradigm, the threshold could be unreachable. Figure 2.11 is a screen shot of the real-time visualization of trial records during the actual pilot experiment, using the staircase method but too small step size. In an ascending sequence, where the step size is too small, many levels below the threshold would be tested, for which the observer is unable to detect/discriminate. However, while converging onto the actual threshold through these undetectable/indistinguishable trials, an observer might correctly select the target purely by chance, despite his/her inability to detect/discriminate, resulting in the termination of the convergence, and the reversal of search direction, away from the threshold. In this specific example, the staircase method reported a threshold value of 0.026, whereas the maximum-likelihood method, as will be described later in this section, reports a threshold value of 0.045, clearly showing the problem with very small step size.

To mitigate the above limitations with staircase methods, we used the maximum-

41
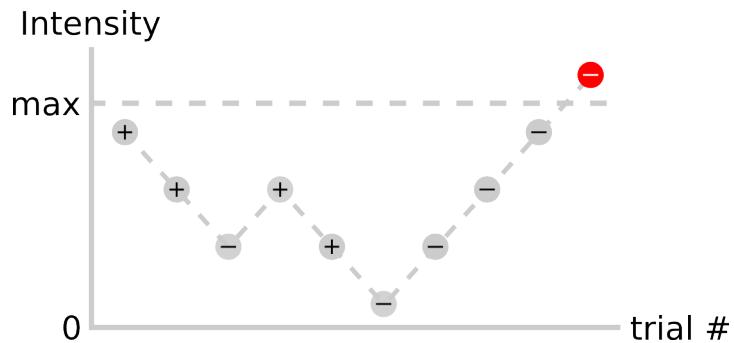
Figure 2.10: Too Large Step Size Causes Overflow. The stimulus to be tested next (in red background) is stronger than the maximum intensity presentable by the device.

Figure 2.11: Too Small Step Size Prevents Convergence. Green triangles are trials with correct response, red squares are trials with wrong response. Blue horizontal line shows actual threshold, which is never reached.

likelihood method in our experiment. We model the underlying psychometric curve as the cumulative density function of Weibull distribution [114], which is a popular choice in psychophysics studies [76, 112].

A Weibull distribution is defined for $x \geqslant 0$. The probability density function (PDF) for a Weibull distribution is:

$$
f(x) = \begin{cases} \frac{k}{\lambda} \left(\frac{x}{\lambda} \right)^{k-1} e^{-(x/\lambda)^k} & x \geqslant 0 \\ 0 & x < 0 \end{cases} \tag{2.9}
$$

and its cumulative distribution function (CDF):

$$
F(x) = \begin{cases} 1 - e^{-(x/\lambda)^k} & x \geqslant 0 \\ 0 & x < 0 \end{cases} \tag{2.10}
$$

where $\lambda \in (0, +\infty)$ is the scale parameter, and $k \in (0, +\infty)$ is the shape parameter.

Some advantages of the Weibull distribution include:

1. It approximates a wide range of sigmoid curves for positive input, covering the shapes of most psychometric curves.

2. Both its PDF and CDF have closed-form expressions, and only two parameters are used to control its shape and scale.

3. Specific to our experiment paradigm, for a target that is no different from the standard stimulus (i.e., a 'catch' trial where no signal/difference is present), the observer would never give a correct response. This implies that the psychometric curve would pass through the origin, which is modeled by the Weibull distribution.

In actual testing, it is found that the fitted Weibull curve would have extreme val-
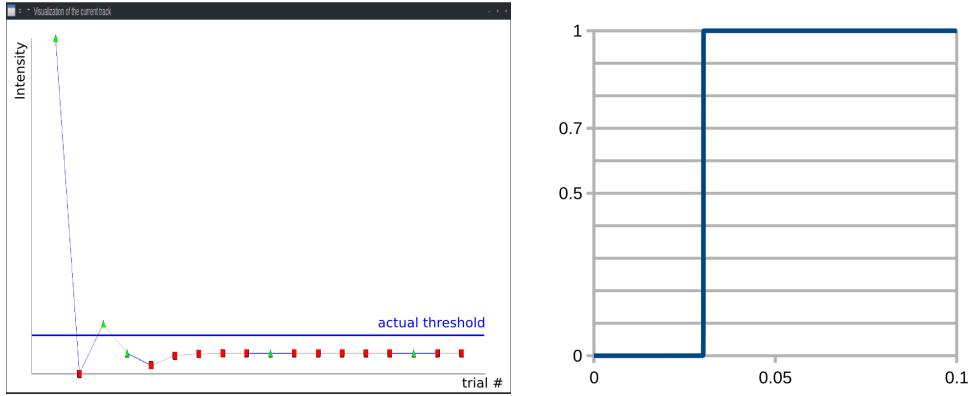
Figure 2.12: Extreme Shape Parameters in Maximum Likelihood Method. Left: the tested levels are constrained within a small interval. Right: the fitted curve is of extreme shape.

ues for its parameters. This is actually an expected behavior. Figure 2.12 shows a track of trials in one of our pilot experiments with such a problem. The observer responds positively to the first trial, and the threshold would be estimated to be infinitesimal, resulting in the next tested level far below the actual threshold, and the observer would respond negatively. Then the maximum-likelihood fitting would estimate the threshold to be an intermediate value between the first two tested levels. And in turn, depending upon the result of the third trial, the threshold would be estimated as an intermediate value between the lowest tested level with a positive response and the highest tested level with a negative response. When more trials are conducted, the threshold estimate is 'trapped' in a tiny range, and the change from negative to positive responses takes place in such a tiny range, that the shape parameter, k, is extremely large. After the last trial in the example in figure 2.12, the maximum likelihood fitting reported an extreme k value of 2.21256E11 and a λ value of 0.030203, whose shape is shown in figure 2.12. It can be seen that the extreme k value would undermine the process of the maximum likelihood threshold estimate, by trapping subsequent trials in a small interval of intensity that might be far from the actual threshold level, preventing it to be ever tested.

44

To cope with this issue, we applied prior probabilities on the two parameters in the calculation of likelihood:

$$H'(\vec{x}) = G(\vec{x}) \, H(\vec{x}), \tag{2.11}$$

where the function $G(\vec{x})$ is the probability of the parameters having value $\vec{x}$.

With this tweak, extreme values for the parameters are penalized, and the threshold estimate is robust against less likely responses. It is found that, on the same scale for which the device brightness range is $[0, 1]$, Gaussian prior on k with a mean of 5.5 and a standard deviation of 2.25 works well. This setting is used in the formal experiments.

Factors

As in the design of controlled experiments, the various factors in the experimentation process are identified as follows.

Independent Variables   Three aspects are of interest about the detection and discrimination of binocular luster: the effect of the magnitude of the inter-ocular difference, the effect of total energy presented to the observer (i.e., sum of energy in the two eyes), and the effect of ocular dominance. This leads to the definition of three independent variables.

Our definition of the BT binocular luster space makes it convenient to choose the B value ($B = (L + R)/2$) as the factor reflecting the total presented energy, and the absolute value of T as the magnitude of inter-ocular brightness difference. Note that the B and T values are related to the true factors of our interest by a scale factor of 2, which preserves linearity.

To explore the effects of ocular dominance, we propose sidedness as a nominal factor of binocular luster stimuli. Sidedness can be either positive or negative. If the dominant eye is presented with higher brightness than the non-dominant eye, the sidedness of this stimulus is considered positive, and negative otherwise. Note that sidedness is relative to eye dominance, instead of absolute side of left or right in the definition of T. To incorporate sidedness, we propose a variant of BT space, the BT' space, where the definition of the T' dimension is 'half of the inter-ocular brightness difference from the **non-dominant** to the **dominant** eye'. This way, the sign of the T' value can be directly used as the sidedness factor.

Dependent Variables   The dependent variables are the detection/discrimination thresholds along the dimensions of B and T' for each standard stimuli.

The thresholds are not measured by a single trial, but through a track of several trials. For a complete and faithful documentation of the experimental process, the response for every trial is recorded, including tested condition (standard stimulus in BT' space, direction of threshold search, and tested level), correctness, response time (elapsed time from onset of the stimulus on the screen till numeric key is pressed as the response), and estimated threshold after that trial.

Control Variables   Control variables are factors that are kept constant throughout the experiment, which include:

- Color of the stimuli, which is none, corresponding to zero U and V values in the YUV color space.

- Background brightness, which we set as black.

- Size and spacing of the 3-by-3 grid of stimuli, whose numeric values are presented later in the introduction of the experimental apparatus.

- Parameters of the display device, such as intrinsic brightness and contrast, and color profile, which we keep as default and constant throughout the experiment.

- Direction of the threshold search, which we always set as the direction of increasing strength of the stimuli. For example, we only measure positive difference threshold of luster strength, i.e., minimum increment, rather than decrement, in luster strength from the standard stimulus to be just noticeable.

Measuring only the positive perceptual thresholds reduces the size of the experiment. It is a valid decision in the experiment design, because the negative threshold can be viewed as the positive threshold from a standard stimulus with a smaller intensity. For example, a negative threshold of $-\Delta I$ from a standard stimuli of I means that stimuli of $I - \Delta I$ is just differentiable from I, and another way to view this fact is that the positive threshold from the stimulus with the intensity of $I - \Delta I$ is ΔI.

Random Variables Random variables are factors out of the experimenter's control. Apart from the demographics of the participants of the experiment, such as gender and age, we are mainly concerned about ocular dominance and visual acuity, which would likely affect the result.

Therefore, prior to the experiment, we measured the participants' ocular dominance using the Miles test [90] and verified that they have normal or corrected-to-normal visual acuity.
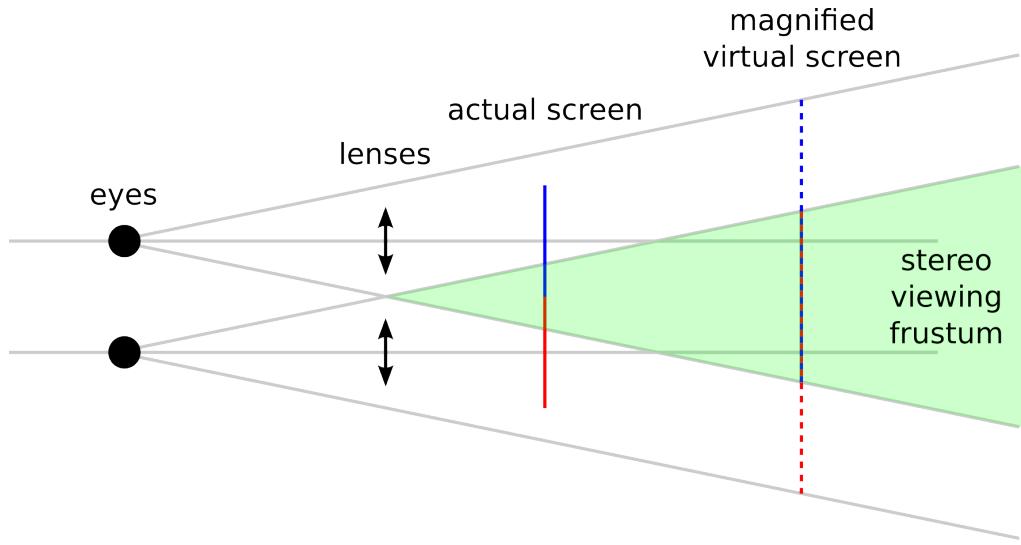
Figure 2.13: Optical Mechanism of Oculus Rift from Top View. Lenses magnify each half screen (blue and red solid lines) for each eye. Virtual screens seen by the eyes (blue and red dashed lines) define the stereoscopic viewing frustum.

It is possible that an observer does not have strong reliance on a particular eye for visual perception. To capture this nature of ocular dominance, the Miles test is repeated for 10 times, and the outcome for each repetition is recorded.

Apparatus

The experiment was carried out with a laptop PC with Intel Core i7 quad-core 2.2GHz processor, 16G memory, and running 64-bit Debian Linux operating system.

The presentation device is the Oculus Rift immersive head-mounted display [6] (DK1, as shown in figure 1.10. Its working mechanism involves a screen directly in front of the eyes, and the accompanying lenses, which magnify and focuses the screen sharply onto the retina of the eyes, creating a frustum for stereoscopic viewing. Figure 2.13 illustrates the optical mechanism of the Oculus Rift device from the top view.

Figure 2.14 illustrates the physical dimensions of the Oculus Rift HMD. The
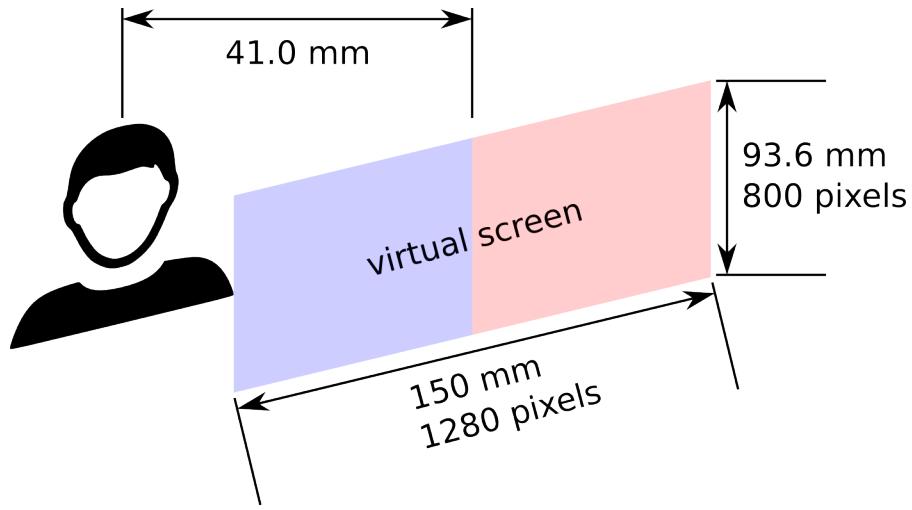
Figure 2.14: Physical Dimensions of Oculus Rift.

apparent dimension of the virtual screen (after magnification by the lenses) perceived by the observer is 150mm of width by 93.6mm of height. The distance from the eye to the screen is 41.0mm. And the resolution of the screen is 1280 by 800 pixels, which is 640 by 800 for each eye.

Figure 2.8 shows an example of a trial presented in the experiment. A 3-by-3 grid of nine squares are presented, with separate brightness for each eye's view. One of the 9 squares is different from the rest, differing in either B or T' values in the BT' space. The side of each square is 5.79 pixels, corresponding to 0.677mm. And the distance between the centers of adjacent squares is 28.9 pixels, corresponding to 3.39mm. With the eye-to-screen distance of 41.0mm, the diagonal angular size of each square is 1.34 degrees, the separation of adjacent square centers is 4.73 degrees horizontally as well as vertically, and the entire 3-by-3 grid occupies a diagonally 14.6 degree region in the center of the field of view. In addition, a rotating cube with different colors on each side is presented stereoscopically all the time, so that participants could ensure proper stereoscopic convergence with this stereo cue.

Figure 2.15: Oculus Rift control box showing brightness and contrast adjustment buttons.

The Oculus Rift device is connected to the experiment PC as an extended display via an HDMI cable to its control box.

The intrinsic brightness and contrast of Oculus Rift can be adjusted (figure 2.15), similar to most computer displays. To insure the comparability of results, these parameters are kept constant throughout the experiment.

The Oculus Rift also provides two other pairs of lenses with two degrees of correction for visual acuity. The participants who wore correction lenses were asked to try them and wear their own spectacles with the Oculus Rift device, and then choose the configuration that they feel provides an optimal experience, in terms of viewing clarity and comfort.

To provide convenient means for participants to respond to the trials, we used the numeric keypad on a full-size keyboard. The target is selected by hitting the number key corresponding to its on-screen location, as illustrated in figure 2.16.

A program is developed for the experiment. It uses OpenGL to render the left and right views of the stimuli onto the Oculus Rift screen. We also implemented the maximum-likelihood fitting algorithm and its underlying numeric maximization
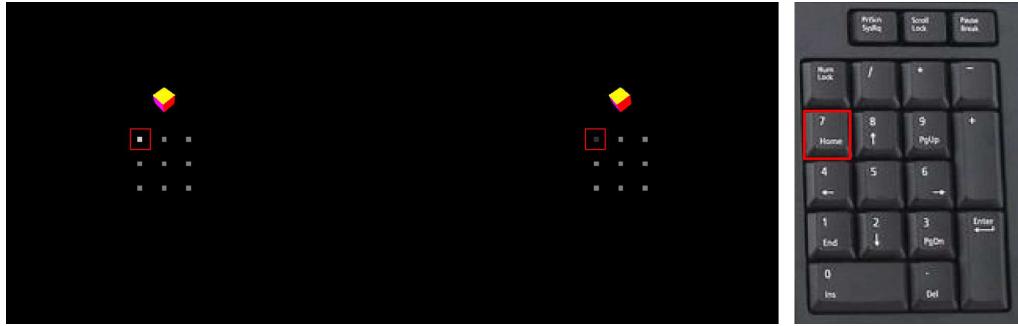
Figure 2.16: Target selection method in the experiment. Target square is selected by pressing corresponding key on the numeric keypad. The target is at the top-left corner, corresponding to the top-left key on the keypad.

algorithm (Nelder-Mead Maximization [65]), so that the maximization can be performed after each trial.

The experiment program uses comma-separated vector (CSV) files for input and output. The input is a single CSV file specifying the conditions of thresholds to be measured in each line. The output is in the form of multiple CSV files, one for each threshold measurement track. In each file, details for each trial in that track are recorded, including tested levels of standard and comparison stimuli, position of the target square, participant's selection, correctness, response time, and estimated threshold after that trial.

The program creates two windows, the experiment window and the visualization window. The experiment window is shown in full screen on the Oculus Rift device, and the visualization window is shown on the built-in screen of the PC, providing intuitive feedback to the experimenter. The detailed information for each trial is also printed to the console in real-time, which is also logged into a file. The visualization and console output are not available to the participant, and no feedback of correctness is provided for them.

Procedure

The experiment starts by conducting the 10 repetitions of Miles ocular dominance tests, and collecting demographics of the participants. Then with the help of an experimenter, the participant puts on the display and adjusts for the optimal viewing condition, including proper positioning of the Oculus Rift device and selection of either correction lenses provided by the Oculus Rift or the participants own spectacles. The participants are introduced with the visual structure of each trial, as shown in figure 2.8. Then they are acquainted with the method of using numeric keypad to respond to the trials. The measurement of the thresholds takes place after several practice trials, through which the participants familiarize themselves with the experimental system.

Figure 2.17 shows a track of the threshold search using maximum-likelihood method with a priori constraint on the k parameter of the underlying Weibull CDF curve. The horizontal axis represents the trial number that indicates the progression of the track, and the vertical axis represents the level tested. Green triangle indicates a correct detection/discrimination by the observer, and red square an incorrect response. As can be seen, the threshold estimate quickly converges after around 10 trials in the track. The track is required to consist of at least 25 trials, and at most 41 trials. For any trial between the 25th and 41st, if the standard deviation of the 10 most recent threshold estimates is smaller than half the highest brightness resolution of the display ($1/255$ on a 0 to 1 scale, for most digital display devices, including the Oculus Rift), the track is terminated as well. This termination criterion translates to: assuming that the estimated threshold is normally distributed around the true threshold, there is a 95% chance that the true threshold falls within the range of $\pm 1/255$ of the
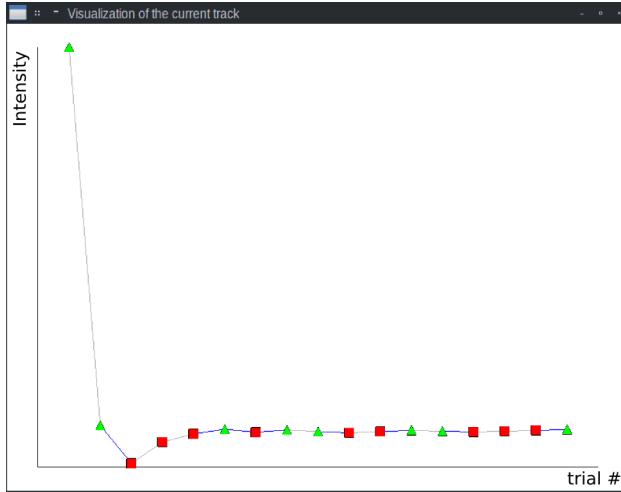
Figure 2.17: Threshold search track using maximum likelihood method with a priori.

presentable brightness range, around the estimated threshold value.

It could happen that the tested level is very close to zero, which will be coerced to zero due to the numerical limits of the computer. However, in such a situation, specific for fitting the Weibull curve in our experiment setting, testing a level at zero would not gain any information for the fitting, since any Weibull curve would pass through the origin, and as a result, the threshold estimate would not be refined after testing at zero. Therefore, instead of testing at zero, we test at a small non-zero level, so that the maximum-likelihood method could proceed. It is found that a minimum testing level of 1E6 works well with our experiment.

Overflow could also happen due to the limited number of observations at the start of the experiment, and less likely responses, such as accidentally answering wrongly for an easy-to-discriminate stimulus. In such cases, a stimulus with intensity greater than the device limit is requested for the next trial. To cope with this issue, a random intensity level within the presentable range is selected for the next trial, so that more observations could be accumulated until the maximum-likelihood process estimates a threshold within the presentable range.

To quickly converge onto a relatively small sub-region close to the threshold, a special routine is employed to bootstrap the maximum-likelihood threshold search. For the first trial in a track, the difference between the target square and the standard stimulus is set at the maximum possible. For example, when searching for the difference threshold along the T' direction, for the point of $B = 0.5$, $T' = 0.1$, and positive sidedness, the first target square in the first trial will be $B = 0.5$, $T' = 0.5$, with positive sidedness. If the observer correctly selected the target square, the tested level is reduced by 90%, and if the observer again responded correctly, the tested level is further reduced by 90%. This process continues until the observer fails to detect/discriminate for the first time. Then the maximum-likelihood method kicks in and selects the next level to test based on the maximum-likelihood estimate of the threshold.

Figure 2.18 shows the standard stimuli for which the thresholds are measured. Arrows from the standard stimuli indicate the direction of the threshold searches. The main focus, as seen, is on the line of $B = 0.5$, with the resolution of 21 different T' values in the range of $T' \in [-0.25, 0.25]$.

Apart from these points of primary interest, four additional points on the line of $T' = 0$ are measured, to investigate the effect of B value on the detection threshold along T', as well as to collect difference thresholds without binocular luster, so as to enable cross validation with previous research of brightness perception. We hypothesize that the difference threshold along the B direction for standard stimuli with zero T' values would follow Weber's Law, in agreement with previous research [102].

To allow investigation of the interaction between the B and T' values on thresholds, 12 more points on neither of the two lines $B = 0.5$ and $T' = 0$ are investi-
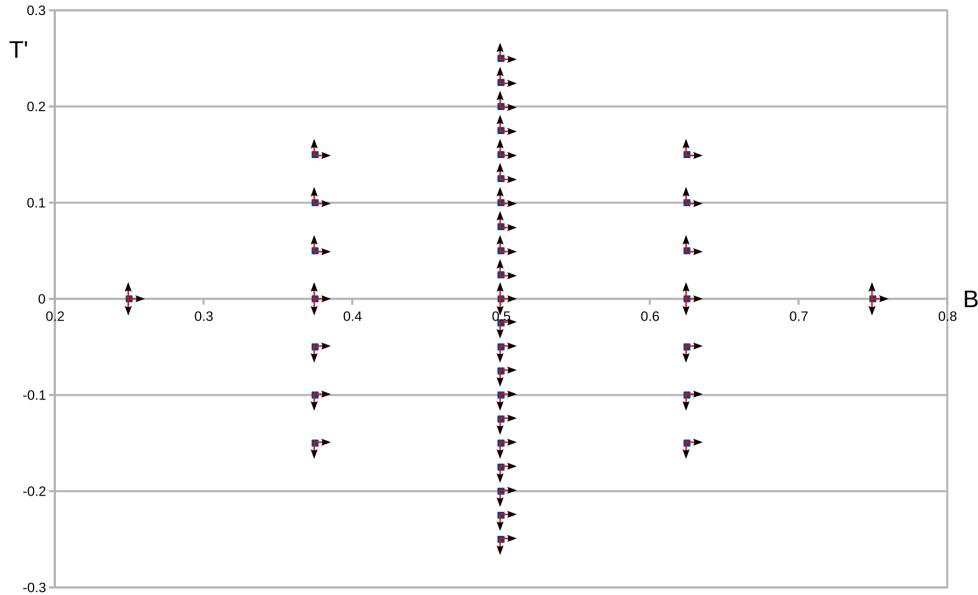
Figure 2.18: Tested thresholds in the experiment. Standard stimuli are shown in BT' space, with arrows indicating directions of threshold search from each standard stimulus.

gated.

Also note that the layout of these points are symmetric about the B axis, so that for each combination of B and T' value, both positive and negative sidedness conditions are tested, to allow investigation of the effect of ocular dominance.

The points of interest described above require measuring of 79 thresholds under different conditions.

It is found in the pilot study that a single measurement of a threshold, consisting of 25 to 41 single trials, usually finishes in about 2 minutes. The total time to measure all 79 thresholds is therefore about $79 \times 2 = 158$ minutes. It is impractical for the participants to finish all the tasks in a single session, as prolonged experiment hinders accuracy of the measurement due to fatigue and lapse of attention. Therefore, the experiment is divided into 5 sessions, each taking around 45 minutes to finish, including the introduction and the practice

55

trials for the participants to familiarize them with the procedure.

It has been noted in previous psychophysics studies that if the thresholds are measured sequentially, the pattern of choice of tested level becomes apparent to the participants, who might be intentionally or unintentionally biased [68, 103]. Following conventional practices, the tracks of threshold measurements in a session are interleaved, by randomly selecting a track to continue after a trial is finished.

A trial might be affected by previous trials, due to the adaptation of the perception system, reducing its sensitivity to the stimuli presented for a prolonged time. To minimize such effects, the screen is blanked for 300ms, to allow for the recovering of the perception system to it normal sensitivity.

Participants

4 female and 8 male participants were invited to the experiment. Their age range is between 23 to 30, with a mean of 26. All of them are right-handed, experiencing no difficulty in selecting the target using the numeric keypad on the keyboard. Two of them are left-eye dominant, and the rest are right-eye dominant.

All participants finished the five sessions of the experiment, over a period of two weeks.

2.3   Results

This section describes the post-processing method on the collected raw results, and the statistical characteristics of the measured thresholds. The statistic tests

are performed with the R statistics software.

2.3.1 Post-Processing of Raw Results

The measured thresholds reflect the sensitivity of the observers with their particular ocular dominance. Instead of being nominally either left or right, ocular dominance can be at an arbitrary position on the continuum from complete left- to complete right-eye dominance. To incorporate this consideration into our comprehension of the experiment results, the outcomes of the 10 repetitions of Miles test of ocular dominance is used to adjust the measured thresholds for each participant.

First, we define the two theoretical extremes of the ocular dominance continuum, as follows.

- **Complete dominance**

  The theoretical situation where the observer's ocular dominance is strongest. For example, if the observer demonstrates left-eye dominance for 8 times out of 10 Miles tests of ocular dominance, the theoretical situation of complete dominance is that this observer is completely left-eye dominant, always demonstrating left-eye dominance in Miles test.

- **Conjugate dominance**

  The theoretical situation where the observer's ocular dominance is opposite to the actual result, and is complete dominance (as defined above). Following the above example, the conjugate dominance is the theoretical situation when the observer is completely right-eye dominant.

Two theoretical thresholds are associated with the respective theoretical dominance situations defined above.

Note that theoretical threshold of complete dominance for one condition is the same as theoretical threshold of conjugate dominance for the same condition with the left- and right-eye views swapped. We define 'symmetric conditions' to account for this observation:

Definition 2.1. *Two conditions of threshold measurement for an observer are said to be symmetric if the standard stimuli and the directions they measure are symmetric about the B axis in the BT' space.*

With these defined concepts, our lemma is described as:

Lemma 2.1. *The theoretical threshold of complete dominance for a condition equals the theoretical threshold of conjugate dominance for its symmetric condition, for a specific observer.*

Figure 2.19 illustrates a pair of symmetric conditions, and the relationship between their theoretical thresholds for a same user. Consider an observer with certain ocular dominance. For a condition, C, with non-negative T' value (i.e., above or on the B axis in the BT' space), denote its theoretical threshold of complete dominance as d, and the theoretical threshold of conjugate dominance as d'. Then, according to lemma 2.1, for its symmetric condition, C', the theoretical threshold of complete dominance is d', and theoretical threshold of conjugate dominance is d, according to the lemma.

Denote the measured threshold for condition C as d, and the measured threshold for its symmetric condition C' as d'. We interpret the pair of measured thresholds as the weighted sum of their respective theoretical thresholds, where the weight is determined by the outcome of the repeated Miles tests.

For example, if an observer demonstrates n times of dominance in one eye, and
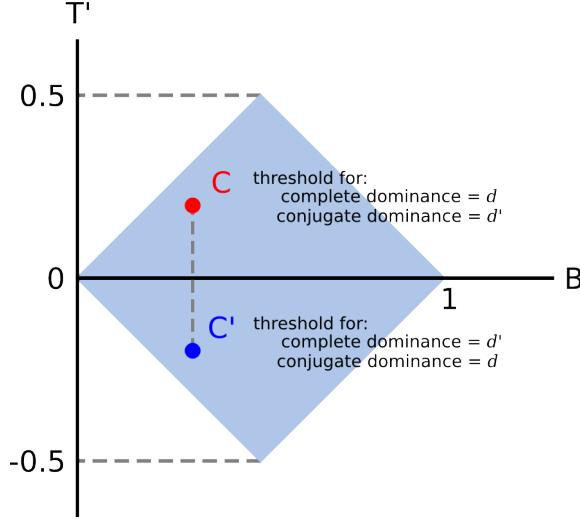
Figure 2.19: Symmetric conditions and the relationship between their theoretical thresholds.

m times in the other, where $n > m$, for $n + m$ repeated Miles tests, for a pair of symmetric conditions C and C', the measured thresholds d and d' are the weighted sums of the theoretical thresholds D and D':

$$d = \frac{nD + mD'}{n + m} \tag{2.12}$$

$$d' = \frac{nD' + mD}{n + m} \tag{2.13}$$

In matrix form, the theoretical thresholds and the measured thresholds are related by:

$$\begin{bmatrix} d \\ d' \end{bmatrix} = \frac{1}{n + m} \begin{bmatrix} n & m \\ m & n \end{bmatrix} \begin{bmatrix} D \\ D' \end{bmatrix} \tag{2.14}$$

Since the experiment measures d and d', we calculate d and d' with the inverse of the matrix as:

$$\begin{bmatrix} D \\ D' \end{bmatrix} = \frac{1}{n - m} \begin{bmatrix} n & -m \\ -m & n \end{bmatrix} \begin{bmatrix} d \\ d' \end{bmatrix} \tag{2.15}$$

After this adjustment, we are able to analyze the effect of sidedness on the theoretical results with more homogeneity, as there would be a smaller effect of different degrees of ocular dominance specific for each participant.

To minimize the interpersonal difference that could arise among the few users participating in our experiment, we also averaged the thresholds for all users for corresponding conditions in the BT' space.

2.3.2 Detection and Discrimination of Binocular Luster Intensity

The T' dimension in the BT' binocular luster space represents the physical intensity of binocular luster. This section presents findings about the detection and discrimination thresholds along this dimension. With respect to the measured thresholds shown in figure 2.18, the detection thresholds of binocular luster are investigated along the $T' = 0$ line in the BT' space, and the discrimination thresholds are investigated along the three lines $B = 0.375$, $B = 0.5$, and $B = 0.625$. The following subsections detail the findings about the thresholds along the T' dimension, along these lines.

Detection Threshold

Figure 2.20 shows the detection thresholds of T', with respect to different B values on the line $T' = 0$, averaged over all participants, for positive and negative sidedness.

The detection thresholds of binocular luster for both sides demonstrate a positive association with the B value of the background stimuli, from which the presence of luster is to be detected. A Pearson's correlation test was performed for both sides. For positive sidedness, the p-value is 0.01132, with a t value of 5.5877 and a df (degree of freedom) of 3. The correlation coefficient is 0.9551633. For negative sidedness, the p-value is 0.01035, with a t value of 5.7698 and a df of 3.
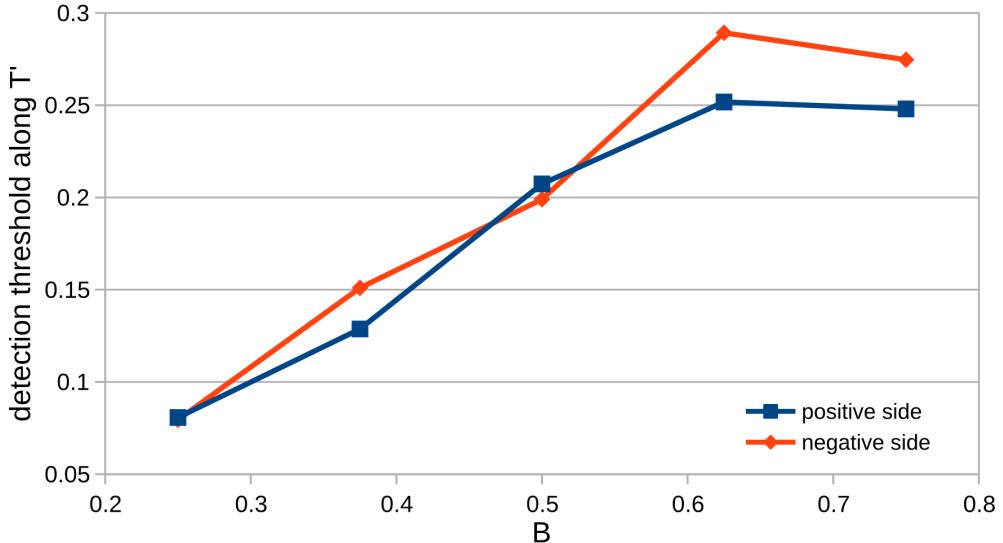
Figure 2.20: Detection threshold of T' with respect to B.

The correlation coefficient is 0.9577757. Both results indicate a strong correlation between the detection threshold and the brightness of background stimuli.

The two curves for the two sidedness almost overlap each other, indicating an absence of a strong effect of sidedness. A paired t-test reports a p-value of 0.1507, with a t value of -1.7741 and a df of 4. This p-value means that the test's hypothesis of 'true difference in means is equal to 0' cannot be rejected, meaning that the effect of sidedness on the detection threshold of binocular luster intensity is not significant.

Discrimination Threshold

The discrimination thresholds of luster intensity are measured along the lines $B = 0.375$, $B = 0.5$, and $B = 0.625$.

Figure 2.21 shows the discrimination thresholds of T', with respect to T' value of the standard stimuli, for both sides, on the three lines measured. It appears that discrimination threshold is inversely associated with T' value of the standard
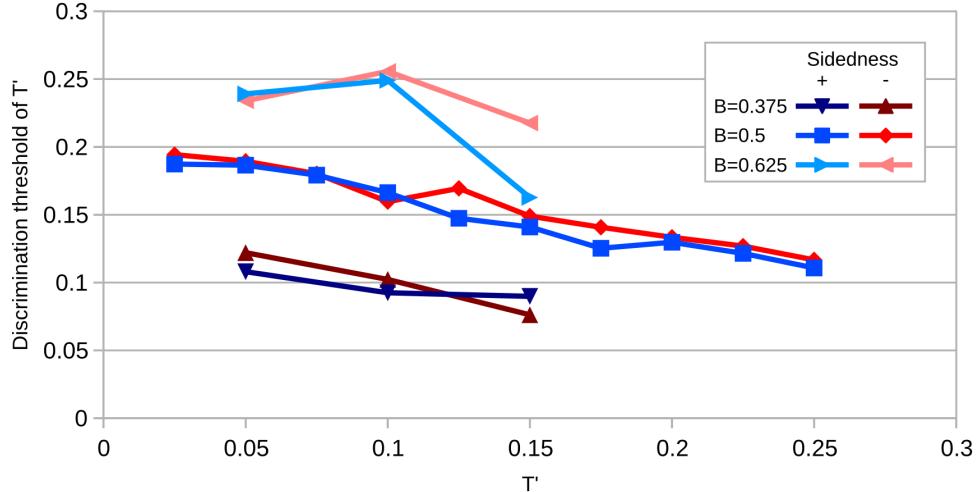
Figure 2.21: Discrimination threshold of T' with respect to T' of standard stimuli. stimuli.

Also observed in this figure is that B value of the standard stimuli might have an effect, demonstrated by the much lower discrimination thresholds for the line $B = 0.375$. Figure 2.22 demonstrates this potential effect more clearly, by plotting discrimination thresholds of T' against B value of the standard stimuli, for different T' values of the standard stimuli.

Sidedness seems to have an effect, but is different for different B values. For the line $B = 0.375$, positive sidedness seems to reduce discriminability, as shown with its higher thresholds than negative sidedness. For the line $B = 0.5$, however, the effect of sidedness seems to be reversed, leading to a higher discriminability for positive side.

Table 2.1 summarizes results of a multi-factor ANOVA test on the data of discrimination thresholds.

As shown, the significance of the effect of B and T' on discrimination threshold of T' is confirmed. In addition, the effect of sidedness is also found to be significant,
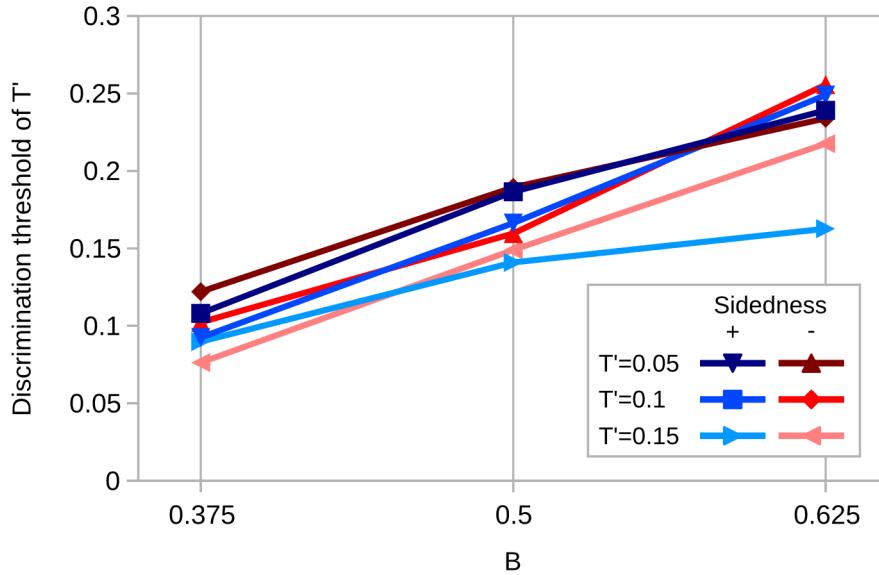
Figure 2.22: Discrimination threshold of T' with respect to B of standard stimuli.

Table 2.1: ANOVA table of discrimination threshold of T' with B, T', and sidedness. Left-most column shows the factors, where the form A:B indicates the interaction between A and B.

	Sum sq	Df	F value	Pr(>F)	
B	0.049060	1	399.1464	< 2.2E-16	***
T'	0.017011	1	138.3963	1.883E-11	**
side	0.000541	1	4.4002	0.04664	*
B:T'	0.000103	1	0.8403	0.36844	
B:side	0.000178	1	1.4460	0.24089	
T':side	0.000027	1	0.2224	0.64150	
B:T':side	0.000959	1	7.8009	0.01009	*
Residuals	0.002950	24			

Signif. codes: 0 '***' 0.001 '**' 0.01 '*' 0.05 '.' 0.1 ' ' 1

Table 2.2: Pearson correlation test for discrimination threshold of T' and T' value.

B	sidedness	t-value	df	p-value	correlation coefficient
0.375	+	-2.4495	1	0.2468	-0.9258199
	−	-12.6326	1	0.05029	-0.9968815
0.5	+	-13.8258	8	7.237E-7	-0.9797091
	−	-15.8965	8	2.455E-7	-0.984537
0.625	+	-1.3755	1	0.4002	-0.8088354
	−	-0.4737	1	0.7184	-0.4281227

so as the three-way interaction between B, T', and sidedness.

To further test the linearity between T' and discrimination threshold of T', Pearson's correlation tests were performed for the 6 combinations of the three B values (0.375, 0.5, 0.625) and the two possible sides (positive, negative). Table 2.2 summarizes the results.

The table shows strong and significant negative correlation between T' discrimination thresholds and T' value of the standard stimuli for the line of $B = 0.5$. For the other two lines, since less samples were collected, although most of the correlation is strong, their effect is not significant. Given the significance of T' reported by the earlier ANOVA test, there is reason to believe that the correlation will become stronger and more significant with more samples collected. It is thus safe to interpret that the discrimination threshold of binocular luster intensity is linearly and negatively associated with the binocular luster intensity of the standard stimuli.

Similarly, the linearity between B and discrimination threshold of T' is tested with Pearson's correlation tests for 6 combinations of the three T' values (0.05, 0.10, 0.15) and the two possible sides (positive, negative). Table 2.3 summarizes the results.

Although for some T' values, the correlation is not significant enough, due to the

Table 2.3: Pearson correlation test for discrimination threshold of T' and B value.

T'	sidedness	t-value	df	p-value	correlation coefficient
0.05	+	8.7324	1	0.07259	0.9935068
	−	8.4801	1	0.07473	0.9931188
0.10	+	30.7629	1	0.02069	0.9994721
	−	6.8776	1	0.09192	0.9895942
0.15	+	4.2913	1	0.1457	0.9739071
	−	58.0835	1	0.01096	0.9998518

limited size of the sample, they all demonstrate strong positive linear correlation between B value of the standard stimuli and the discrimination threshold of T'. Given the significance of B reported by the earlier ANOVA test, there is reason to believe that the correlation will become stronger and more significant with more samples collected. It is thus safe to interpret that the discrimination threshold of binocular luster intensity is linearly and positively associated with the total energy of the standard stimuli.

Unifying Detection and Discrimination Thresholds

Interestingly, if the detection thresholds are plotted together with the discrimination thresholds for T', as shown in figure 2.23, it seems that the previous results still hold.

To confirm this, a multi-factor ANOVA is performed on the unified data, reported in table 2.4.

The significance of the effect of both B and T' is confirmed, and the effect of sidedness is no longer significant, possibly due to different significance from previous results on detection and discrimination thresholds alone.

Additional Pearson's correlation tests are performed for 6 combinations of the three B values (0.375, 0.5, 0.625) and the two sides (positive, negative), on the
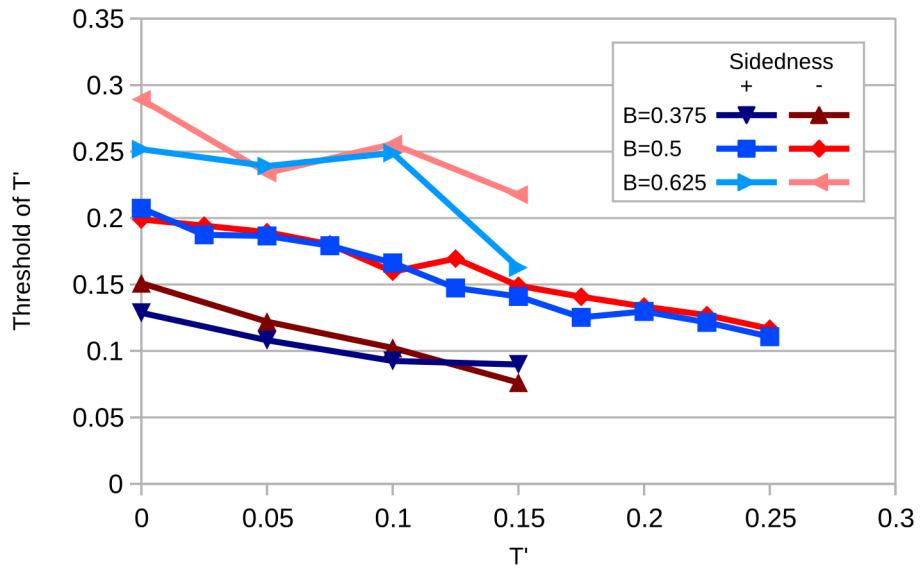
Figure 2.23: Detection and discrimination threshold of T' with respect to T' of standard stimuli.

Table 2.4: ANOVA table of detection and discrimination threshold of T' with B, T', and sidedness. Left-most column shows the factors, where the form $A{:}B$ indicates the interaction between A and B.

	Sum Sq	Df	F value	Pr($>$F)	
B	0.096090	1	345.8998	< 2.2e-16	***
T'	0.025785	1	92.8180	3.003e-11	***
side	0.001034	1	3.7228	0.06205	.
$B{:}T'$	0.000957	1	3.4441	0.07216	.
$B{:}$side	0.000429	1	1.5425	0.22274	
$T'{:}$side	0.000008	1	0.0303	0.86281	
$B{:}T'{:}$side	0.000223	1	0.8040	0.37622	
Residuals	0.009445	34			

Signif. codes: 0 '***' 0.001 '**' 0.01 '*' 0.05 '.' 0.1 ' ' 1

Table 2.5: Pearson correlation test for detection and discrimination threshold of T' and T' value.

B	sidedness	t-value	df	p-value	correlation coefficient
0.375	+	-4.5594	2	0.04489	-0.9551096
	−	-20.5273	2	0.002365	-0.9976352
0.5	+	-16.5856	9	4.7E-8	-0.9840321
	−	-18.1169	9	2.168E-8	-0.9865654
0.625	+	-1.7922	2	0.215	-0.7850302
	−	-1.9228	2	0.1944	-0.8055778

Table 2.6: Changes in p-value and correlation coefficient after unification of detection and discrimination threshold of T'.

B	sidedness	change in p-value	change in correlation coefficient
0.375	+	-0.20191	-0.0292897
	−	-0.047925	-0.0007537
0.5	+	-6.767E-7	-0.004323
	−	-2.2382E-7	-0.0020284
0.625	+	-0.1852	0.0238052
	−	-0.524	-0.3774551

unified data. Table 2.5 summarizes the results:

Table 2.6 further shows the change in the p-value and the absolute value of correlation coefficient after unification of detection and discrimination threshold for these respective Pearson's correlation tests.

The table clearly shows that by unifying the detection and discrimination thresholds, both significance of the effect of T' and its linearity with the unified thresholds improve. Note that negative change in correlation coefficient indicates improved linearity, since the correlation coefficient is negative.

Summary

The characteristics of detection and discrimination of binocular luster intensity, i.e., along the T' dimension in BT' space, are summarized as follows.

Firstly, perception of binocular luster might not be a completely independent perceptual modality. This is seen from the data analysis that unifying detec-

tion and discrimination thresholds uncovers same effects of B and T', and even improved linearity. This finding contradicts our expectation based on prior experience in psychophysics studies. This property might indicate that, our hypothetical 'detection' task might not reflect the actual mechanism of binocular luster perception. Instead of being a completely independent perceptual modality, the perception of binocular luster is very likely to be correlated with brightness perception without luster. In this light, it might be appropriate to make no distinction between the detection and discrimination thresholds, and simply refer to them as the perceptual thresholds of binocular luster intensity.

Secondly, as the intensity of binocular luster increases, the sensitivity to its change also increases: a smaller increase in physical binocular luster intensity would instigate a larger increase in the perceptual experience. This is seen from the data analysis that the perceptual threshold of binocular luster intensity is inversely associated with the binocular luster intensity where the threshold is measured. This somewhat remotely resembles the linearity described by Weber's Law, but differs in its negative slope of the line and non-zero intercept.

Thirdly, larger total energy in the two eyes makes the perception of binocular luster intensity less sensitive. This is exhibited in the data as the effect of B value of the standard stimuli, with larger B resulting in larger threshold, which corresponds to a reduced sensitivity to intensity change in binocular luster.

Fourthly, perception of binocular luster intensity seems to be unaffected by sidedness, as reflected by the insignificance of the effect of sidedness on perceptual threshold in the experimental data. This could suggest that the perception of inter-ocular brightness difference might be symmetric, and swapping brightnesses in the dominant and non-dominant views might have no significant effect on the
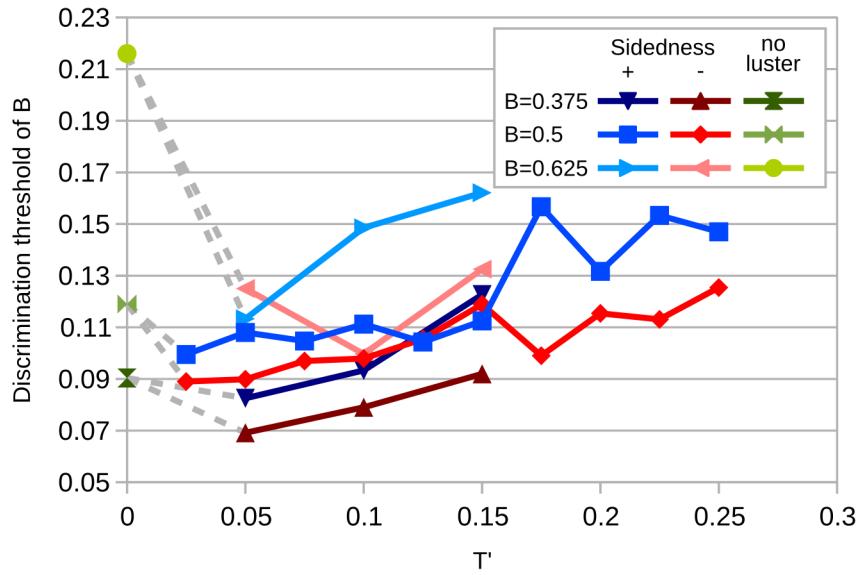
Figure 2.24: Discrimination threshold of B with respect to T' of standard stimuli.

perception. It can be further deduced that a pair of binocular luster stimuli with left- and right-eye views swapped might appear very similar to the observer.

2.3.3 Discrimination of Total Energy

The B dimension in the BT' binocular luster space represents the total energy in a binocular luster stimulus. The discrimination thresholds of total energy are measured for all standard stimuli shown in figure 2.18.

Figure 2.24 shows discrimination thresholds with respect to the intensity of binocular luster, for different total energy values (0.375, 0.5, 0.625) and sidedness (positive, negative).

It appears that discrimination threshold of total energy is positively correlated to the intensity of luster, but only for non-zero luster. Keeping total energy (i.e., B) the same, when no luster is presented (i.e., $T' = 0$), the discrimination threshold is much higher then when there is some luster presented (i.e., $T' \neq 0$).

Table 2.7: ANOVA table of discrimination threshold of B for non-zero luster. Left-most column shows the factors, where the form A:B indicates the interaction between A and B.

	Sum Sq	Df	F value	Pr($>$F)	
B	0.0048997	1	41.7067	1.117E-6	***
T'	0.0056106	1	47.7581	3.800E-7	***
side	0.0028706	1	24.4351	4.801E-5	***
B:T'	0.0000054	1	0.0463	0.8314	
B:side	0.0000059	1	0.0501	0.8248	
T':side	0.0004589	1	3.9065	0.0597	.
B:T':side	0.0000720	1	0.6129	0.4414	
Residuals	0.0028195	24			

Signif. codes: 0 '***' 0.001 '**' 0.01 '*' 0.05 '.' 0.1 ' ' 1

Due to this observation, the data is partitioned into two parts, based on whether there is luster presented, and is analyzed separately.

Discrimination with Non-Zero Luster

As shown in figure 2.24, it seems that the thresholds of total energy are affected by intensity of binocular luster and sidedness, but not total energy of the standard stimuli. These observations are tested with a multi-factor ANOVA test, whose result is shown in table 2.7.

The table shows significance for the effect of luster intensity and sidedness, and rejects the effect of total energy and any interactions.

The effect of luster intensity is further tested for linearity. Table 2.8 shows the results of Pearson's correlation tests for three B values (0.375, 0.5, 0.625) and two sides:

The Pearson's tests report quite strong correlations, although not all correlations are significant, due to limited sample size.

To further investigate the significant effect of total energy, the correlation is tested with Pearson's correlation tests, and the results are summarized in table 2.9:

Table 2.8: Pearson correlation test for discrimination threshold of B and non-zero T' value.

B	sidedness	t-value	df	p-value	correlation coefficient
0.375	+	3.745	1	0.1661	0.9661493
	−	13.0055	1	0.04885	0.997057
0.5	+	4.5331	8	0.001916	0.8484004
	−	5.1151	8	0.0009126	0.8751225
0.625	+	3.9021	1	0.1597	0.9686959
	−	0.2234	1	0.8603	0.2176954

Table 2.9: Pearson correlation test for discrimination threshold of B and B value.

T'	sidedness	t-value	df	p-value	correlation coefficient
0.05	+	2.6362	1	0.2308	0.9349903
	−	6.7258	1	0.09397	0.9891268
0.10	+	4.9291	1	0.1274	0.9800348
	−	2.0846	1	0.2847	0.9016295
0.15	+	1.1417	1	0.4579	0.7522535
	−	5.2427	1	0.12	0.9822908

The above results verify that there is a correlation between total energy of standard stimuli and the discrimination threshold of total energy.

The size of the effect of sidedness is calculated as the mean of the pairwise differences between symmetric conditions. It is found to be 0.01443256, where the threshold for positive side is slightly larger, suggesting that sensitivity to total energy change is slightly reduced if the brighter light is presented to the dominant eye. This might be explained based on prior experience on monocular brightness discrimination. By Weber's Law, monocular brightness discrimination threshold increases with the increase in brightness of the standard stimuli, resulting in a reduced sensitivity. This might be what happens in the dominant eye for discriminating total energy when a stimuli with positive binocular luster is presented. By definition of ocular dominance, an observer is more reliant on the dominant eye, which could also be the case in such a task. Thus, for two stimuli with a same luster intensity, but opposite sides, the dominant eye is presented with higher brightness for the positive luster stimulus than in the negative luster stimulus, and the measured threshold might reflect the difference in monocular
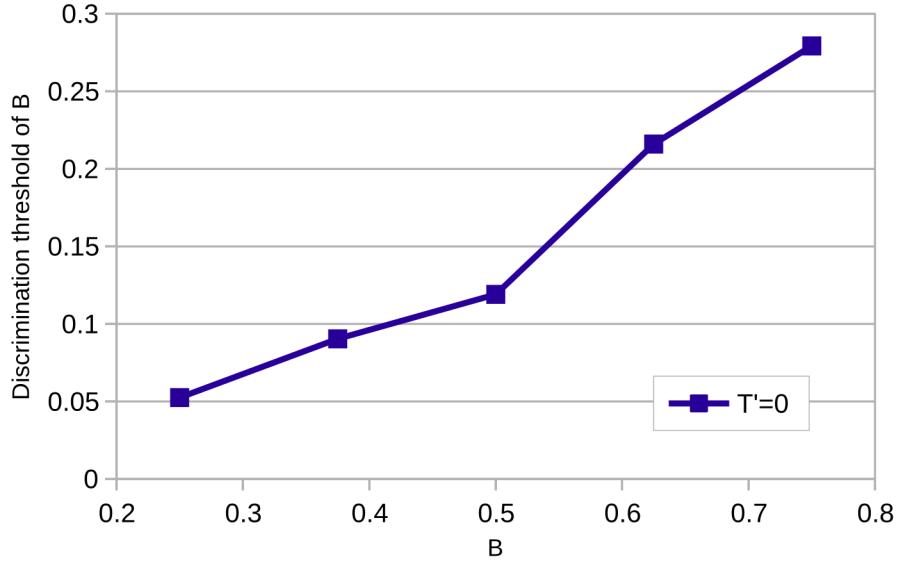
Figure 2.25: Discrimination threshold of B with respect to B value of the standard stimuli with zero luster.

brightness discrimination sensitivity in the dominant eye.

Discrimination without Luster

Discrimination threshold of total energy without luster in the standard stimuli is essentially brightness discrimination, which has been studied in previous psychophysics research. Alternatively, brightness perception could be viewed as a special case in the higher-dimensional binocular luster space. These thresholds are measured along the line $T' = 0$, as shown in figure 2.18.

Figure 2.25 shows the discrimination threshold of total energy with respect to total energy of the standard stimuli, with no luster effect (i.e., $T' = 0$).

The discrimination threshold seems to be linear with respect to total energy of the standard stimuli. A Pearson's correlation test reports a p-value of 0.00393, with a t value of 8.1022 and a df of 3. The correlation coefficient is 0.9779048. This confirms the observed linear effect.

Table 2.10: Changes in p-value and correlation coefficient after inclusion of discrimination thresholds of B without luster.

B	sidedness	change in p-value	change in correlation coefficient
0.375	+	0.0426	-0.1748674
	−	0.7748	-0.8206484
0.5	+	0.004571	-0.0870631
	−	0.0796274	-0.3265176
0.625	+	0.4577	-1.3513124
	−	-0.566	-0.9233473

Additionally, to show that discrimination without luster is indeed different from other discrimination thresholds, Table 2.10 shows the changes in significance and correlation coefficient after inclusion of discrimination thresholds without luster in the Pearson's tests for the correlation between threshold value and binocular intensity (table 2.8).

Clearly, our decision of separate analyses is supported, since not doing so would reduce the significance of the effect (i.e., increased chance of the null hypotheses that T' does not have an effect), and also reduce the strength of the correlation (i.e., decreased correlation coefficients from the original positive correlation coefficients).

Summary

As a summary, discrimination of total energy for binocular luster demonstrates the following characteristics.

Firstly, as intensity of luster increases, the sensitivity to total energy change decreases, which is described by the significant effect of T'.

Secondly, total energy of the standard stimuli does not significantly affect the sensitivity.

Thirdly, sidedness has a significant effect, where sensitivity is slightly higher for

a standard stimuli where the non-dominant eye is presented with the brighter light.

Fourthly, in the absence of luster, which reduces to conventional condition of brightness discrimination, the sensitivity is reduced.

2.4 Empirical Modeling

Results in the previous section statistically describe the qualitative characteristics of binocular luster and its relationship with monocular brightness perception without luster. This section describes the procedure to fit an empirical model to the results. The usage of the model is explained, which includes predicting the perceptual thresholds for a certain condition, and building a numeric perceptual scale that relates the physical parameters of binocular luster to the strength of the experience of the observer.

2.4.1 Mathematical Formulation

To formulate a quantitative model of binocular luster perception, the first agenda is to define the dependent variables of the model, in other words, the entities described and/or predicted by the model.

Perception of binocular luster could be viewed as a new modality completely independent of the perception of monocular brightness without luster. However, the experiment is not devised to prove the complete independence of this modality. In addition, the presentation space of binocular luster stimuli is inclusive of monocular brightness stimuli. With the above considerations, instead of making an aggressive assumption of the complete independence of the perceptual

modality of binocular luster, it is more reasonable to assume that the perception of binocular luster and monocular brightness are somewhat related. In turn, this leads to our view of a single scalar to represent the perceptual response of binocular luster and monocular brightness. We denote this scalar response as P.

The previous section has shown that B, T', and sidedness are all important factors contributing to the perception of binocular luster. Of these three factors, B and T' take continuous values, and sidedness is a nominal factor with only two possible discrete values. To capture this, we model P as a piecewise function of B and T', with each piece modeling P for a certain sidedness. Mathematically, this formulation is expressed as:

$$P_+ = f(B, T') \tag{2.16}$$

$$P_- = g(B, T') \tag{2.17}$$

where P_+ and P_- are pieces of the model for positive and negative sidedness respectively.

In psychophysics studies, JND is often used as the unit of perceptual response on an interval scale [98]. On an interval scale, distances between points can be compared. For example, if a pair of stimuli, A and B, are separated by 1 JND, and another pair, M and N, are also separated by 1 JND, then the perceptual difference between A and B is considered to be the same as that between M and N: an observer would have the same difficulty in distinguishing between A and B, as to distinguish between M and N, although the differences of physical strengths between A and B and between M and N could be different, due to Weber's Law. We follow this convention and use JND as the unit of the value of the P scalar.
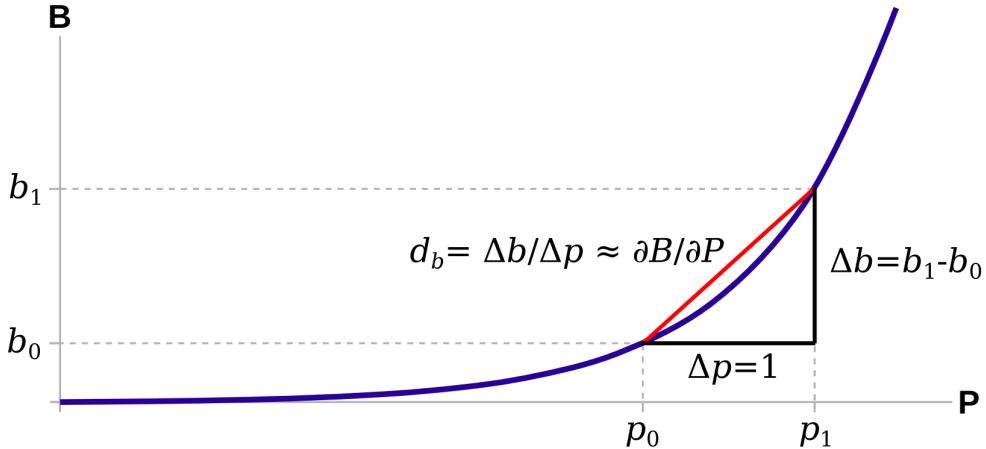
Figure 2.26: Relationship between B and P values. Measured threshold is the change in B corresponding to a unitary change in P (i.e., 1 JND).

In this perspective, the measured thresholds are changes in physical stimuli that instigate unitary changes in perceptual responses, i.e., 1 JND. Figure 2.26 illustrates this relationship between the changes in physical stimuli strength and the changes in perceptual response, using threshold along B dimension as an example. Given a standard stimulus with B value of b_0, assume its unknown P value is p_0. The threshold search procedure finds a threshold d_B, so that another stimulus with B value of $b_1 = b_0 + d_B$ is just-noticeably different from the point of b_0. Assuming that this stimulus has the unknown P value of p_1, by definition of JND, we have $p_1 - p_0 = 1$. Then the measured threshold, d_B can be expressed as

$$d_B = \frac{b_1 - b_0}{p_1 - p_0}. \tag{2.18}$$

Note that in our investigation, there is no need to differentiate between detection and discrimination threshold. This is because the previous section has shown that the detection threshold of binocular luster intensity (i.e., along T' dimension) does not significantly deviate from the difference threshold. Therefore, treating detection and discrimination thresholds separately will not increase the goodness

of fit, or its predictive power, but only to complicate the model. However, it is still advisable to respect the previous shown result that conventionally studied brightness discrimination without luster effect is a special case in the binocular luster space, and should be treated separately.

Analogous to the derivation of Fechner's Law based on Weber's Law [77], this relationship can be transformed into integral form as

$$D_B = \frac{\partial B}{\partial P} \tag{2.19}$$

Note the use of capital D instead of lowercase d for the threshold, to indicate the transformation from measured threshold to theoretical threshold. Also note the partial derivative sign above, since P is a function of both B and T'. Similarly, the theoretical thresholds along T' dimension could be viewed as

$$D_{T'} = \frac{\partial T'}{\partial P} \tag{2.20}$$

The problem for empirical model fitting, therefore, is:

Problem 2.1. *Given the measured thresholds as samples of inverse of partial derivatives, $\partial B/\partial P$ and $\partial T'/\partial P$, recover an empirical model of P, as a function of B and T', for both sides of binocular luster.*

A two-step approach can be taken to fit the empirical model. First, fit a model that describes/predicts the thresholds along B and T' dimensions. This essentially recovers the first-order partial derivatives of P, with respect to its independent variables, B and T'. Next, the function of P about B and T' can be recovered by solving the partial differential equations. Note that, as discussed earlier, the model is fitted piecewise.

Previous section has shown that both B and T' are linear with the measured thresholds, so linear models can be used to fit the measured partial derivatives.

77

Table 2.11: Fitted model coefficients and mean square error of cross validation.

piece	side	Coefficient values				MSE
		intercept	B	T'	$B \cdot T'$	
$\frac{\partial T'}{\partial P}$	$+$	-0.007461	0.393547	-0.522975	0.414955	0.0007076894
	$-$	-0.01117	0.42301	-0.92248	1.19073	0.0003901167
$\frac{\partial B}{\partial P}$	$+$	0.02321	0.13245	0.08946	0.34802	0.0002202
	$-$	-0.02367	0.21725	0.45229	-0.61201	0.0001355
$\frac{\partial B}{\partial P}\big|_{T'=0}$	n/a	-0.08027	0.46338	n/a	n/a	0.0008862238

For sake of accuracy, the full model including interaction terms are used. The full model (i.e., including the interaction term between B and T') for positive sidedness is expressed as:

$$\frac{\partial T'}{\partial P} = \vec{\alpha} \cdot \begin{bmatrix} 1 & B & T' & B \cdot T' \end{bmatrix}^T \tag{2.21}$$

$$\frac{\partial B}{\partial P} = \vec{\beta} \cdot \begin{bmatrix} 1 & B & T' & B \cdot T' \end{bmatrix}^T \tag{2.22}$$

$$\frac{\partial B}{\partial P}\bigg|_{T'=0} = \vec{\theta} \cdot \begin{bmatrix} 1 & B \end{bmatrix}^T \tag{2.23}$$

where $\vec{\alpha}$, $\vec{\beta}$, and $\vec{\theta}$ are the coefficient vectors for the four terms, including the intercept. The last expression is the form of the conventional brightness discrimination, which is treated separately, as per the discussion in the previous section. The full model is defined similarly for negative sidedness.

2.4.2 Model Fitting

A linear regression for the above piecewise model is carried out. In addition, 10-fold cross validations are performed for each piece of the model. Table 2.11 summarizes the coefficients and mean square error (MSE) of cross validation, for each piece of the model.

The mean square errors from the 10-fold cross validations show that the fitted model is robust and quantitatively captures the empirical relationship between

78

B, T' values and the measured thresholds.

2.4.3 Derivation of Perceptual Scale

Given the fitted linear model and the view that the measured thresholds are the inverse of partial derivatives, we can try to recover a closed-form function of P with respect to B and T'.

For a piece in the model corresponding to thresholds along B dimension, for either sidedness, the measured threshold is in the following linear form

$$\frac{\partial B}{\partial P} = \beta_0 + \beta_1 B + \beta_2 T' + \beta_3 BT' \tag{2.24}$$

where β_n are the fitted coefficients for each of the terms in the linear model.

To solve this partial differential equation, first rearrange the terms to get:

$$\partial P = \frac{\partial B}{\beta_0 + \beta_1 B + \beta_2 T' + \beta_3 BT'} \tag{2.25}$$

Then, substitute the partial term ∂B as follows:

$$\partial P = \frac{\partial \ln(\beta_0 + \beta_1 B + \beta_2 T' + \beta_3 BT')}{\beta_1 + \beta_3 T'} \tag{2.26}$$

Treating T' as a constant, and integrating on both sides, we get:

$$P(B) = \frac{\ln(\beta_0 + \beta_1 B + \beta_2 T' + \beta_3 BT')}{\beta_1 + \beta_3 T'} + f(T') \tag{2.27}$$

where $f(T')$ is a function of T', which is free with respect of B.

Thus, we have derived the form of P as a function of B. Similarly, the form of P as a function of T' can be derived as:

$$P(T') = \frac{\ln(\alpha_0 + \alpha_1 B + \alpha_2 T' + \alpha_3 BT')}{\alpha_2 + \alpha_3 B} + g(B) \tag{2.28}$$

where $g(B)$ is a function of B, which is free with respect to T'.

To combine the above partial representations into a complete analytical form of P, P has to be smooth. Mathematically, this requires that

$$\frac{\partial^2 P}{\partial B \cdot \partial T'} = \frac{\partial^2 P}{\partial T' \cdot \partial B} \tag{2.29}$$

Substituting our fitted coefficients, the left-hand side becomes:

$$\frac{\partial^2 P}{\partial B \cdot \partial T'} = \frac{\partial}{\partial T'}\left(\frac{\partial P}{\partial B}\right) = -\frac{\beta_2 + \beta_3 B}{(\beta_0 + \beta_1 B + \beta_2 T' + \beta_3 B T')^2} \tag{2.30}$$

And the right-hand side becomes:

$$\frac{\partial^2 P}{\partial T' \cdot \partial B} = \frac{\partial}{\partial B}\left(\frac{\partial P}{\partial T'}\right) = -\frac{\alpha_1 + \alpha_3 T'}{(\alpha_0 + \alpha_1 B + \alpha_2 T' + \alpha_3 B T')^2} \tag{2.31}$$

Equating the two sides, we have:

$$-\frac{\beta_2 + \beta_3 B}{(\beta_0 + \beta_1 B + \beta_2 T' + \beta_3 B T')^2} = -\frac{\alpha_1 + \alpha_3 T'}{(\alpha_0 + \alpha_1 B + \alpha_2 T' + \alpha_3 B T')^2} \tag{2.32}$$

Collecting the terms having like powers of B and T' results in a long polynomial expression, whose coefficients are summarized in table 2.12.

The numeric values of the coefficients are calculated for each piece, shown in table 2.13:

Ideally, the above coefficient matrices should be zero, for an analytical solution of P to exist. From the above tables, the sum of squares are calculated, as a measure of how far the empirical model is from an analytical solution. The sum of squares is 0.0004792 for the positive side, and 0.8020 for the negative side. Although the positive side of the model seems to be closer to the ideal situation, conservatively, it cannot be assured that perception of binocular luster has an analytical form, as a function of B and T'.

Table 2.12: Coefficients of smoothness criterion of the empirical model.

power of B	power of T'	coefficient
3	3	0
	2	$-\alpha_3^2\beta_3$
	1	$-2\alpha_1\alpha_3\beta_3$
	0	$-\alpha_1^2\beta_3$
2	3	$\alpha_3\beta_3^2$
	2	$\alpha_1\beta_3^2 - 2\alpha_2\alpha_3\beta_3 - \alpha_3^2\beta_2 + 2\alpha_3\beta_1\beta_3$
	1	$-2\alpha_0\alpha_3\beta_3 - 2\alpha_1\alpha_2\beta_3 - 2\alpha_1\alpha_3\beta_2 + 2\alpha_1\beta_1\beta_3 + \alpha_3\beta_1^2$
	0	$-\alpha_1\left(2\alpha_0\beta_3 + \alpha_1\beta_2 - \beta_1^2\right)$
1	3	$2\alpha_3\beta_2\beta_3$
	2	$2\alpha_1\beta_2\beta_3 - \alpha_2^2\beta_3 - 2\alpha_2\alpha_3\beta_2 + 2\alpha_3\beta_0\beta_3 + 2\alpha_3\beta_1\beta_2$
	1	$-2\left(\alpha_0\alpha_2\beta_3 + \alpha_0\alpha_3\beta_2 + \alpha_1\alpha_2\beta_2 - \alpha_1\beta_0\beta_3 - \alpha_1\beta_1\beta_2 - \alpha_3\beta_0\beta_1\right)$
	0	$-\alpha_0^2\beta_3 - 2\alpha_0\alpha_1\beta_2 + 2\alpha_1\beta_0\beta_1$
0	3	$\alpha_3\beta_2^2$
	2	$\beta_2\left(\alpha_1\beta_2 - \alpha_2^2 + 2\alpha_3\beta_0\right)$
	1	$-2\alpha_0\alpha_2\beta_2 + 2\alpha_1\beta_0\beta_2 + \alpha_3\beta_0^2$
	0	$-\alpha_0^2\beta_2 + \alpha_1\beta_0^2$

Table 2.13: Coefficient values of smoothness criterion of the fitted empirical model.

	Positive side			
	T' power			
B power	3	2	1	0
3	0	-4.408E-6	4.535E-5	-0.0001167
2	-3.265E-7	-0.0004078	0.003937	-0.009417
1	-5.479E-5	-0.003107	0.01724	-0.0003150
0	-0.002298	0.006953	0.003745	0.0001966

	Negative side			
	T' power			
B power	3	2	1	0
3	0	0.2756	0.1119	0.01136
2	0.2277	-0.5929	-0.1432	-0.002718
1	-0.3654	0.3617	0.02981	-0.003348
0	0.1465	-0.05093	0.01511	-0.0004809

The next subsection describes an approach to still calculate P, based on the piecewise empirical model, and some approximation.

2.4.4 Calculation of Perceptual Difference

Perceptual difference is an important measure in psychophysics. Expressed in number of just-noticeable differences between two stimuli, the perceptual difference quantitatively describes how much they differ, in terms of psychological experience, rather than directly measurable physical quantities. The larger the perceptual difference between two stimuli, the more easily they can be distinguished. And two pairs of stimuli with a same perceptual difference have the same difficulty in distinguishing them.

Perceptual difference is usually calculated from the known values of physical parameters of two stimuli. In the ideal case where an analytical form exists for the perceptual response, this is as trivial as calculating the perceptual response of the stimuli, and taking the difference. As revealed by the previous subsection, the empirical model does not have an analytical form, so to calculate the perceptual difference between two arbitrary stimuli, some assumptions and approximations are needed.

First, we can assume that the partial models along each direction of B and T' are accurate. This allows the calculation of perceptual difference between two stimuli with same B or T' values. For two stimuli with different T' values of T'_0 and T'_1, but same B value of B_0, their perceptual difference is calculated as:

$$P(T'_1) - P(T'_0) = \frac{\ln\left(\frac{\alpha_0 + \alpha_1 B_0 + \alpha_2 T'_1 + \alpha_3 B_0 T'_1}{\alpha_0 + \alpha_1 B_0 + \alpha_2 T'_0 + \alpha_3 B_0 T'_0}\right)}{\alpha_2 + \alpha_3 B_0} \tag{2.33}$$

Similarly, for two stimuli with different B values of B_0 and B_1, but same T' value
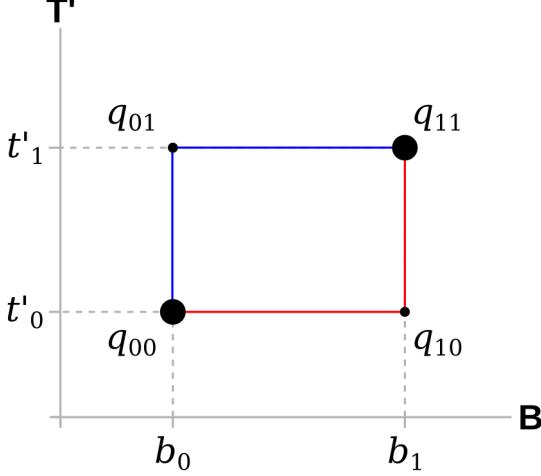
Figure 2.27: Two Manhattan paths connecting two arbitrary points in the BT' Space. From the point q_{00} to q_{11}, the red path passes through q_{10}, and the blue path passes through q_{01}.

of T_0', their perceptual difference is calculated as:

$$P(B_1) - P(B_0) = \frac{\ln\left(\frac{\beta_0 + \beta_1 B_1 + \beta_2 T_0' + \beta_3 B_1 T_0'}{\beta_0 + \beta_1 B_0 + \beta_2 T_0' + \beta_3 B_0 T_0'}\right)}{\beta_1 + \beta_3 T_0'} \tag{2.34}$$

Now that perceptual difference could be calculated between pairs of stimuli with same B or T' value, it could be calculated for pairs of arbitrary stimuli, by integrating from one stimulus to the other, through the Manhattan paths connecting them. Figure 2.27 illustrates this approach. For two stimuli as two points in BT' space, with $q_{00} = [B_0, T_0']$ and $q_{11} = [B_1, T_1']$, there are two possible shortest Manhattan paths between them, through two intermediate points, $q_{01} = [B_0, T_1']$ and $q_{10} = [B_1, T_0']$, respectively. The two Manhattan paths are $q_{00} \Rightarrow q_{01} \Rightarrow q_{11}$ and $q_{00} \Rightarrow q_{10} \Rightarrow q_{11}$.

In theory, the two paths should calculate same perceptual difference, by integrating along each sub-path using the corresponding partial model. However, in practice, this could be different for the two possible paths, due to the numerical imprecision of the model. In addition, due to the logarithmic terms in the partial models' analytical forms, the perceptual value P is not defined for all

possible B and T' values, and the calculated result, if such 'out-of-bound' points are involved, might be complex numbers. To alleviate these two limitations, the perceptual difference along each path is calculated, and if differences calculated from both paths are complex, we refrain from calculating a meaningful difference. If only one path is complex, we use the perceptual difference calculated from the other path. If neither is complex, and that difference between the two perceptual differences is smaller than 1 JND, than the average perceptual difference of the two is used.

The perceptual difference is used to numerically represent psychological experience of binocular luster on a perceptual scale, by assigning an arbitrary stimulus in BT' space with a perceptual value of zero, and expressing all other stimuli by their perceptual difference from that reference stimulus. The resulting perceptual scale is an interval scale [98], and not a ratio scale. This means that only the degrees of difference can be inferred by comparing value on the perceptual scale. For example, for two stimuli, A and B, with values of 2 and 4 on the perceptual scale, it can only be inferred that B is more different from the reference stimulus than A (i.e., $4 - 2 = 2$), but not twice more different (i.e., $4/2 = 2$), which is only possible with a ratio scale. Compared to an arbitrary selection of the zero point on an interval scale, a ratio scale has a unique meaningful stimulus of zero value, such as the absence of mass in weight perception, so that judgments like 'twice as heavy' are valid.

The most suitable zero point for a ratio scale in binocular luster space would be the point of complete darkness in both eyes. However, this condition is not easily measured, since our display device, being a backlit LCD display, is not able to present such a condition.
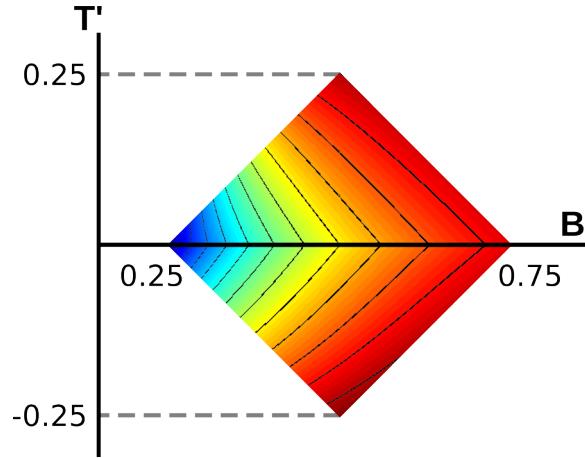
Figure 2.28: Color map of the perceptual difference and the contour of equal perceptual difference for stimuli in BT' space. Color indicates perceptual difference from the point $[0.5, 0]$ in BT' space, and stimuli on a same black contour line have same perceptual difference from the point $[0.5, 0]$.

Although a zero point is arbitrary and unnecessary in some cases, such as calculating perceptual difference between two stimuli, we conventionally use the point of $[0.5, 0]$ in the BT' space as the zero point on the perceptual scale, since it is located at the center of the points we have measured.

Figure 2.28 shows a color map of the perceptual difference from various stimuli in the BT' space to the zero point of $[0.5, 0]$, as well as contour lines of equal perceptual difference. It clearly shows that the perceptual scale is different from the value of the physical parameters of the stimuli.

We have thus far created a model that is able to assess perceptual differences between two stimuli in the BT' binocular luster space.

2.5 Creating Multi-View Images with Binocular Luster

Being shiny and dynamic [105, 104], a binocular luster stimulus is very different from what is seen in the left or right eye alone. This experience is mostly exclusive for the binocular viewing condition, since different brightness values need to be presented to separate eyes to instigate this experience. The notion that perceptual value of a binocular luster is different from perceptual values of its individual eyes' views is interesting, since it also implies that the perceptual differences between two binocular luster stimuli could be different from the perceptual differences between their respective single eye's views. It could then happen that the two binocular luster stimuli might appear more different than their differences in the left- or right-eye views, or vice versa.

Consider a binocular luster stimulus of $[x, y]$ in the BT' space. Its perceptual difference to the zero point $[0.5, 0]$ is calculated by the empirical model presented in the last section. If the observer views only with the dominant eye, the perceptual difference between the two stimuli is governed by the brightness presented to the dominant eye only. It can also be calculated with the empirical model, as the perceptual difference between $[x + y, 0]$ and $[0.5, 0]$. Similarly, the perceptual difference between the two stimuli in the non-dominant eye only is the perceptual difference between $[x - y, 0]$ and $[0.5, 0]$. Figure 2.28 in the previous section shows perceptual differences from each binocular luster stimulus to the point $[0.5, 0]$ in BT' space. Figure 2.29 shows perceptual differences from the dominant and non-dominant view of each stimulus to the corresponding views of the $[0.5, 0]$ stimulus. Figure 2.30 shows discrepancies between the three views in

86
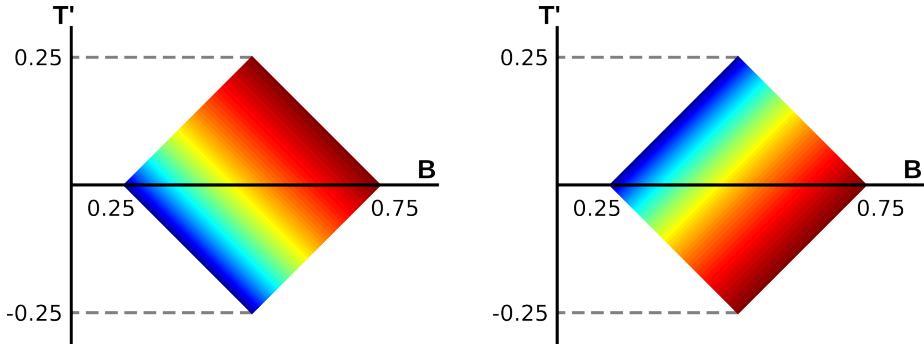
Figure 2.29: Perceptual difference in individual eyes to the $[0.5, 0]$ stimulus in BT' Space. Left: perceptual difference in the dominant eye. Right: perceptual difference in the non-dominant eye.
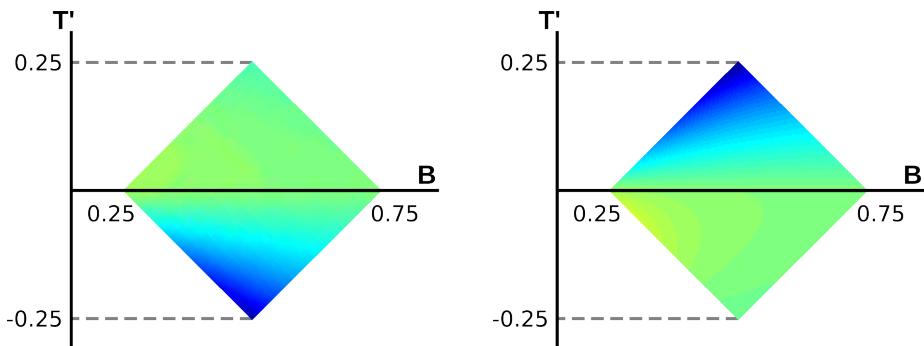
Figure 2.30: Discrepancy between perceptual difference in individual eyes and binocularly. Left: for discrepancy between dominant view and binocular view. Right: for discrepancy between non-dominant view and binocular view.

perceptual difference, for each stimulus to the $[0.5, 0]$ stimulus.

Clearly, there exist some stimuli whose perceptual similarity to the point of $[0.5, 0]$ is very different in the binocular view from the single-eye view, suggesting the large discrepancies for those stimuli. It is therefore possible to create visual artifacts with different appearances depending on whether they are viewed binocularly or monocularly. We refer to these artifacts as 'multi-view images', and explain our approach to create them.

2.5.1 Viewing Conditions

There are three to four viewing conditions of a binocularly presented image: binocularly, monocularly with the dominant eye, monocularly with the non-dominant eye, and, depending on the display technology, the average of the two monocular views. This last viewing condition is only applicable to technologies such as active shutter and polarized light. For these technologies, the left and right views are displayed on the same physical space, and special glasses are required to demultiplex the signals into left and right views to be delivered to each eye. Without the glasses as demultiplexers, the left and right signals would usually be available to both eyes, resulting in perceiving the average of the two views.

We refer to these four viewing conditions as 'binocular view', 'dominant view', 'non-dominant view', and 'merged view'.

2.5.2 Problem Statement

This subsection provides a mathematical formulation of the problem of multi-view image, by defining mathematical forms for several entities, followed by the definition of the problem.

As our investigation is on luster only, the scope of the problem is gray-scale images without any color. A monocular gray-scale image is essentially a function that maps a pixel's 2D positional vector $\begin{bmatrix} x & y \end{bmatrix}^T$ to the scalar brightness value of that pixel:

$$M_{\mathrm{mono}}(x, y) : \mathbb{R} \times \mathbb{R} \mapsto \mathbb{R} \tag{2.35}$$

For raster images, a more convenient notation is in matrix form: $M_{h \times w}$, where

h and w are the height and width of the image, and the element m_{ij} is the brightness value of the pixel at location $[i, j]$ of the image.

A binocular gray-scale image allows for different brightness in each eye. It differs from a monocular gray-scale image in that the brightness value is a 2D vector, instead of a scalar. Function of binocular image:

$$M_{\text{bino}} : \mathbb{R}^+ \times \mathbb{R}^+ \mapsto \mathbb{R} \times \mathbb{R} \tag{2.36}$$

In matrix form: $M_{\text{bino},h \times w}$, where the element $m_{ij,1}$ and $m_{ij,2}$ correspond to the pixel values at $[i, j]$, presented to the dominant and non-dominant eye respectively. Note that monocular gray-scale images are special cases of binocular gray-scale image, for which the brightness values in the dominant and non-dominant eyes are always the same.

A similarity measure encapsulates the process to assess visual similarity between the two binocular gray-scale images. Given two such images, the similarity measure is a function, E, that outputs a scalar value negatively associated with the similarity between the two images. The smaller the similarity measure between the two images, the more similar they are.

The problem of creating multi-view image thus becomes:

Problem 2.2. *Given four target gray-scale images, M_{bino}, M_{d}, M_{nd}, and M_{merged}, corresponding to the four views defined earlier, find a binocular gray-scale image, $L = [L_{\text{d}}; L_{\text{nd}}]$ so that its four views,*

1. *$L_{\text{bino}} = [L_{\text{d}}; L_{\text{nd}}]$ for binocular view,*

2. *$L_{\text{d}} = [L_{\text{d}}; L_{\text{d}}]$ for dominant view,*

3. *$L_{\text{nd}} = [L_{\text{nd}}; L_{\text{nd}}]$ for non-dominant view, and*

4. $L_{\text{merged}} = [(L_{\text{d}} + L_{\text{nd}})/2; (L_{\text{d}} + L_{\text{nd}})/2]$ *for merged view*

each minimizes its similarity measure with the corresponding target views.

In mathematical terms the problem is to calculate L_{d} and L_{nd} in the following equation:

$$
\begin{aligned}
[L_{\text{d}}; L_{\text{nd}}] = \arg\min E([L_{\text{d}}; L_{\text{nd}}], [M_{\text{bino}}; M_{\text{bino}}]) + \\
E([L_{\text{d}}; L_{\text{d}}], [M_{\text{d}}; M_{\text{d}}]) + \\
E([L_{\text{nd}}; L_{\text{nd}}], [M_{\text{nd}}; M_{\text{nd}}]) + \\
E([(L_{\text{d}} + L_{\text{nd}})/2; (L_{\text{d}} + L_{\text{nd}})/2], [M_{\text{merged}}; M_{\text{merged}}])
\end{aligned}
\tag{2.37}
$$

The subsequent sections introduce a generic solution to this problem, then discuss few specific approaches to specialized problems in practice.

2.5.3 Generic Approach

The general approach to the multi-view images problem is quite straight forward. First we need to explicitly define the similarity measure, then we use already established numerical methods to solve this as an optimization problem.

To define similarity measure, we are aware that two images could be perceptually similar, even if their overall brightness is very different, as long as their edge maps remain similar. To implement this view into the similarity measure, we adapt the conventional edge detection routine so that it also copes with binocular luster. Edge detection is conventionally achieved by convolving a filter, also known as a kernel, with the image. Among several popular choices, we use the Sobel kernels

to detect horizontal and vertical edges:

$$K_x = \begin{bmatrix} -1 & 0 & 1 \\ -2 & 0 & 2 \\ -1 & 0 & 1 \end{bmatrix} \quad K_y = \begin{bmatrix} -1 & -2 & -1 \\ 0 & 0 & 0 \\ 1 & 2 & 1 \end{bmatrix} \tag{2.38}$$

Instead of working on values of the physical parameters of the image, we first need to map the image onto perceptual space, so that the result of edge detection reflects the edge perceived by the observer, instead of the edge physically presented by the device. We use the empirical model from the previous section, which is essentially a function, J, that maps a binocular luster stimulus to a scalar perceptual value:

$$J(B, T') : \mathbb{R} \times \mathbb{R} \mapsto \mathbb{R} \tag{2.39}$$

For a binocular image L, which is a candidate for the desired multi-view image, each of its pixel could be represented as a point in BT' space:

$$L : l_{ij} = [B_{ij}, T'_{ij}] \tag{2.40}$$

Its four perceived images, P_{bino}, P_{d}, P_{nd}, and P_{merged}, could be calculated as:

$$
\begin{aligned}
P_{\text{bino}} &: p_{\text{bino},ij} = J(B_{ij}, T'_{ij}) \\
P_{\text{d}} &: p_{\text{d},ij} = J(B_{ij} + T'_{ij}, 0) \\
P_{\text{nd}} &: p_{\text{nd},ij} = J(B_{ij} - T'_{ij}, 0) \\
P_{\text{merged}} &: p_{\text{merged},ij} = J(B_{ij}, 0)
\end{aligned}
\tag{2.41}
$$

Similarly, we can calculate the perceived images for the four target views, Q_{bino}, Q_{d}, Q_{nd}, and Q_{merged}.

Next, the perceived images are filtered with the Sobel kernels, and a pair of perceptual edge maps along the x and y directions of the image are generated

91

for each of the viewing conditions of the candidate, as well as the target views. Denote perceptual edge maps of the candidate as G, and those of the target views as H:

$$G_{\text{bino}} : [P_{\text{bino}} \circledast K_x; P_{\text{bino}} \circledast K_y]$$

$$G_{\text{d}} : [P_{\text{d}} \circledast K_x; P_{\text{d}} \circledast K_y]$$

$$G_{\text{nd}} : [P_{\text{nd}} \circledast K_x; P_{\text{nd}} \circledast K_y]$$

$$G_{\text{merged}} : [P_{\text{merged}} \circledast K_x; P_{\text{merged}} \circledast K_y]$$

$$H_{\text{bino}} : [Q_{\text{bino}} \circledast K_x; Q_{\text{bino}} \circledast K_y]$$ \hfill (2.42)

$$H_{\text{d}} : [Q_{\text{d}} \circledast K_x; Q_{\text{d}} \circledast K_y]$$

$$H_{\text{nd}} : [Q_{\text{nd}} \circledast K_x; Q_{\text{nd}} \circledast K_y]$$

$$H_{\text{merged}} : [Q_{\text{merged}} \circledast K_x; Q_{\text{merged}} \circledast K_y]$$

where the symbol $\circledast$ denotes the convolution operation.

Then the perceptual edge maps for each viewing condition of the candidate image need to be compared with the corresponding target views' perceptual edge maps. To account for both the magnitude and orientation of the edge, we treat an edge as a vector with x and y components from each orientation of Sobel filter results, and compute the vector difference between the candidate and the target perceptual edge maps for the corresponding pixels:

$$D_{\text{bino}} : d_{\text{bino},ij} = [\ g_{\text{bino},ij,x} - h_{\text{bino},ij,x}\ ,\ g_{\text{bino},ij,y} - h_{\text{bino},ij,y}\ ]$$

$$D_{\text{d}} : d_{\text{d},ij} = [\ g_{\text{d},ij,x} - h_{\text{d},ij,x}\ ,\ g_{\text{d},ij,y} - h_{\text{d},ij,y}\ ]$$

$$D_{\text{nd}} : d_{\text{nd},ij} = [\ g_{\text{nd},ij,x} - h_{\text{nd},ij,x}\ ,\ g_{\text{nd},ij,y} - h_{\text{nd},ij,y}\ ]$$

$$D_{\text{merged}} : d_{\text{merged},ij} = [\ g_{\text{merged},ij,x} - h_{\text{merged},ij,x}\ ,\ g_{\text{merged},ij,y} - h_{\text{merged},ij,y}\ ]$$

\hfill (2.43)

Then, we compute the sum of squares of the magnitude of all pixels in D as the

final similarity measure, for that specific view:

$$E_{\mathrm{bino}} = \sum_{i=1}^{h} \sum_{i=1}^{w} (d_{\mathrm{bino},ij})^2$$

$$E_{\mathrm{d}} = \sum_{i=1}^{h} \sum_{i=1}^{w} (d_{\mathrm{d},ij})^2$$

$$E_{\mathrm{nd}} = \sum_{i=1}^{h} \sum_{i=1}^{w} (d_{\mathrm{nd},ij})^2 \qquad (2.44)$$

$$E_{\mathrm{merged}} = \sum_{i=1}^{h} \sum_{i=1}^{w} (d_{\mathrm{merged},ij})^2$$

And the final similarity measure is the weighted sum of the similarity measure in each view:

$$E = w_{\mathrm{bino}}E_{\mathrm{bino}} + w_{\mathrm{n}}E_{\mathrm{n}} + w_{\mathrm{nd}}E_{\mathrm{nd}} + w_{\mathrm{merged}}E_{\mathrm{merged}} \qquad (2.45)$$

where w_{bino}, w_{d}, w_{nd}, and w_{merged} are the weights.

The above process shows how the total similarity measure is a function of the candidate binocular image. The problem therefore is transformed into an optimization problem, i.e., to find a candidate image that minimizes the total similarity measure. The total similarity measure is non-negative, because we take the square of the vector difference between the candidate and target perceptual edges. There exist established methods to solve such optimization problems. One commonly used method is the Nelder-Mead optimization method [65]. Being a so-called 'derivative-free' optimization method, it does not need to evaluate the gradient of the target function, as often needed in other methods such as gradient descent.

Although this generic approach is theoretically correct, it is not computationally tractable. The Nelder-Mead method creates $N + 1$ points in N dimensions, and evaluates at least one more such point as input to the target function during each iteration, where N is the number of independent variables in the argument for

maximization. In our case, the argument for maximization are two images, and N would be two times the number of pixels in a target view.

2.5.4 Specific Solutions

It is seen from the previous subsection that the generic approach is not computationally practical. In this subsection, we propose two specializations of the problem of multi-view images, which are practically usable and computationally affordable.

Naive Dual-View Image for Binocular and Merged Views

The first specialized problem is how to present different perceptions in the binocular view and the merged view.

For a binocular pixel with $[b, t']$ value in the BT' space, the merged view would appear as a monocular point with brightness of b, the dominant view would appear as $b + t'$, and the non-dominant view would appear as $b - t'$. It is noticed that the merged view is not affected by the intensity of luster at all. Therefore, an easy way to provide separate perceptions in the merged view and one of the remaining three views, is to use B in the BT' space to encode the information for the merged view, and use T' to encode information for the other target view.

Mathematically, the solution to this specialized problem is as follows. For the target view of M_{bino}, and M_{merged}, calculate the dominant and non-dominant images of the multi-view image as follows:

$$L_{\mathrm{d}} = (1 - w) \cdot M_{\mathrm{merged}} + w/2 + w \cdot M_{\mathrm{bino}}/2$$
$$L_{\mathrm{nd}} = (1 - w) \cdot M_{\mathrm{merged}} + w/2 - w \cdot M_{\mathrm{bino}}/2$$

(2.46)

where w is a weighting factor controlling the intensity of the binocular view relative to the maximum intensity presentable by the display device. We assume that the brightness values used to represent the images have the range of $[0, 1]$.

Note that although the merged view is completely free from interference of the other view encoded in the T' value, the other target view might suffer from slight interference, due to the fact that the perception is not completely independent of the information encoded in B. However, this problem can be mitigated with the knowledge from figure 2.24 and figure 2.21, that with increasing luster intensity, the sensitivity to total energy change reduces, while the sensitivity in luster change increases, so that the information encoded in B would become less noticeable than T', for binocular viewing.

Figure 2.31 shows an example of a multi-view binocular image created in this way. It uses a w value of 0.8. Also note that figure 2.31 performs the same treatment on the U and V channels of the image in YUV color space, to provide additional color information. However, the colors and brightness are inverted in the dominant and non-dominant eyes, resulting in only one of the eyes being able to perceive the intended information. The perceptual edges in the dominant and non-dominant views are of the same strength, but of opposite orientation, thus violating our previous definition of perceptual edge map difference. However, we still feel that this is an easy-to-understand approach to create dual-view images, and might be potentially useful in applications where we need to add a simple luster effect in the binocular view to facilitate graphic annotation, while keeping the merged view unaltered. This technique also needs no calibration, and is device independent, as long as the left- and right-eye views are equal, in terms of the presentation duration, for active shutter based stereo, or the brightness,

Figure 2.31: Naive dual-view image. Dominant (left) and non-dominant (center) views, when viewed binocularly, would instigate much stronger sensation of the baboon image than the image in the merged view (right). The luster effect is completely absent from the merged view, with degradation in contrast, controlled by the weighting factor w.

for polarized or color filter based stereo.

Palette Search for Binary Target Images

The second specialized problem is to create multi-view images where the target views are binary images, instead of continuous-value gray-scale images.

To address this problem, we designed an algorithm to search for a palette of binocular stimuli that tries to satisfy the perceptual constraints between them, required by the target views.

Determining participating views The input is up to four binary images as target views. The binary levels in every target view is denoted as 1 and 0, and a binary number up to four digits is used to label each pixel in the corresponding views. From the most significant to least significant bits, the digits corresponds to the level in binocular view, dominant view, non-dominant view, and merged view. Clearly, there are at most $2^4 = 16$ possible labels for all the pixels in the target views. And the objective of the algorithm we developed is to find an assignment of binocular luster stimuli in BT' space to the labels, which we call

a 'palette'.

A valid palette must satisfy certain perceptual constraints. For example, consider two labels, 1101 and 0110, each representing a binocular luster stimulus. In binocular view, i.e., for the first bit from the left, 1101 must be sufficiently different from 0110, and must have a larger perceptual value, since its corresponding bit is 1, whereas the other label's corresponding bit is 0. For the second bit from the left, i.e., in dominant view, since the two labels have a same bit, they must be sufficiently similar, to appear as representing the same level in that view. We can express all constraints between each pair of all the 16 labels, and any valid palette must satisfy these constraints to produce the target multi-view image.

An 'edge criterion' controls the tolerance of constraint checking. It defines two entities:

1. **Maximum Similarity**

   The maximum perceptual difference between two stimuli that can be considered the same.

2. **Minimum Difference**

   The minimum perceptual difference between two stimuli that can be considered different.

We recommend the edge criteria of $[1, 2]$, considering that perceptual difference of 1 means a just-noticeable difference, which is not reliably acknowledged by the observer. When the perceptual difference increases to 2, the probability of indiscrimination is $0.5 \times 0.5 = 0.25$, and the probability of discrimination becomes 0.75, which we consider an acceptable minimum difference for an observer to reliably distinguish between the stimuli.

97

Determining perceptual discrepancy profile Given a palette, the total number of constraints to check is $\binom{16}{2} \times 4 = 480$, and each constraint is checked with a calculation of the perceptual difference in the respective view, between the pair of stimuli being checked. If any of the constraints is not satisfied, then the palette is not valid.

While checking a palette could be computationally trivial, enumerating all possible palette is not possible, since there are infinite possible palettes in the continuous binocular luster space.

We present a method to first limit the possible palettes to a finite set, and then greatly reduce the number of palettes to be enumerated and checked, by removing those stimuli that are not possible in any valid palette.

To limit the number of choices of stimuli to a finite number, we discretize the continuous binocular luster space with a certain resolution. For example, a B resolution of 10 in the range of $[0, 1]$ means that only 10 discrete B values equally spaced in the range would be considered as candidates of the palette. Next, we create four matrices of pairwise perceptual difference in the four target views. For example, if 10 discrete B values and 10 discrete T' values are used, then there are a total of 100 stimuli in the BT' space to be considered as the potential palette members. The size of a pairwise perceptual difference matrix would be 100 by 100, where the row and column indices are the 100 stimuli. There are a total of 10000 elements in each of the four matrices. The value of each element is the perceptual difference from the stimulus represented by the column index to the stimulus represented by the row index. Each of these matrices, denoted by W, have the property that $-W = W^T$, so the actual number of calculations of perceptual distance is $(10000 - 100)/2 = 4950$. Figure 2.32 shows the four
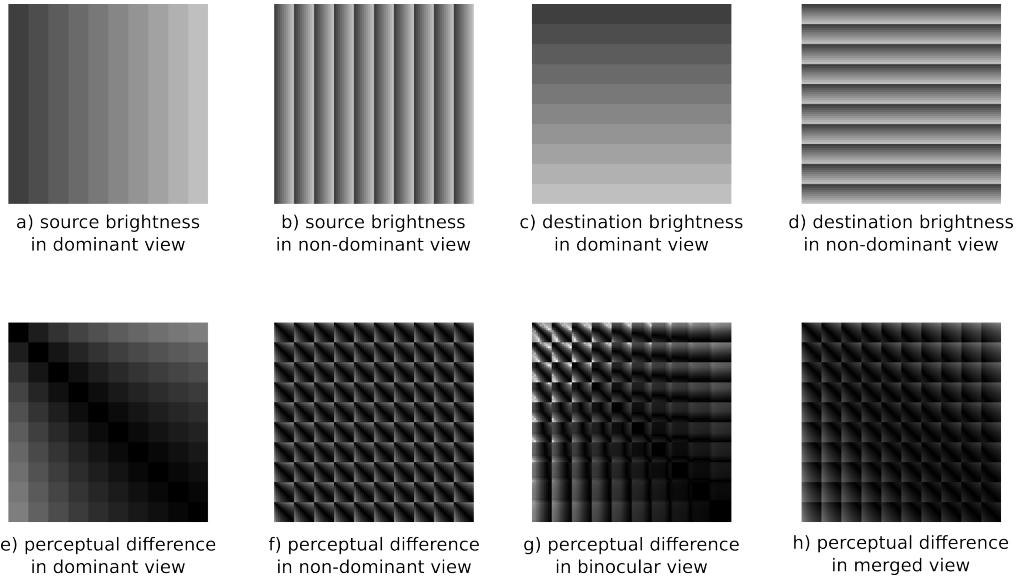
Figure 2.32: Pairwise perceptual difference matrices. a) to d): source and destination binocular colors. e) to h): perceptual differences from source to destination binocular colors in each view.

perceptual difference matrices in this example.

Finding and labeling palette candidates   To permute a maximum of 16 stimuli from 10000 to form a palette and check for constraints is still intractable, there are 9.881e63 possible palettes to check. To further reduce the number of enumerations, we introduce the concept of 'solitary edge', and use it to express a simple lemma that helps narrow down the search space of valid palette members.

A solitary edge is a pair of stimuli that are different only in one view, and same in all the other views, according to an edge criterion. A solitary edge corresponds to a location in the pairwise perceptual difference matrices, and only one element in one of the four pairwise perceptual difference matrices is larger than the minimum difference, while the remaining three are smaller than the maximum similarity, according to the edge criterion.

To find possible palette members, we further observe that a solitary edge can have two possibilities, from 1 to 0 or 0 to 1, in its view, which is determined by

the value of the element in the respective pairwise perceptual difference matrix. We call a solitary edge from 0 to 1 as a *rising edge*, and 1 to 0 as a *falling edge*.

We show the following lemma of solitary edge:

Lemma 2.2. *For any member stimulus in a valid palette satisfying all constraints, there must exist four solitary edges in different views, on the row and column representing that stimulus, and the label of a potential palette candidate is determined by the directions of the solitary edges on its corresponding row in the pairwise perceptual difference matrices.*

Figure 2.33 explains this lemma, using 3 views as an example. For a valid palette shown in the figure, for any of its member stimuli, consider its three-digit label for dominant, non-dominant, and binocular views, respectively from left to right, there must exist another label that differs only by one digit. And the stimulus assigned to that label forms a solitary edge with this stimulus. The labels are determined by the directions of its solitary edges. For example, the label 101 is determined by its falling edge in the dominant view, rising edge in the non-dominant view, and falling edge in the binocular view. Based on this, we find all possible candidates for each label in the palette.

Based on this lemma, we can first find solitary edges in each view's pairwise perceptual difference matrix, and then try to find stimuli satisfying this lemma, and finally enumerate possible palettes from these stimuli.

Verifying constraints between palette candidates Next, we enumerate all possible palettes using these candidates for each label, and check for other constraints. For example, in figure 2.33, the label 101 and 110 have to satisfy additional constraints that their dominant views should be similar, non-dominant
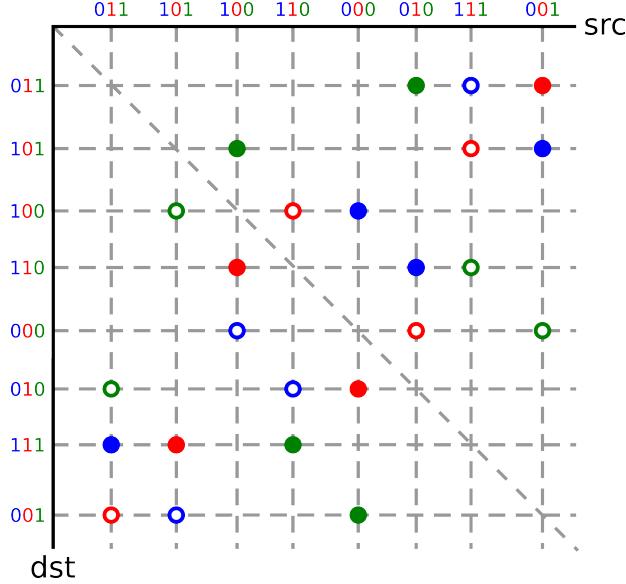
Figure 2.33: Finding and labeling palette candidates. A valid palette for three views is shown, with corresponding solitary edges in each view, blue for dominant view, red for non-dominant view, and green for binocular view. Rising edges are marked with solid filled circles, and falling edges are marked with unfilled circles.

views from 101 to 110 should be a rising edge, and binocular views should be a falling edge.

By the above process, we are able to greatly reduce the number of palettes to enumerate. This is mainly because solitary edges are sparse, as shown in figure 2.34.

There could be more than one valid palette satisfying all constraints. To select

solitary edges
in non-dominant view

solitary edges
in binocular view
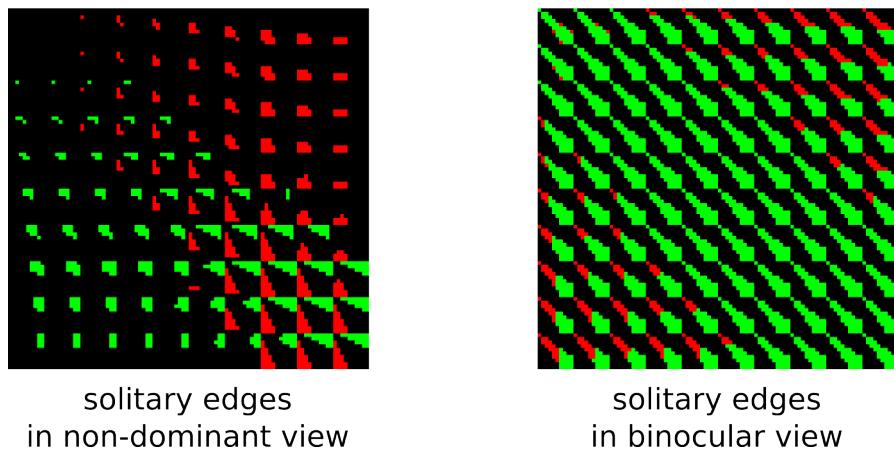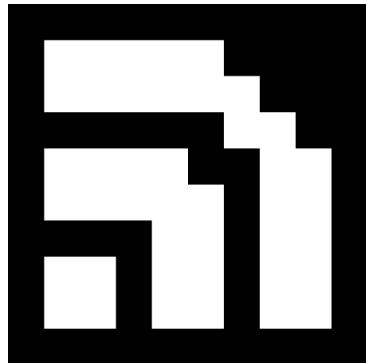
Figure 2.34: Solitary edges for two views. Red points show rising solitary edges, green points show falling solitary edges.

the best palette, we have to define the quality of a palette. A palette is of good quality if the rising and falling edges are clearly distinguishable. We use the minimum of the strength of the rising and falling edges for all pairs of candidates in the palette as the measure of its quality. This ensures the lower bound of the perceptual difference for edges in the palette. And to select the best palette out of all valid palettes, we select the palette whose minimum edge strength is the largest among all.
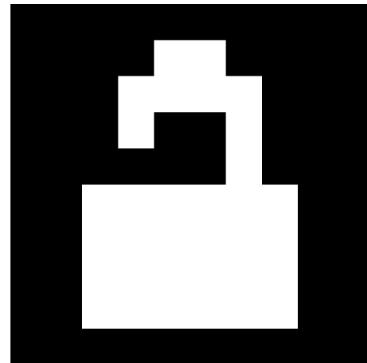
As as a final step, the selected palette, which consists of assignments of binocular luster stimuli to labels, is used to paint the pixels in the corresponding target views. The image for the dominant and non-dominant eye are thus determined.

Figure 2.35 shows a dual-view binary image created with the above method. It is noticed that when two pixels are placed close to each other, the visual boundary in the monocular views would interfere with the perception of binocular luster stimuli. To mitigate this, we also separate the pixels with black spacings.
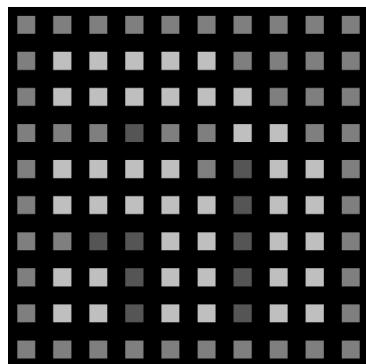
Although the method described above supports creation of multi-view image with up to four views, it is found that specifically for the Oculus Rift device, for which we have fitted an empirical model, only two views are supported, since with three or more views, there are no valid palettes available in the modeled perceptual space of binocular luster. However, since this method could designate two target views to any two of the four views, and other devices could be calibrated through the experimentation and modeling process described in the previous two sections, there could still be some application scenarios that can benefit from this technology. The next subsection analyzes the design space for dual-view applications.
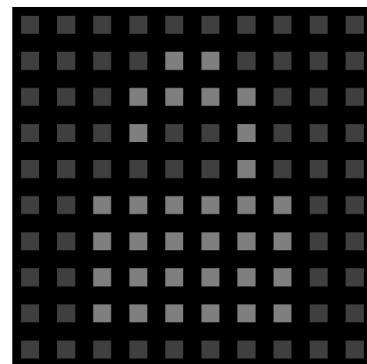
Target binocular view

Target non-dominant view

A wifi icon
shown in
dominant view

A lock icon
shown in
non-dominant view

Output binocular image
in dominant view
without spacing

Output binocular image
in non-dominant view
without spacing

Figure 2.35: Dual-view binary image. The intended perception is a wifi icon in binocular view, and a lock icon in non-dominant view, shown in the top row. The output binary binocular image is shown in the middle row, with black spacing between them to prevent the interference by the edges in monocular views, shown in the bottom row.

2.5.5 Design Space for Dual-View Applications

We begin this subsection by defining several factors that help formulate requirement of potential dual-view applications. Then, we identify some key technological aspects that help match application requirement with appropriate stereoscopic display solution. Lastly, we introduce several potential interesting dual-view applications, and analyze their requirement and technological choices for implementation. Mock-up screen shots of the proposed potential applications are created to help conceptualize the usage scenarios.

Requirement of Dual-View Applications

An activity could be analyzed with several factors that uncovers opportunities to apply dual-view images in such scenarios.

Number of roles The first factor is the number of roles participating in the activity for which the application is designed. A role in an activity is a party functioning towards an indivisible objective. An activity can involve multiple roles, each with its own objectives requiring different tasks, which are carried out usually in parallel or interleaved with other roles' tasks.

For example, in a professional training scenario, there are usually two roles, instructor and trainee. The objective of instructors is to transfer skills and knowledge to the trainees, through the explanation of instructional materials and demonstration. The objective of trainees is to acquire the skill and knowledge, usually through comprehension, active note-taking, and repeated exercises. The two roles conduct their activities concurrently during the training session.

Number of users in each role   The second factor is the number of users taking each role. There could be as few as one user in a certain role, or even a same user involved in multiple roles, depending on the current phase of the activity.

For example, there are two roles in a quiz activity, the tester and the test taker. The objective of a tester is to articulate the question, without revealing the correct answer, to the test taker. And the objective of a test taker is to attempt at that question. The format of the quiz could be a formal examination, where the testers would usually be the teaching staffs of the class, and test takers the students. This is the case where the roles are taken by different groups of people. Alternatively, in an informal paired quiz during a class, the tester and the test taker are usually neighboring students, and their roles can exchange as they take turns to ask and answer questions. Moreover, if a student is doing self-testing, the two roles are taken by a same person.

Switchability   The third factor is whether the users in each role are allowed to switch between views. For the quiz scenario, the role of the test taker is constrained with only one view showing the question, and the tester role is allowed to switch between the question view and the answer view.

View persistence   The fourth factor is whether each view needs to be persistent, i.e., requiring minimal or no extra effort to remain in that view.

In some usage scenarios, such as a quick glance for the time, or for the power status of the laptop computer's battery, the access of information is very quick and easy. Therefore, no persistence is required for that view, and it can be

designated to the dominant or non-dominant view, to be accessed by closing one eye temporarily.

Information resolution   The fifth factor is information resolution, which concerns how much information needs to be presented in each view.

In the quiz scenario, the information could be as simple as text for a multiple-choice question in the test taker view, and highlighting of the correct option in the tester view. In the professional training/simulation scenario, the information in the instructor view might be as complex as an anatomical diagram with presenter notes and markings scattered around, whereas the student view might be simply the diagram itself.

Interactivity   The sixth factor is interactivity in each view, referring to how much interaction is allowed in that view.

For example, in an informal quiz scenario, no interaction is required for each question, since after the test taker provides an answer, it can be checked for correctness without changing the visual presentation in each view. Contrary to this, in an interactive visualization application incorporating binocular luster effect, users need to be able to manipulate the visualizations, such as selecting and dragging data points in an interactive scatter plot.

Visual/semantic correspondence   The last factor is correspondence, i.e., whether object locations in one view are independent of the other view.

In the quiz scenario, the test taker view shows only the question, and the tester view shows the answer next to the question. The object locations in the two

views are dependent upon each other, and are thus considered to be 'aligned', in terms of correspondence. In some rare scenarios, as will be introduced later in this subsection, the two views do not have much correspondence. Consider an advertisement showing a product image in the binocular view, and the QR code for its coupon to be scanned through the phone in the merged view, these two objects in each view are independent, and thus require no correspondence.

Technological Aspects

Knowledge about the characteristics and constraints of various stereoscopic display technologies is essential in choosing the most appropriate of them for the target application scenario. This subsection describes these aspects of several popular stereoscopic display technologies.

We consider the following technologies:

- Head-mounted displays (HMD) such as Oculus Rift and Vuzix VR920 devices

- Active shutter technologies such as NVidia 3D Vision

- Polarized display systems such as RealD cinema, and HP 2311gt 3D display

- Color filtering technologies, such as Dolby 3D

- Autostereoscopic displays such as EyeFly 3D lenticular sheets for mobile devices

Image presentation technology The first factor concerns the properties of the image presentation technology.

Most HMDs use ordinary screen (e.g., Oculus Rift) or projection and prism systems (e.g., Vuzix VR920), which are the same as mainstream display and projection technologies. Active shuttering based technologies require display or projection with high refresh rate, usually 120Hz. Polarized display technologies require screens or projectors with additional components for polarization. In addition, polarized projection requires special metallic screen to preserve polarization after the projected light is reflected by the screen. Polarized projection is often used in 3D cinemas (i.e., RealD). Color filter based technologies such as Dolby 3D requires projection of two images with different tricolor primaries, using specific color filters. Autostereoscopic displays usually have special optical films such as a lenticular sheet attached to the surface of the screen.

The displayed size and the easiness of system setup are the main considerations for this factor. For example, while both are able to display on a large area, polarized 3D projection requires special screens, whereas active shuttering 3D projection can virtually project onto any surface and object, making it more suitable for projected augmented reality, on which dual-view applications could be based.

Demultiplexing mechanism The second factor is the demultiplexing mechanism, which concerns how a separate view is delivered to each eye.

For HMDs, the two views are naturally separated. For active shuttering based technologies, the two views are so-called 'time-multiplexed', showing each view in an interleaved fashion, and active shutter glasses synchronize with the signal, so that the respective glass panel in front of each eye would unblock and show the screen only for the respective frames. For polarized technologies, a passive

polarization glass is used to allow only the signal with the respective polarization orientation. For color filter based technologies, a passive color filter glass is used, with each eye's filter allowing a different set of tricolor primary wavelengths. For autostereoscopic technologies, the two eyes' views are projected to different spatial directions, so that no glasses are needed.

The demultiplexing mechanism determines whether the four views are technically achievable, for example, HMDs, using separate display area for each eye, do not support a merged view. And neither do autostereoscopic technologies, since the two views are not mixed during presentation.

View switch method   The third factor is the view switch method, which concerns with how a user switches between the supported views of each technology.

For HMDs, no merged view is supported, and the remaining three views are switched by closing one eye. For active shuttering, besides closing one eye, the merged and binocular view can be switched by putting on and taking off the glasses. Specifically for NVidia 3D Vision technology, the power button on its glasses can temporarily disable the shuttering, thus enabling switching to the merged view by holding down the power button. For polarized and color filtering technologies, the merged view and binocular view can only be switched by putting on and taking off the glasses. For autostereoscopic technologies, merged view is not supported, so switching between binocular and monocular views can only be done by closing one eye.

Scalability   The last factor is scalability, concerning the cost of increasing number of users.

For HMDs, the cost with every additional user is large, since a whole display system is needed, let alone the computation resource and infrastructure required. For active shuttering, additional users need additional shutter glasses, which cost less than full HMD sets but still involve cost of electronic components and batteries. For polarized and color filtering technologies, the increasing number of users merely requires an increasing number of cheap passive glasses. For autostereoscopic technologies, no additional monetary cost is required for additional users, but since the ideal viewing range of the image is limited in space, this cost of decreased viewing space becomes a constraining factor of the scale of the application.

The scalability factor needs to be considered especially for applications with a potentially large number of users, such as in the professional training scenario.

Potential Applications

This subsection showcases several concepts of potential applications for the dual-view technology, through textual description and mock-up images of the application.

Quiz The first application is the quiz application mentioned several times earlier. There are two roles, the tester and the test taker in this application. The tester view is assigned to the binocular view, and test taker view to the merged view. Both views show an image with the question, whereas tester view shows the answer in addition.

The quizzing activity can be conducted in the classroom mode, or the self-test mode. In the classroom mode, the questioning and answering could happen
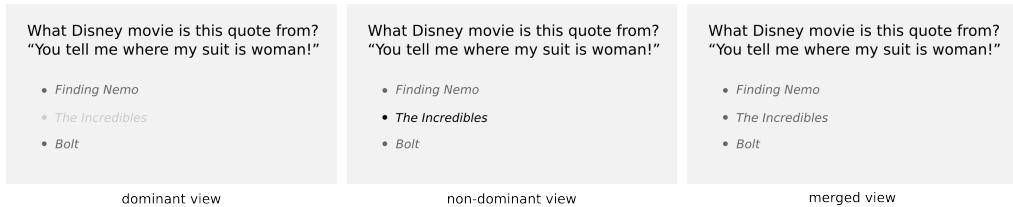
Figure 2.36: Quiz with two views. Left: dominant view. Center: non-dominant view. Right: merged view that hides the answer with binocular luster.

between two groups of users, either teacher and student, or pairs of neighboring students taking turns for each role. In this mode, to facilitate large number of participants, large-screen stereo projection systems with cheap passive glasses are preferable, such as polarized or color filter based systems.

In self-test mode, the user first sees the question in merged view, and switches to binocular view to check the answer. To satisfy this requirement, NVidia 3D Vision technology is preferable, since it provides convenient switching between the two views, and this mode usually does not need to scale to large group of participants.

Figure 2.36 illustrates this application, showing the question in the merged view, and the dominant and non-dominant views that reveal the answer with binocular luster.

Radiology   Oftentimes, doctors need to interpret X-ray images in relation with the corresponding body parts of the patient. This can be a tedious process, involving cross comparing two images, one in X-ray, the other in normal light, back and forth, to find the correspondence between the two. The X-ray image lacks sufficient details of the contour of the patients outer body, whereas the normal image does not show where the internal structures are, such as bone and joints.

dominant view   non-dominant view   merged view
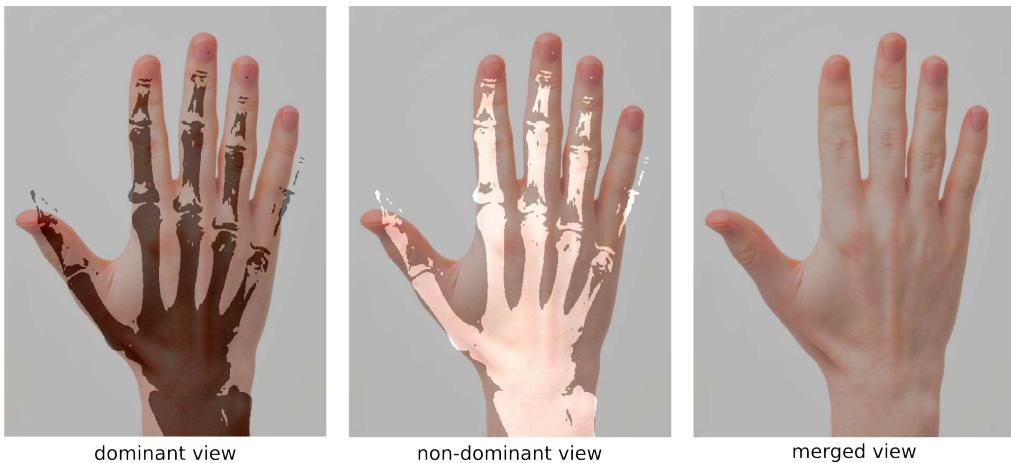
Figure 2.37: Overlaying an X-ray image with a normal image.

To help with this situation, the two images could be overlaid, with the normal image using the merged view, and the X-ray image using the binocular view with luster. The doctors might benefit from the convenience of quickly switching between the two images that are spatially collocated.

Figure 2.37 shows an example of such a dual-view image that overlays the X-ray image of a hand on its normal image.

Since the illustrated scenario of finding correspondence between the X-ray and the normal images are usually performed by a single doctor, active shuttering technologies are appropriate, especially when coupled with the NVidia 3D Vision glasses to allow for quick switching.

Advertising   Advertisers are doing everything to catch people's attention, and binocular luster is a new visual effect to play with.

Figure 2.38 shows a mock up ads against smoking.

Due to the mass adoption of 3D glasses and the situations where commercials are played prior to the start of the movies, the 3D cinema is an appropriate venue

112

| dominant view | non-dominant view | merged view |
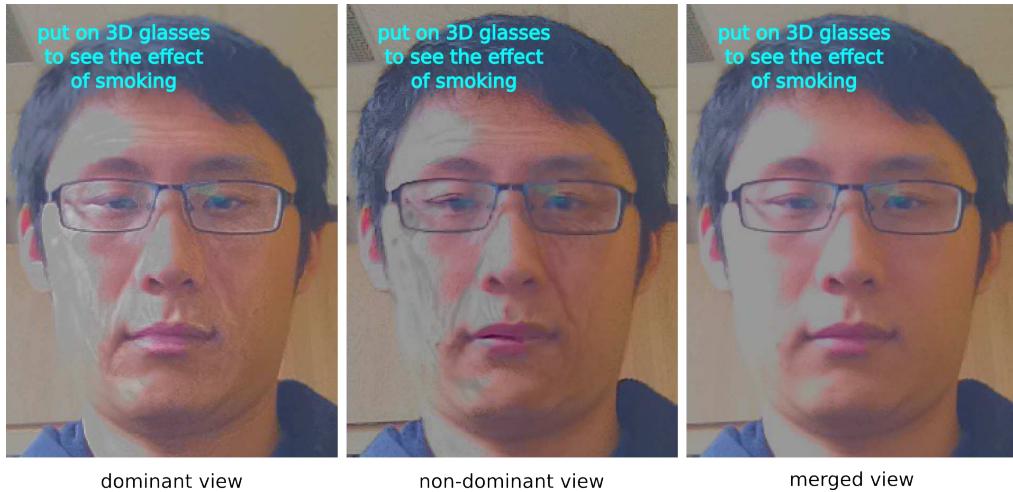
Figure 2.38: Mock-up anti-smoking advertisement. The monocular view encourages people to put on 3D glasses to see the effect of smoking, which is revealed in binocular view.

for this application.

Binocular Icons   Figure 2.35 shows an interesting application using binary dual-view images. By showing the Wi-Fi icon in the binocular view, when the user is normally using the computer, the user is able to access the information such as the status of the connectivity. Temporarily closing the dominant eye, the user is able to quickly and temporarily access further details of the connection, such as whether it is securely encrypted.

This application mainly involves one role of computer user, and there is usually a single user in that role. Therefore, personal stereoscopic display devices such as the range of HMDs can be used. As the output image is low in resolution, the most appropriate place could be the notification icons such as those in the task bar of the desktop.

2.6 Conclusion

In conclusion, this chapter presents a psychophysics study that explores perceptual characteristics of binocular luster, in terms of the detection and discrimination thresholds. The data is further used to fit an empirical model of binocular luster perception. The fitted model is piecewise and does not have a closed form. The empirical model is able to describe and predict the perceptual difference between pairs of binocular luster stimuli in the BT' binocular luster space. Leveraging on this model, a method to create multi-view images is presented. Practically, it is possible to present a binocular image that has two different appearances in two of its four possible viewing conditions. The design space of dual-view images in HCI are discussed, and several potential applications are demonstrated with mock-up concept images.

Chapter 3

ColorBless: Augmenting Visual Information for Color Blind People with Binocular Luster Effect

This chapter presents a study of an application of binocular luster in the field of digital color blind aids. Two prototype techniques are developed, ColorBless and PatternBless, to investigate the effectiveness of such aids and to exemplify the potential applications of luster effect. User studies and interviews revealed that luster-based aids were fast and required lower cognitive effort than the existing aids, and were preferred over other aids by the majority of the color blind participants. We infer design implications of the luster effect from the study and propose potential applications in augmented visualization.

3.1 Introduction

Color blindness, also known as color vision deficiency, is a medical condition that affects around 200 million people in the world [40]. It is characterized by an impaired ability to distinguish between certain colors in the visible light spectrum. There are three main types of color blindness: protan, deutan, and tritan, each corresponding to a defect in red, green, and blue cones in the human eye respectively (total color blindness is much less common compared to the three). The severity of the defect has two levels: dichromacy, in which the cone is absent or dysfunctional; and anomalous trichromacy, in which the cone's spectral sensitivity is altered but is still functional. Both protan and deutan are considered as red-green color blindness while tritan is blue-yellow color blindness. Among the people with a Northern European ancestry, there are approximately 8% of men and 0.5% of women who suffer from red-green color blindness [28].

Existing digital color blind aids help color blind people to distinguish colors by either substituting confusing colors with colors of higher contrast or applying visual patterns on top of confusing colors to augment visual information. While both are useful, each has its own set of limitations in actual usage [91]. The two techniques presented in this chapter overcome some of these limitations by employing binocular luster as a means of annotating confusing colors.

As illustrated in figure 3.1 [53], binocular luster effect is very salient and often associated with the perceived glossiness of metallic surfaces [104]. While it has been recently applied to produce highlights in 3D images [124], and enhance perceived image quality [122, 124], its perceptual strength as a function of color, contrast and difference in brightness has not been measured.

116
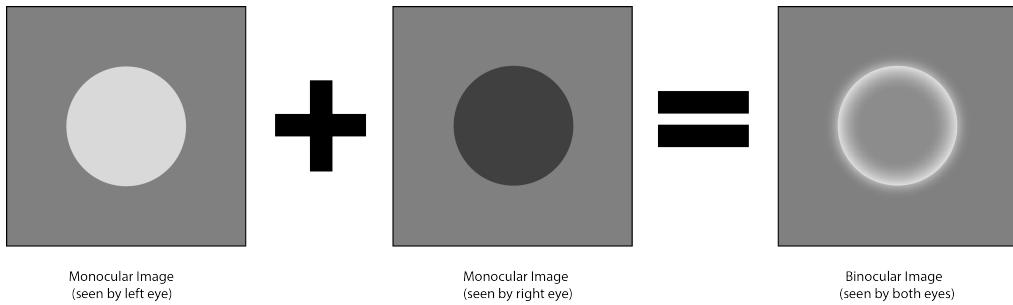
Figure 3.1: Visual illustration of the binocular luster effect.

Like hue and saturation, the luster effect can be used in visual encoding to represent information, especially for users who are unable to perceive other encoding variables. Based on this principle, wavelength-selective filter lenses such as the X-chrom lens have been used to create a brightness difference between the two eyes to help color blind people in distinguishing hues [96]. However, there is a lack of evidence to show that such lenses could distinguish colors in all situations, and it has also been shown to impair the user's depth perception [45].

The two prototypical color blind techniques described in this chapter apply binocular luster in two different ways to augment visual information for color blind people. A user study was conducted with 10 deutan color blind people to compare our approach with two other existing digital color blind aids. It is revealed that our approach is faster and requires less cognitive effort in decoding color information. The majority of the color blind users in the study also preferred our approach. Lastly, the observations from our study suggest large potential for using the binocular luster effect for unobtrusive information visualization overlays.

The contribution of this research is three-fold.

- First, a set of basic implementation guidelines are provided for applying

binocular luster with stereoscopic 3D by conducting basic psychophysical studies.

- Second, two prototypical luster-based color blind techniques, ColorBless and PatternBless, are designed and implemented. A user study is conducted to assess the usability and practicality of stereoscopic luster-based aids.

- Third, potential applications of binocular luster in HCI domain are proposed based on the implications from our study.

3.2 Background and Related Work

Apart from the knowledge of binocular luster introduced in chapter 1, we review existing color blind aids and summarize them in the following section.

In general, there are three strategies for color blind people to distinguish confusing colors. They are (i) contextual inferences, (ii) substituting colors, and (iii) augmenting visual information.

3.2.1 Contextual Inferences

Contextual inferences refer to the color blind people's strategy to discern colors by relying on the learnt or memorized association between the meaning and context of an object and its color. One notable example is the traffic light, whose position infers color information. However, many objects do not have a consistent and universal color in our daily life, and hence limiting the usefulness of this strategy.

3.2.2 Substituting Colors

Color blind aids in this category substitute colors in the content with other colors to enhance color contrast from the color blind users' point of view. This could be done in two ways: one from the content creator's end by using a color-blind-friendly color scheme, and another by changing the colors after the contents have been created. The former is known as pre-publication aid (a term to describe methods that modify the content while it is being created), and the latter is known as post-publication aid.

Pre-publication aids are not widely adopted for several reasons. Firstly, it limits the color palette a content creator can use in designing content. Secondly, it disrupts the semantic meaning of the colors with which as least 90% of the population is already familiar with (like red, yellow, and green in traffic lights). Here, we see an intrinsic three-way trade-off between the content creator's need to convey creative expressions or semantic meanings of colors, color blind people's need to decode color information, and finally normal people's need to capture color semantics accurately.

There is thus a need for post-publication aids where the color blind users can simply enable on their devices to enhance the color contrast by themselves. One physical technique is to wear filter lenses such as X-chrom lenses that change the wavelength of the lights received [96]. While filter lenses enhance color contrast, they alter the color perception of the entire scene (equivalent to wearing a tinted glasses), changing the perceived hue of initially unconfused colors in their color vision. In addition to that, their efficacy in distinguishing colors in different situations is largely unproven and it has been shown in a previous study to impair the depth perception of the color blind users [45].

In a digital setting, post-publication aids for color blind people focus on enhancing color contrasts in the image by replacing the original color with a different one. Most digital color blind techniques are primarily designed for dichromats, a more severe form of color blindness, due to the absence of a single type of color cone cell. However, these techniques are also usable by anomalous trichromats, a less severe form of color blindness that constitutes the majority of the color blind population, since it is a less restrictive form of defective color vision than dichromatic vision [79].

The recoloring techniques change the colors in a content-specific manner to resolve potential color confusion. A number of related work and solutions have been proposed in this category [1, 64, 75, 89, 109]. Daltonize, one of the earliest and most widely used in this category, works by increasing the red/green contrast, brightness, and blue/yellow coloration in the images [1]. Wakita and Shinamura proposed a recoloring technique that allows "author's intention" to be preserved in the documents by adjusting the mapping algorithm [109]. In comparison with the two previous works, Rasche et al. focused on the differences between the confusing color pairs rather than the similarity of the mapped colors to the original ones [89]. Kuhn et al. presented an automatic and efficient recoloring technique that preserves the naturalness of the colors [64]. Recently, Machado and Oliveira presented an automatic recoloring technique that preserves temporal coherence [75].

While a lot of work has been done on improving these recoloring techniques, they still share similar limitations. First, they are not very effective in resolving color ambiguities with images that contain many colors [91]. As a color is changed, the resulting color could potentially be confused with other existing colors in the

image. Second, recoloring techniques inadvertently affect the color perception of normal people since the underlying original colors are changed. Therefore, they are not very effective in scenarios where the colors convey semantic meaning and are presented for both normal and color blind people.

3.2.3 Augmenting Visual Information

Unlike substituting colors, these color blind aids append additional visual elements onto the image to augment visual information. These visual elements are usually in the form of shapes, positions, line types, and different patterns. In designing images like bar, pie, and line charts, these elements could be added to assist in interpreting data other than decoding colors. An example here is the ColorAdd® Color Identification System[1] that uses five simple symbols to represent different colors. These augmentative visual elements are added in a pre-publication manner. Unfortunately, pre-publication strategies are not widely implemented and standardized in the industry, and the color blind people recruited for our study still find it difficult at times to decode color information in images.

Recently, one approach has demonstrated the use of patterns to encode color information for color blind users in a post-publication manner [91]. This technique overlays patterns on the images in a content-independent fashion without recoloring the images. Applying patterns of lines with different slopes onto different colors, these colors can be identified (with learning) in addition to just being distinguished from each other. This patterning method minimizes ambiguities associated with the recoloring technique. However, recognizing patterns (with

---

[1]http://www.coloradd.net

different slopes) to distinguish and identify colors requires a higher cognitive effort, which makes decoding color information slower.

3.3　Designing Luster-based Digital Color Blind Aids

Motivated by the unique characteristics of binocular luster that could potentially overcome some of the limitations in existing color blind aids, two techniques are developed that apply luster effect with active shutter 3D to augment color information in images. The first technique, ColorBless, encodes color information by first determining the confusing colors in an image and applies different levels of luster effects to these colors. With ColorBless, color blind people use the luster effect applied on colors as a visual cue to distinguish confusing colors. Unlike physical luster-based aids like the X-chrom lens, ColorBless applies the luster effect to the confusing color regions only, not the entire scene. The second technique, PatternBless, applies the luster effect to stripe patterns of different slopes overlaid onto the colors as a way to augment visual information in the image. Figure 3.2 shows the two techniques with two other conventional techniques.
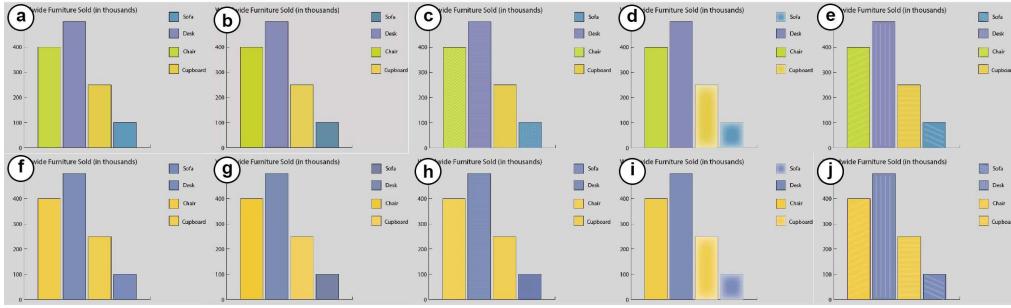
Figure 3.2: An overview of the effects of the four color blind aids. Bar graph images on top row represent the colors seen by the normal people while the bottom row is the colors seen by the color blind. (a) and (f) are the untouched images, (b) and (g) are the images recolored by the Daltonize technique [1], (c) and (h) are the images augmented with fine patterns (zooming in to see the patterns more clearly) [91], (d) and (i) are the images with luster effect (ColorBless), and (e) and (j) are the images with lustered patterns (PatternBless). Note that images with luster effect (d, e, i, j) are illustrations. Actual effects can be seen with 3D glasses.

For these two techniques to be usable and be better than some of the existing aids in an actual setting, the techniques need to fulfill three design requirements:

- First, the color distinguishing speed has to be fast.

- Second, it should minimize the underlying color change.

- Third, the luster effect should be perceivable at a comfortable level.

Based on the design requirements and our motivation stated in the beginning of this section, we propose the following research questions in this paper:

RQ1: What are the inter-ocular brightness difference levels (noted 'dY') required for the luster effect to be just noticeable and comfortable? What are the possible factors that could affect the two based on previous work in physical studies?

RQ2: Compared to the Daltonize recoloring technique [1] and pattern technique [91], is applying binocular luster an effective way to augment visual information while minimizing the underlying color change?

RQ3: What are the subjective evaluations of ColorBless and PatternBless com-

pared to the recoloring and pattern technique? Which color blind aids would the color blind users prefer in several common use cases?

User studies were conducted to evaluate ColorBless and PatternBless based on the three design requirements and research questions. The next section elaborates the implementation of both these techniques and how the color change is minimized at the algorithmic level.
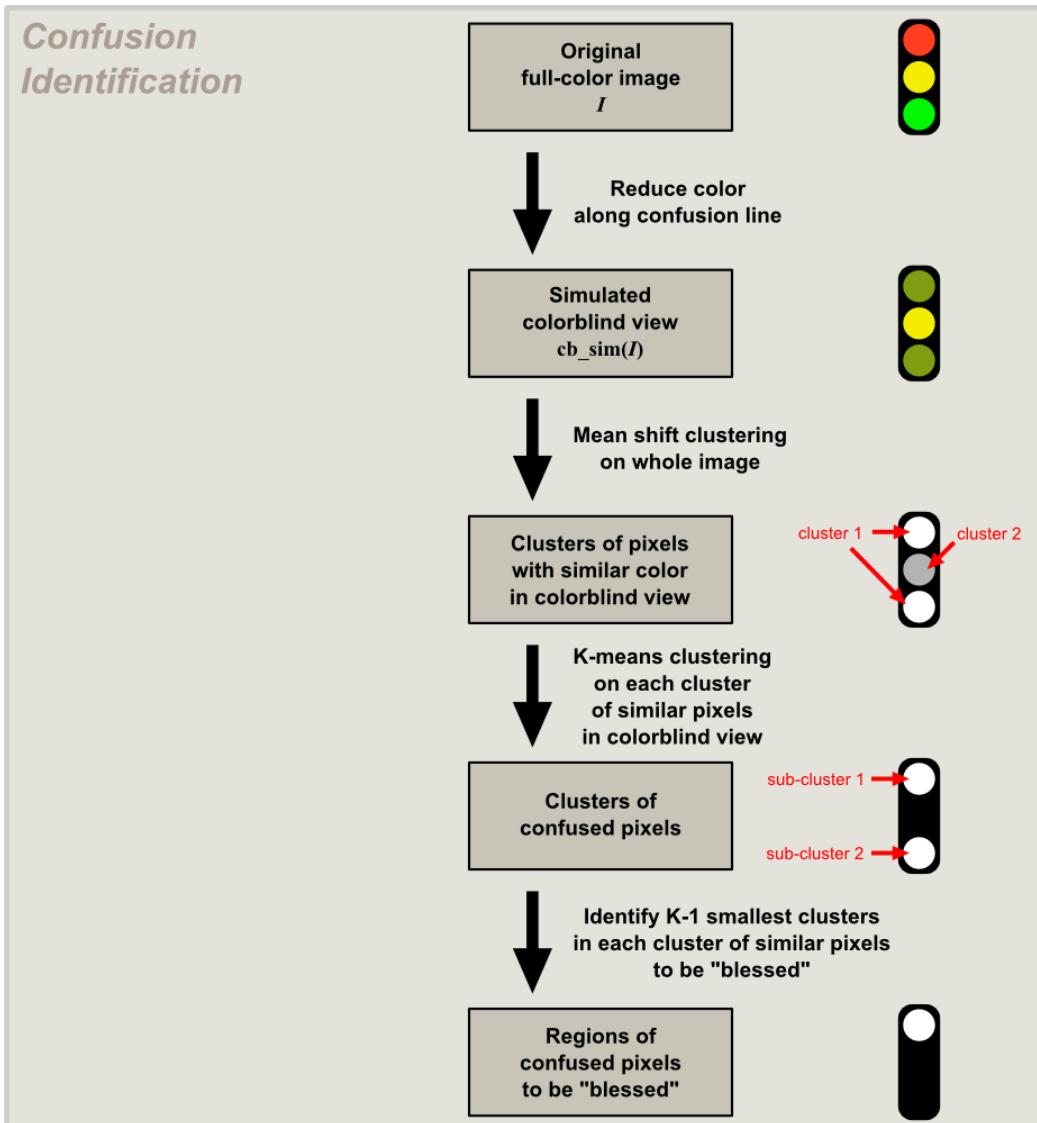
3.4 Implementation

The sections below describe how regions with confusing colors are identified, the different strategies for the ColorBless and PatternBless techniques, and how the luster effect is applied. A flowchart diagram of all the steps involved is shown in Figure 3.3.
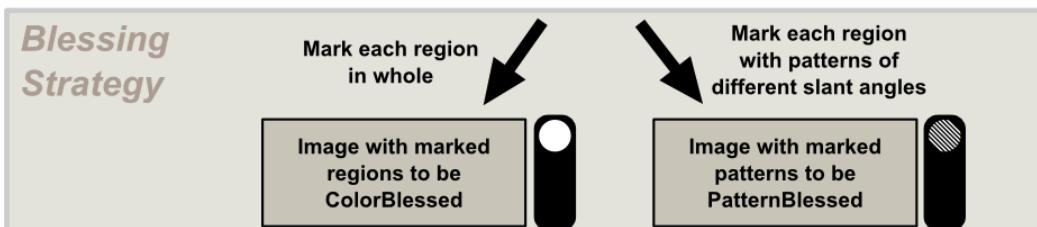
3.4.1 Identifying Clusters of Confusing Colors

The first step in the algorithm is to determine colors in an image I that are confusing to the color blind people. To do this, we apply the color blind simulation algorithm by Meyer and Greenberg to determine the pixel regions that get transformed into the same color in the simulated image [79]. This algorithm transforms image I to an image cb_sim(I) by reducing colors that lie along the dichromatic confusion line (the line parallel to the axis of the missing photoreceptor) to a single color. The colors along the confusion line, which is different for protan, deutan, and tritan, in the CIE1931 color space are indistinguishable for color blind people. This algorithm helps identify the confusing color regions of image I.
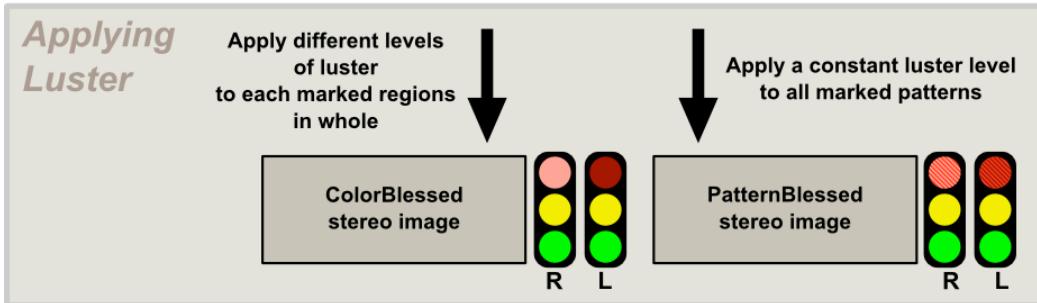
Figure 3.3: A flowchart summary of the implementation of the ColorBless and PattenBless techniques.

We then apply mean shift clustering to the simulated image cb_sim(I) [21], to classify pixels into clusters of similar color. We use a combination of pixel distance and the CIE color distance metric [118] to define the cluster distance and a default mean-shift 'bandwidth' parameter of 0.05. Larger bandwidth generates fewer and bigger spatial clusters of similar color and vice versa. While each cluster in the simulated image cb_sim(I) appears to be a single color for color blind observers, it contains pixels of different colors in the original image I. For example, red and green pixels in I may have been transformed into a single color cluster in cb_sim(I), and it is these colors that we now wish to distinguish in I using binocular luster. For the pixels within each cluster, k-means clustering is applied based on their colors in the original image I, so that each cluster of confusing colors is further separated into k discrete sets. For example, if we only wish to distinguish two primarily confused colors we set $k = 2$.

3.4.2 Blessing Strategies

There are two strategies with which luster can be applied to the confusing color regions ('blessed'), as introduced below.

ColorBless Technique

For the ColorBless technique, we distinguish the k sets by applying $k-1$ different levels of binocular luster to $k-1$ smallest sets, leaving the largest set of prevalent color in the image I unaltered (no luster). Our studies later show that up to 3 different levels of binocular luster can be perceived, i.e. a value of $k \leqslant 4$ can be used.

PatternBless Technique

PatternBless applies luster to stripe patterns of different slopes with the same luster level onto different confusing color regions in the image, to provide augmented color information. We compute the pixel regions corresponding to the k sets of color we would like to distinguish following the k-means algorithm. After applying k-means clustering, we then map the hue of each of the representative k colors to a line slant ϕ, which can qualitatively convey the hue in a region. Then, we use the size of the clustered region's bounding box to define the spacing, s, of line stripes. Finally, we apply luster to the pixels that would lie on horizontal lines s pixels apart after a rotation by an angle of $-\phi$.

3.4.3 Applying the Luster Effect

To apply the luster effect, we convert the RGB values of an image to YUV color space, whose Y component controls the luminance while U and V control the chrominance components. Then, two copies of this YUV image are created: one for the left eye, and the other for the right eye. The left image is tuned by decreasing the Y values for the target pixels to be 'blessed', and the right image is created by increasing the Y values for them. The color change created by the program is minimized by increasing and decreasing the Y value by the same amount, while keeping values of the U and V components unchanged. This process is mathematically described as:

$$\text{leftImage}_{ij} \leftarrow \text{YUVImage}_{ij}.Y - dY \tag{3.1}$$

$$\text{rightImage}_{ij} \leftarrow \text{YUVImage}_{ij}.Y + dY \tag{3.2}$$

where YUVImage represents the original image in YUV color space, dY represents the brightness differences created on the targeted pixels, leftImage represents the image for the left eye, and rightImage represents the image for the right eye. The two images are then combined to generate a 3D-image file viewable with a 3D setup.

3.5 Study Methodology and Design

A user study was performed to compare and evaluate ColorBless and PatternBless technique against other existing post-publication aids. We picked the Daltonize recoloring technique [1], which is a widely used substitution-based color blind aid, and pattern technique by Sajadi et al. [91], which augments color information with line patterns of different slopes, as a comparison against our approaches.

3.5.1 Participants

10 deutan color blind participants and 10 normal color vision participants (age range 21 to 30 years old) recruited from the host university volunteered for this study. All participants have normal or corrected-to-normal eye vision. Color blind screening test was done with the HRR Pseudoisochromatic Plates [80, 44, 12] with all participants before the studies to verify their color vision. The color blind participants were recruited for the sections S1, S2, and S4 of the experiment while the normal color vision people were recruited for the sections S1 and S3. Details on the different experimental sections are elaborated in the experimental design and protocol section.

3.5.2   Apparatus

In our user study, the 'blessed' image in 3D image file format was presented using the active shutter 3D-enabled Alienware M17x laptop equipped with NVIDIA 3D Vision (GPU: NVIDIA Geforce GTX 560M). External color calibration tool Spyder 4Pro was used to calibrate the M17x's display to ensure accurate color representations.

3.5.3   Experimental Design and Protocol

The user study was divided into four sections. The first section (S1) investigates the binocular luster effect with active shutter 3D, which answers RQ1. The second section (S2) investigates the color distinguishability of each color blind technique, which answers RQ2. The third section (S3) investigates the color differences produced by the color blind techniques, which answers RQ2. Finally, the fourth section (S4) answers RQ3 by acquiring color blind participants' subjective evaluation of the techniques.

Section 1 (S1): Investigating luster in active shutter 3D

The goal in S1 was to determine the average just-noticeable (JN) brightness differences (dY) levels, the average comfort threshold (CT) dY levels, and the average number of discrete luster levels that participants can differentiate between the two limits (JN and CT dY). Besides, we also looked into the effect of different colors, contrast polarity, and the participants' color vision (normal and color blind) onto the three dependent variables above.

As described in figure 3.4, nine non-luster stimuli images, each with 10 luster

129

Figure 3.4: The nine non-luster stimuli images in S1. Three different colors and backgrounds (with different luma Y values in the YUV color space) were applied respectively.

variants (where luster effect was applied onto the colored square in the middle) were presented to each participant (a total of 99 stimuli images). To create stimuli with different contrast polarity, three gray-scale backgrounds with different luminance values in the YUV color space ($Y = 18$, 128, 238) were applied, and the Y values of the three colors were kept at 128. Hence, contrast polarity is present in stimuli with background of $Y = 128$, and no contrast polarity stimuli with background of $Y = 18$ and 238. The 10 luster variants were created with a dY increment of 10 ($dY = 10$, 20, 30, 40, 50, 60, 70, 80, 90, 100) to investigate the average JN and CT dY levels.

The participants were asked to answer three questions for each of the images shown. The first is a YES/NO question to whether they can perceive the luster effect on the colored square. The second is a ten-point Likert-scale rating on the saliency of the luster effect, 1 being not visible at all and 10 being extremely salient. The third is a five-point category rating scale of the experienced viewing comfort for the luster image relative to the non-luster image. This scale was previously used by Kooi et al. in investigating visual comfort of 3D displays [62].

For each set of stimuli (e.g. 11 images of blue with background of $Y = 128$, dY

from 0 to 100), JN dY is determined by the lowest dY level where the participant indicated YES in the first question. CT dY is determined by the highest dY level where the participant rated a '2' for the experienced viewing comfort level, a threshold also used by Kooi et al. in their work [62]. The number of discrete luster levels was determined by presenting the stimuli between JN dY and CT dY to the participants and they were told to indicate the number of perceptually different luster levels among the stimuli shown.

When presenting each of the nine stimuli set, the non-luster stimulus was always shown first, followed by the stimulus with $dY = 100$ to give participants a sense of the maximum luster levels. Then, the presenting sequence of the stimuli with dY between 0 and 100 were randomized, so that the participants were unaware of the dY level of the stimulus shown. The non-luster stimulus was always shown on the right side of the display to facilitate the answering of the questions.

Section 2 (S2): Measuring color distinguishability

To measure the color distinguishability of different color blind technique (re-coloring, pattern-applying, ColorBless, PatternBless), participants were told to indicate the square with a different color in the stimuli images, as illustrated in figure 3.5. Their response and color distinguishing time (timer starts when the image appears and ends when they indicate their response) for each stimulus image were recorded with a key press. Numbers 1, 2, 4, 5, 7, 8 on the number pad were chosen due to the resemblance of the positions of the colored square in the stimuli.

A within-subject design was used, where each participant would encounter four groups of stimuli in which each of the four techniques was applied. An additional
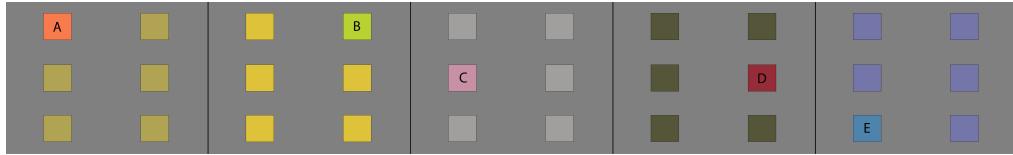
Figure 3.5: Stimuli used in S2. Five confusing color pairs were prepared, and pre-test was done to determine the three pairs that were the most confusing for each color blind participant. During the pre-test, participants were instructed to quickly point out the color square that had a different color from the rest for each of the five stimulus, and we picked three stimulus in which their responses were either incorrect or delayed. In each actual trial, subjects were told to indicate the square with a different color using a number pad. The different colors in each stimulus, named A to E, were used in S3 (the letters in this figure are not shown in the stimuli).

group of stimuli with original, untouched images were included in this section to ensure the colors are confusing for the color blind participants. The presenting sequence of stimuli block (where one block represents a color blind technique) was counterbalanced across the participants using a Latin square. Within each stimuli block, there were 18 stimuli images combining three different confusing color pairs and six possible square positions ($3 \times 6 = 18$ stimuli), which were also counterbalanced to prevent ordering effects.

To investigate the techniques' effectiveness in InfoVis images, we also measured the participants' response time in solving tasks in bar, pie, and line graphs with confusing colors. To accommodate five conditions (untouched, recoloring, pattern-applying, ColorBless, and PatternBless), five variants for each type of graphs (bar, pie, and line) were designed with different data but with same number of data categories and with same colors. One example of the bar graphs used is shown in figure 3.2. The five variants were controlled with the same number of data categories and colors used. A Latin square was used to counterbalance the presenting sequence of technique-applied stimulus across the participants.

The dependent variables in this section were error rate (ER) and task completion

time. ER was defined by the number of wrong responses over the total responses in each block. Color distinguishing time (DT) was measured in the color distinguishing tasks (with stimuli shown in figure 3.5) while the reaction time (RT) was measured in completing the task in the InfoVis stimuli (with stimuli shown in figure 3.2).

Section 3 (S3): Evaluating color differences

The perceptual color differences produced by the recoloring, pattern, and luster-based aids were evaluated by the normal color vision people. We selected five colors from the stimuli used in S2, indicated by A, B, C, D, E in figure 3.5. The RGB hex value of color A, B, C, D, E is #F77B4D, #B8D232, #C790A4, #952C37, #4E84AC respectively. Participants were told to evaluate the color differences between the original color and the modified colors.

Color name distance, a measure of similarity between colors based on naming patterns created by Heer and Stone in CHI 2012 [48], was used to evaluate the perceived color differences as we associate each color name with its semantic meaning. To measure color name distance, the participants were first asked to name and input the colors in the Color Dictionary. The Color Dictionary[2] was constructed from the standard CIELAB color space and the color distance metric with the current standard CIEDE2000, since RGB color space is a poor model to study human color perception [48]. Then, participants were told to choose one RGB hex value either from the 20 palettes that are provided by default, or from the additional palettes in similar colors that best matches the color being evaluated. After all the responses had been collected, the four RGB hex values of

---

[2]http://vis.stanford.edu/color-names/dictionary/
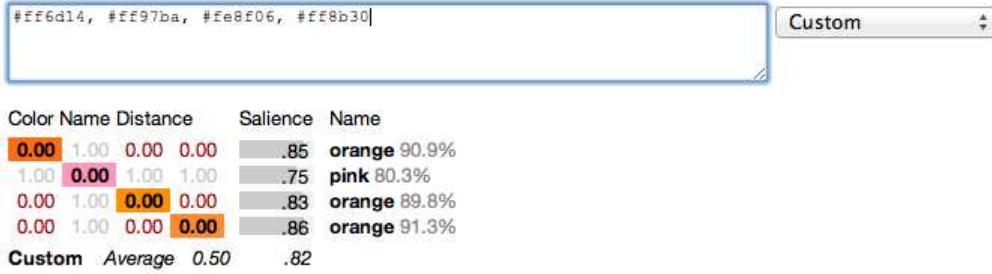
Figure 3.6: An instance of the use of Color Palette Analyzer [48] in our study to evaluate the color differences of the recolored, pattern-applying, and lustered colors from the original color based on their respective pairwise color name distances. The color palette and the hex values in the figure belong to original, recolored, pattern-applying, and lustered color A from the left to the right.

the perceived original and modified (recoloring, pattern, and luster-based) colors were then inputted into the Color Palette Analyzer[3] to calculate the color name distance from the original color, as shown in figure 3.6.

Section 4 (S4): Subjective evaluation

Post-study questionnaire (detailed in appendix A) and interviews were conducted with the color blind participants to collect the subjective evaluation of the techniques studied. They were conducted after the color blind participants had completed sections S1 and S2 of the user study. All the responses were recorded using Google Form.

First, each technique was evaluated individually with a 5-point Likert scale based on several metrics, including the perceived distinguishing speed, cognitive effort required to distinguish between colors, comfort level, and the obviousness of the effects. One example of the question used in the questionnaire to evaluate ColorBless's comfort level in distinguishing confusing color is the following: "Rate the comfort level of using ColorBless to distinguish confusing colors.", followed by a 5-point Likert scale with 1 representing "not comfortable at all" and 5

---

[3]http://vis.stanford.edu/color-names/analyzer/

representing "very comfortable".

After evaluating the techniques, the participants were asked to indicate the color blind techniques they most preferred in several common use-cases such as working alone, working collaboratively with people with normal color vision, working alone with figures containing many colors, and working collaboratively with figures containing many colors. The color blind participants' preferences in these use-cases were collected with multiple- choice questions, where only one technique could be chosen. In the end, brief interviews were conducted to understand their needs and common issues in decoding color information from digital content.

3.6 Results

3.6.1 S1: Investigating Binocular Luster in Active shutter 3D

Two-way repeated measures ANOVA was used to analyze the effects of two factors, colors and contrast polarity, on the three dependent variables: just noticeable dY, comfort threshold dY, and the number of discrete luster levels. The data in S1 is summarized in table 3.1. In terms of just noticeable dY, there is a significant effect in contrast polarity ($F_{1,9} = 41.78, p < 0.001$), which means that contrast polarity is a factor in the noticeability of the luster effect. Stimuli with opposite contrast polarity have a lower just noticeable dY (13.66) than the same contrast polarity (25).

However, no similar significant effect is observed for color ($p > 0.05$), which means that the different colors used in the experiment did not affect the just noticeable dY value. The same conclusion can be made for color blind participants (data not shown).

Table 3.1: Average just noticeable dY, comfort threshold dY, and number of discrete luster levels for normal color vision and color blind participants when encountering stimuli with same contrast polarity and opposite contrast polarity.

	Normal (N=10)		Color blind (N=6)	
	same contrast polarity	oppo. contrast polarity	same contrast polarity	oppo. contrast polarity
just noticeable dY	25	13.66	21.66	10.55
comfort threshold dY	62.33	50.66	58.61	33.88
No. of luster levels	3	3	3	3

For comfort threshold dY, we noticed a similar statistically significant effect for contrast polarity ($F_{1,9} = 23.457, p < 0.01$) but not with color ($p > 0.05$). Again, stimuli with opposite contrast polarity have a lower comfort threshold dY (50.66) than with the same contrast polarity (62.33). Same significant trend can be seen for the color blind participants (data not shown).

However, for the number of discrete luster levels that the normal color vision participants could differentiate, no significant effects were observed in either contrast polarity ($p > 0.05$), or colors ($p > 0.05$). Color vision of the participants does not affect this conclusion (data not shown for the color blind participants). All participants reported that they could reliably differentiate three levels of shininess between the just noticeable dY and the comfort threshold dY.

3.6.2   S2: Measuring Color Distinguishability

Figure 3.7a shows the average error rate of the four techniques in color distinguishing tasks. Repeated measures ANOVA determined that there is an over-
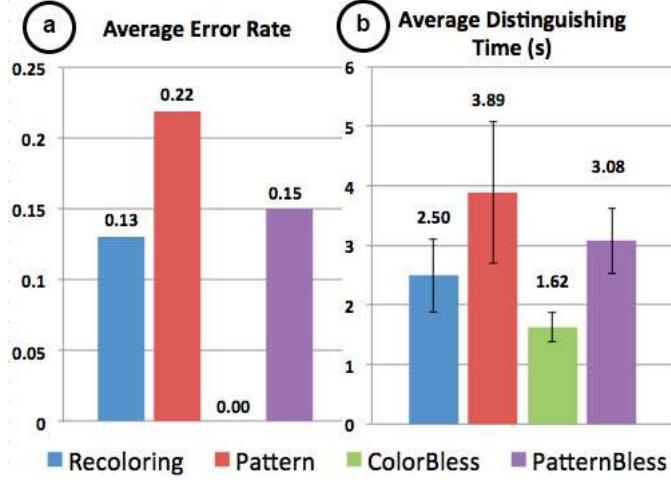
Figure 3.7: (a) Average Error Rate (ER) and (b) Distinguishing Time (DT) of the 10 color blind participants in completing simple color distinguishing tasks. Error bars represent standard deviation.

all significant difference between the mean error rates of the four techniques ($F_{3,27} = 4.481, p < 0.05$). However, pairwise comparison with Bonferroni correction only shows statistically significant difference between ColorBless (0.00) and pattern technique (0.22), indicating that ColorBless produces significantly less errors than that pattern technique ($p = 0.034$), while difference between ColorBless (0.00) and recoloring (0.13) is not significant ($p = 0.15$).

In terms of distinguishing time, there is an overall significant difference between the means of different techniques after Greenhouse-Geisser correction ($F_{1.623,12.514} = 19.637, p < 0.0005$). The average distinguishing time is shown in figure 3.7b. Post-hoc tests using the Bonferroni correction revealed that ColorBless (1.62s) is faster than other techniques with statistical significance (recoloring is 2.5s with $p < 0.01$, pattern is 3.89s with $p < 0.001$, PatternBless is 3.08s with $p < 0.001$), and recoloring (2.5s) is faster than pattern (3.89s) ($p = 0.02$). No significant differences were found in other pairwise comparisons.

Table 3.2 shows the error and response time of solving tasks in graphs. There are no overall significant differences in the response time of solving tasks in

Table 3.2: Error rate and reaction time (in seconds) of using different color blind techniques in solving tasks in graphs.

	Recoloring		Pattern		ColorBless		PatternBless	
	ER	RT	ER	RT	ER	RT	ER	RT
Bar	0.20	5.56	0	5.92	0	5.84	0	6.27
Pie	0.60	5.07	0	5.46	0	4.89	0.11	6.17
Line	0.60	9.14	0.60	11.84	0.25	10.02	0.22	9.93

bar ($p = 0.752$), pie ($p = 0.461$), and line ($p = 0.458$) graphs. Referring to table 3.2, error rates of the augmentation techniques are lower than the recoloring technique in bar and pie charts. Interestingly, for line charts, the error rate for both recoloring and pattern technique is very high (both 0.60) compared to ColorBless (0.25) and PatternBless (0.22).

3.6.3 S3: Evaluating Color Differences

Figure 3.8 shows the average color name distance of each technique, where a higher value represents a larger color difference. Using repeated measures ANOVA, the within-subject main effects of the three techniques are statistically significant in color A ($F_{2,18} = 14.82, p < 0.01$), color D ($F_{2,18} = 8.51, p < 0.01$), and color E ($F_{2,18} = 6.88, p < 0.01$), but not in color B and C. Post hoc pairwise t Tests using Bonferroni correction shows a significant difference between recoloring and luster technique in color A ($p < 0.001$) and color D ($p < 0.01$). No significant differences are found between recoloring and pattern technique in colors A, D, E. Overall, ColorBless retains the original color better than the recoloring technique in 3 of the 5 colors tested.

3.6.4 S4: Subjective Evaluation

Participants were asked to evaluate the color blind techniques by rating their (i) perceived speed in distinguishing colors, (ii) cognitive effort required in using the
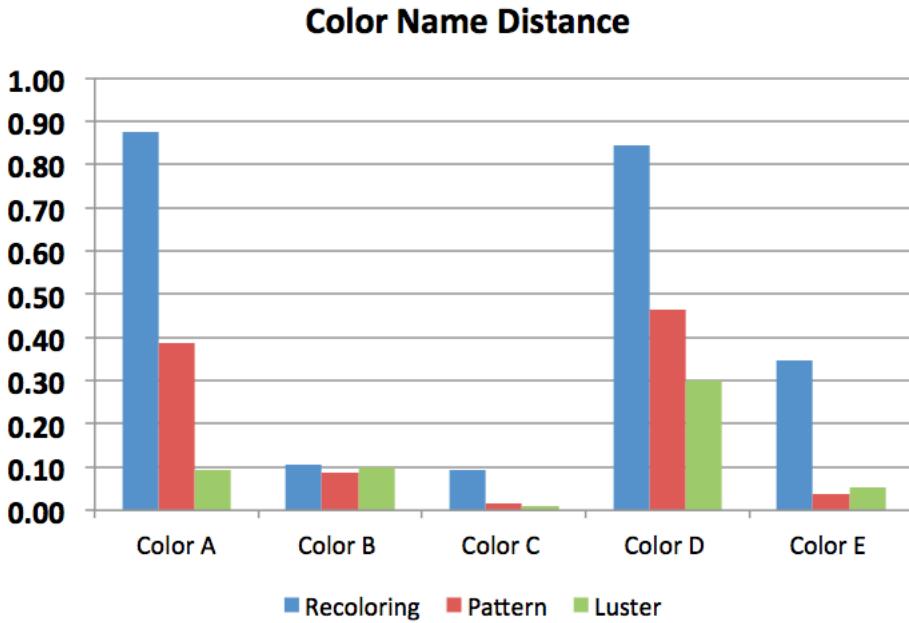
Figure 3.8: Color name distance of original color vs. modified color with recoloring, pattern, and luster (ColorBless).

technique, (iii) comfort level, and (iv) obviousness of the effect created by the technique. Figure 3.9 shows the average mean values of the rating score given by the 10 color blind participants. ColorBless was evaluated to be the fastest, and demanding the least cognitive effort. However, it was also evaluated to be the most uncomfortable among the techniques shown.

Besides, the color blind participants were asked which technique they preferred the most in the four common use-case scenarios, as shown in figure 3.10. In all cases, ColorBless was the most preferred, followed by PatternBless and Pattern technique. Only two participants preferred recoloring technique when they are working alone with graphs. In general, augmentation-based techniques were more preferred than the substitution-based ones.
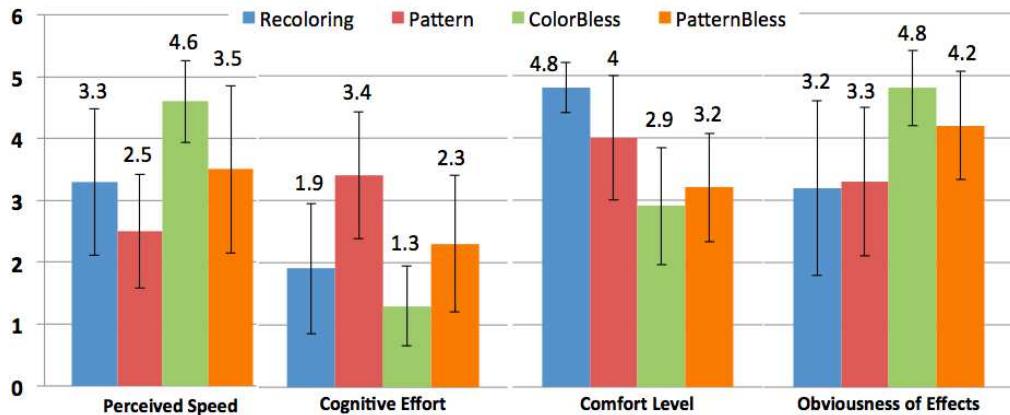
Figure 3.9: Subjective evaluation of the color blind techniques based on the four metrics (a) perceived speed, (b) cognitive effort required, (c) comfort level, (d) obviousness of the effects. Participants rated each using a 5-point Likert-scale and the average mean values for each technique are plotted, with error bars representing standard deviation.
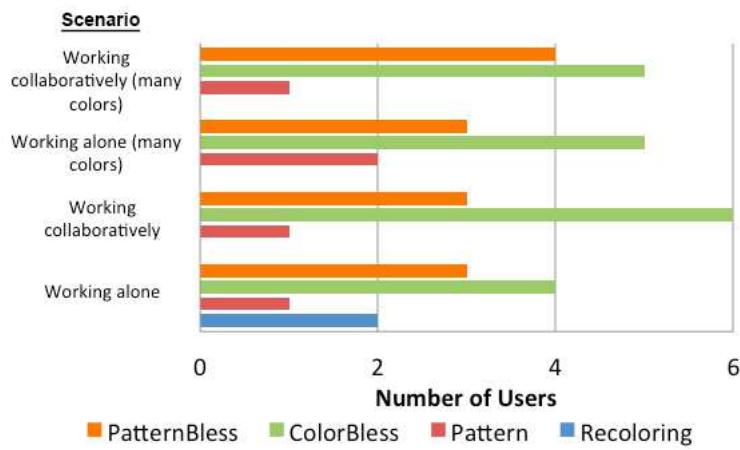
Figure 3.10: Color blind participants' top preferences of the four techniques studied in four different use-case scenarios, working with InfoVis graphs.

3.7 Discussion

In discussing our findings from all four sections of the study we set out to answer the three research questions.

3.7.1 Implementation Guidelines for Binocular Luster in 3D

Concurrent with previous work, our findings show that given the same brightness differences (dY), the luster effect is more salient and noticeable when contrast polarity of the left and the right image is opposite to each other [13]. On average, a higher luminance difference ($dY = 24$) is needed to perceive the luster effect on stimuli with the same contrast polarity across two eyes, compared to $dY = 13$ on those with opposite polarity. In addition to that, the findings suggest that contrast polarity is not affected by the colors of the luster regions. At the same time, the difference in colors does not have any effect on the perceptual saliency of the luster effect, at least for the three distinct hues (red, green, and blue) that we studied. This suggests that the term 'contrast' polarity only refers to the difference in luminance, and not the color.

The average comfort threshold dY value for stimuli with same contrast polarity across two eyes ($dY = 61$) is also significantly higher than stimuli with opposite polarity ($dY = 44$) [62]. Again, this factor is not affected by colors, and it does not affect the comfort threshold. This points to the interesting observation that, for images with same contrast polarity, while they require a higher dY value to start perceiving the luster effect, their comfort threshold dY is also higher. This implies that for images where the luster effect is to be applied with the same contrast polarity, a higher dY should be used. Between the just noticeable dY

and the comfort threshold dY, there are on average three distinct luster levels where the participants could tell apart. Both contrast polarity and hue do not seem to affect the number of discrete and observable luster levels.

In summary, for researchers, our findings provide a basic theoretical understanding on the perceptibility of the binocular luster effect using active shutter 3D. For implementers who are interested in using the luster effect to encode and augment information visually, our findings provide a brief implementation guideline for the luster effect in active shutter 3D, including the dY values to apply in different images and the number of luster levels differentiable.

3.7.2 Efficacy of Binocular Luster in Distinguishing Colors

Binocular luster effect was applied in two different ways (ColorBless, PatternBless) to augment visual information in images. Our findings suggest that ColorBless is the fastest and the most unambiguous in color distinguishing tasks. With ColorBless, the shininess on top of the confusing colors serves as a visual augmentation element, like line patterns for the pattern technique. However, due to the straightforwardness and higher saliency of the luster effect, ColorBless allows users to interpret the color information in a faster manner with lower cognitive effort.

Similarly, with PatternBless, our findings suggest that it is also slightly faster and less error-prone than the pattern technique. However, since PatternBless augments color information with patterns rather than using the entire area, it is slightly slower than the recoloring and the ColorBless techniques due to the additional cognitive effort required in delineating the patterns.

Our findings also suggest that recoloring and pattern techniques are not accurate (both error rate = 0.60) in disambiguating confusing colors in small areas like the legends and lines in line graphs. ColorBless, on the other hand, is more accurate (error rate = 0.25). The participants commented that distinguishing colors in small areas is inherently difficult. For the pattern technique, they felt that the line patterns are hard to detect in small areas, while the luster effect does make the small areas easier to distinguish due to its high saliency in binocular vision.

Color differences wise, ColorBless retains the original color better than the recoloring technique in 3 of the 5 colors we tested. Interestingly, for one of the colors that ColorBless failed to show significance in retaining colors, color B, we found that most of the errors color blind participants made in distinguishing colors with recoloring in S2 were on stimuli with color B (also, see figure 3.2f and figure 3.2g for comparisons of the recolored hues from the color blind users' perspective). This shows that the recoloring technique is not always effective in enhancing color contrasts and disambiguating colors, as previous work has shown [91]. Our findings also suggest that ColorBless retains the color slightly better than the pattern technique as there are no pairwise significant differences between the recoloring and the pattern technique.

3.7.3   Evaluation and Feedback from Color Blind Users

From the post-study questionnaire and interviews we conducted, we understand that color blind users place huge emphasis on reliability and speed when interpreting color-coded information. This is even more important in a collaborative scenario with normal color vision people. Indeed, when asked to rate the importance of speed in distinguishing colors (with a five-point Likert scale), 8 out of

10 rated it very important when they are alone and all rated it very important in a collaborative setting.

Referring to figure 3.10, color blind users generally preferred aids that augment visual information rather than substituting colors. When asked the rationale behind their preferences, they commented that while recoloring technique could resolve color confusion, color blind users generally avoid using color hues exclusively in interpreting information due to the anxiety of being erroneous in the process. This problem is more prominent in images with many colors, in which the recoloring technique has been shown in previous work to be less effective in resolving color ambiguity [91].

From the subjective evaluation and post-study interviews we conducted, we hypothesized that the cognitive effort involved in decoding color information is an important factor in the majority preference of ColorBless over the pattern technique. Assuming two colors are confusing, recognizing the presence of luster on those two colors was perceived to demand a lower cognitive effort (and less mental steps) than detecting the presence of patterns on the two colors and discerning their difference in orientation. This in turn, together with luster effect's acute perception of saliency in human vision, makes ColorBless (significantly) and PatternBless (slightly) faster than the pattern technique.

3.8   Potential Applications of Binocular Luster

The findings from our study suggest that applying luster as a visual cue in a differentiation task facilitate fast and accurate performance, due to saliency of the luster effect. The ability to create 'invincible' visual elements with a lustrous

appearance allows users to turn their attention to the visuals quickly. From our study, we also discovered that for color blind people, using luster effect is more effective than hue in augmenting information in small visual areas.

The fact that the luster effect could only be seen with 3D glasses enables new ways of interaction in a collaboration scenario, where one party requires an additional layer of information. Together with our findings that users could comfortably differentiate three discrete levels of luster, luster effect could potentially be used to represent ordinal data (with four levels, including the non-luster ones) or even interval data. For example, when visualizing noise level, instead of using heat map, which obscures and changes the color of the original underlying image, luster effect could be used to encode the noise level of different areas without the disadvantage of the former approach. In that sense, the ability to create different levels of binocular luster with a stereoscopic setup could enable the visualization of additional 2D scalar function over an image without obscuring or changing its original color and texture.

3.9   Limitations

There are several limitations with both luster techniques and the use of binocular luster in augmented visualization in general. First, in order for the 'blessed' colors to appear unaltered to users with normal color vision, the techniques require a glass-based 3D setup such as active shutter, passive lenses, and Dolby 3D. Second, viewing binocular luster effect with a high dY is uncomfortable for the user. Third, as mentioned in the introduction, our implementation are prototypical and were designed to determine the usability and practicality of luster-based aids. Hence, the algorithms do not handle background color and background

145

brightness of the image, which could be explored in future work.

3.10   Conclusion

In this work, we are interested in the application of binocular luster effect for color blind aids. We developed two prototypical color blind aids, ColorBless and PatternBless that applies luster effect with an active shutter 3D setup and investigated their effectiveness in augmenting visual information. In the study, we validated findings from previous work that binocular contrast polarity is a major factor to the perceived saliency of the luster effect, and the participants can perceive three discrete shininess levels comfortably. In addition, our findings suggest that ColorBless is significantly faster and unambiguous than the other techniques, while PatternBless trails the recoloring technique slightly in both speed and error rate. Color blind users also preferred luster-based aids over the others due to the higher visual saliency and the lower cognitive effort involved. Finally, we inferred design implications of applying binocular luster effect from the study and believed that it could be potentially used in application domain for augmented visualization.

Chapter 4

Beyond Stereo: An Exploration of Unconventional Binocular Presentation for Novel Visual Experience

This chapter reports our explorations on the various visual effects created with not only binocular luster, but binocular rivalry in general, in practical context. A user study is conducted to understand the user experience upon viewing these binocular visual effects. The potential applications of these effects in HCI domain are discussed.

4.1 Introduction

Scientists have studied binocular rivalry mainly to understand the neural mechanisms of human brain and perception [15, 33, 58, 121] where two dissimilar images are presented to study which features are more dominant in visual perception. Differing from these scientific works, we sought to answer this question from an engineering perspective, i.e., how we can constructively exploit human binocular vision system in unconventional ways to present novel visual experience for practical applications.

To explore this, we proposed a set of non-stereo binocular presentation techniques inspired by cognitive science literature, and conducted an informal study to validate the viability of these techniques as well as collecting subjective accounts of the actual visual experience. We first describe our study procedure, and then detail the design and findings of each technique.

4.2 Study Procedure

We used a Vuzix VR920 binocular head-mounted display (figure 1.9). It produces an image of 32° diagonal visual angle at 4:3 aspect ratio, focused at 9 feet, for each eye. The overlap between the two eyes' views was set to 100%. Each participant adjusted the tiltable section of the device to clearly see the entire display. Participants looked with both eyes unless otherwise instructed.

For each presentation technique that we tested, six static image pairs were used[1].

---

[1]Some test images based on:
http://pages.cs.wisc.edu/~csverma/CS766_09/HDRI/hdr.html
http://ivrg.epfl.ch/supplementary_material/cvpr11/
http://vision.middlebury.edu/stereo/data/scenes2006/
and Vuzix JPS Viewer:
http://www.vuzix.com/support/downloads_drivers.html

As we expect our techniques to be integrated with stereo images in practice, where applicable our stimuli also included regular stereo cues. The stimuli were presented to the two eyes at 30Hz refresh rate each. Each image pair was presented twice with the left/right views swapped; and as a baseline comparison, for each pair of images, we also used the same device to present to both eyes an average image that is equally alpha-blended between the image pair. The stereo cues were kept intact in all three conditions whenever possible. Upon participants' request, all stimuli could be freely revisited.

Upon presentation of each stimuli, participants were asked to describe in their own words what they were seeing in as much detail as possible. Only when they could not discover the special visual effects by themselves did we provide hints for regions of interest, however without suggesting the actual effect expected. The study was audio recorded for further analysis. Six people (2 females) aged between 24 and 35 participated. All had normal or corrected-to-normal vision, normal stereo vision, and normal color vision. The participants were tested for eye dominance using the Miles test [90] with several repetitions: 3 participants (male) were generally right-eye dominant, while the rest were generally left-eye dominant.

4.3   Taxonomy

Inspired by cognitive science research, we considered three general dimensions along which we can produce non-stereo difference between the pair of images: Color, Sharpness, and Semantic Content. As we are interested in practical applications, we also consider the following four general categories of visual effects: Highlighting, Compositing, Hiding, and Wowing. Table 4.1 illustrates this design

149

Table 4.1: Application domains and production procedures of usable binocular rivalry effects in HCI.

		Color	Sharpness	Semantics
Highlighting	Color highlighting	✓		
Compositing	Dynamic range	✓		
	Pseudo color	✓		
Hiding	Color dot pattern	✓		
	Hiding by blurring		✓	✓
Wowing	Hyper color	✓		
	Ghosting			✓

space, and summarizes the techniques we explored and their attributes by these two criteria, to be detailed in the following subsections.

4.4   Effects

This section describes how the various effects are created and the user experience they instigate found through the user study.

4.4.1   Highlighting

The highlighting effect aims at making certain regions of interest more noticeable to the viewer, and currently includes one technique: color highlighting. Figure 4.1 shows an example of highlighting. This is produced by painting the region with two different colors (90-180° hue difference, 0-13% saturation difference, and 0-66% brightness difference). For example, in Figure 1a, the square icon in the circular game map differs between violet in one image, and green in the other.

Our study revealed that regions of highly saturated color pairs that differ in hue were particularly prominent, as long as the size of the region is above a certain threshold ($\approx 0.44°$ in view angle). Participants described the effect either positively (4/6, i.e. 4 of 6 participants) as "highlighted", "blinking", or negatively

| right eye view | left eye view |

Figure 4.1: Binocular highlighting effect. The differences between the two eyes' views are marked by red boxes. The two eyes' views are swapped to facilitate crossed-eye stereo viewing.

(2/6) as "distracting", "annoying". More interesting descriptions include "fluorescent", "bright and colorful emissive light", and "floating". 2 participants were reminded of the special optical materials they are familiar with, such as lenticular or refractive films, as these materials may also display view-dependent colors. Eye dominance had a noticeable effect, where different sensations were reported when shown inverted pairs. On the other hand, these sensations were unstable, as typical in binocular rivalry [15]. Unsurprisingly, in the baseline image where the two views were averaged, the regions of interest became even less prominent because averaging two contrasting colors results in desaturation.

The power of color highlighting has thus been confirmed. One thing worth noting is that neither of the single colors in the contrasting pair needs to be prominent from its surroundings in each monocular image, so highlighting can be achieved without compromising the image composition.

The highlighting effect could be theoretically suggested by the perceived shininess of a surface [104]: in real world, some "shiny" materials with specular reflection or refraction properties display drastically different hues and brightness from different view angles. Our proposed highlighting technique produces a similar color rivalry [58] effect that resonates with this principle of perceived shininess,

right eye view   left eye view

Figure 4.2: Compositing dynamic range. The two eyes' views are swapped to facilitate crossed-eye stereo viewing.

thus highlighting the rivaling regions as "shiny" areas.

4.4.2 Compositing

The compositing effect aims at presenting two images of the same scene, however are complementary in terms of information spectrum along a certain dimension. We expect that the human perception system may be able to composite such information to receive a higher bandwidth than is possible with a single view. We explored such compositing effects along two different dimensions:

Compositing Dynamic Range

Compositing dynamic range concerns a pair of photographs taken at different exposures, each missing part of the illumination range of the scene. Figure 4.2 illustrates.

When shown image pairs with different exposures, participants were able to describe details that are only available in one of the two images, where the corresponding region in the counterpart image is subject to overexposure or underexposure due to limited dynamic range of the camera. This may be explained

right eye view   left eye view
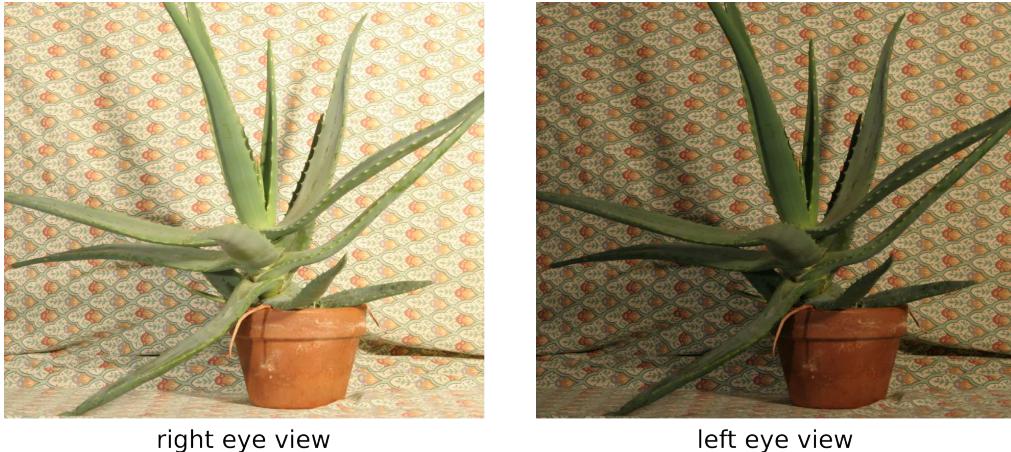
Figure 4.3: Compositing dynamic range in a stereoscopic setting. The two eyes' views are swapped to facilitate crossed-eye stereo viewing.

by contour dominance [121], where the rich contours in one image effectively suppressed the more uniform over/under exposed regions in the other image.

Comparatively, although the baseline average image also incorporates these features, they were less prominent, as averaging reduced the overall image contrast. Interestingly, swapping the left and right eye images also resulted in a perceived change of global brightness; and two participants further perceived change in light source, although they could not determine the nature of that change. The global brightness was biased towards the dominant eye.

This effect can also be incorporated into a stereoscopic image setting, as shown in figure 4.3.

Compositing Pseudo Color

In pseudo color images, pixel values do not represent true visible light intensities, but some other physical channels such as temperature or near infrared (NIR) response. By letting the viewer composite ordinary RGB images with such pseudo color images, we expect that they would be able to make sense of

right eye view   left eye view
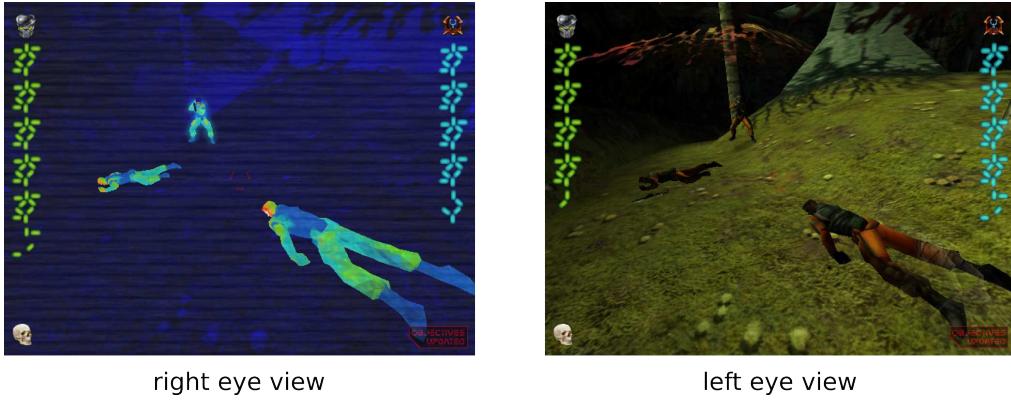
Figure 4.4: Compositing with pseudo color representing temperature. The two eyes' views are swapped to facilitate crossed-eye stereo viewing.

right eye view   left eye view

Figure 4.5: Compositing with pseudo color representing near-infrared light. The two eyes' views are swapped to facilitate crossed-eye stereo viewing.

the complementary nature of different channels. Examples are given in figure 4.4 and 4.5.

For RGB-temperature image pairs, all participants reported seeing bright human figures. It is hard for them to see the human figures' actual color, but they could identify the green color of the background land. One participant described the effect as the contour "shaking". When shown the naive average between the two images, participants responded that more colors could be observed on the human figure, but that the background color is less obvious. For RGB-NIR image pairs, all participants reported that the boundaries of plants, brightly colored blankets, and sign boards are "bright", "confusing", and sometimes (2/6) "floating", which "does not fit well" into the scene. When shown the averaged baseline, participants

154

reported that the color is not as vivid as in the previous case, but the feeling of "unfitness" also disappeared. The effect of eye dominance is mainly on the overall perceived saturation: when the gray scale NIR image is shown to the dominant eye, participants reported reduced saturation as compared to viewing the other way round.

The response from the participants meets our expectation: in the RGB-temperature image pair, textured background of the RGB image suppressed the almost the uniform background of the temperature map; the strong edges of the human figure in the temperature map suppressed the perception of its normal color; and in RGB-NIR image pairs, large luminance difference between the RGB and the NIR images on the plants and the painted sign boards creates strong response that the participants could not overlook. This effect could also be exploited in real-time vegetation inspection applications, by feeding RGB video and NIR video to each eye, while letting the human brain to work out the distracting areas as the possible contours of vegetation.

Besides the contour dominance factor, the aforementioned highlighting effect may also play a role here: regions with rivaling colors would appear bright and catches more attention. The result shows that humans are able to effectively incorporate multi-spectrum visual information through binocular vision and make sense of them. Essentially, by leveraging the "computation power" of the human visual perception system, we may alleviate or eliminate the need for computers to algorithmically fuse such information [43], which is not always possible or straightforward to do.

4.4.3 Hiding

The hiding effect aims at a seemingly counterintuitive goal: to turn visible information in monocular images invisible in the binocular view. In other words, we attempt to hide some information from the viewer when both eyes are open, while revealing it once the viewer closes one of the eyes. This may provide a lightweight mechanism for switching between information layers. For example, in video games, users keep both eyes open to see the regular game view, but may occasionally close one eye to access additional information such as player statistics. This is achieved without active sensing of the user's eye movement.

Hiding using Color Dot Pattern

Research in binocular color fusion [58] has discovered several possible outcomes when the human brain attempts to fuse two different colors presented to two eyes, ranging from stable uniform fused color, to color sensation that vary both in space and in time. Regardless of the outcome of the color fusion, it is usually difficult for humans to determine which eye is seeing which. This suggests that if we present a pair of different colors to both eyes, it may become indistinguishable from the sensation of the same pair presented with the left and the right eye color swapped. Therefore, by rendering a shape in one eye using a foreground and a background color, and rendering the same in the other eye but with the foreground and background color swapped, it becomes possible that in binocular views at any point the user sees the result of color fusion, which are more or less consistent regardless of which color originates from each eye's view. Thus the information would become invisible to the viewer.

right eye view   left eye view
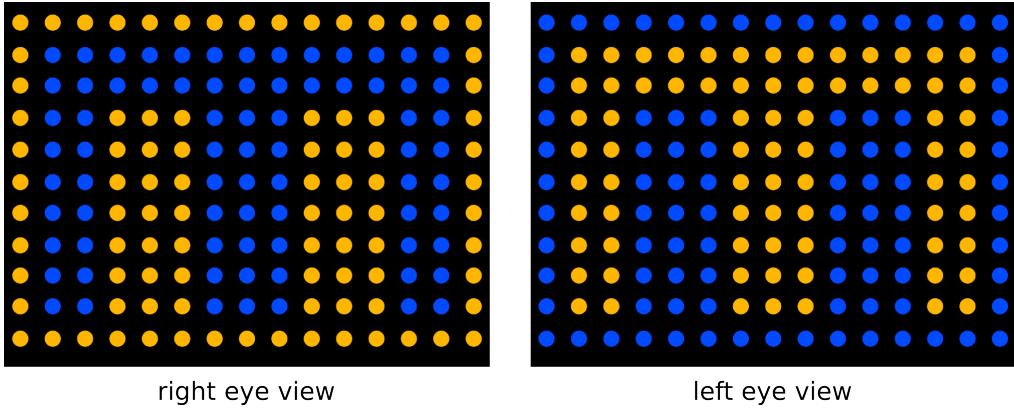
Figure 4.6: Hiding using low-resolution color dot pattern. The two eyes' views are swapped to facilitate crossed-eye stereo viewing.

right eye view   left eye view
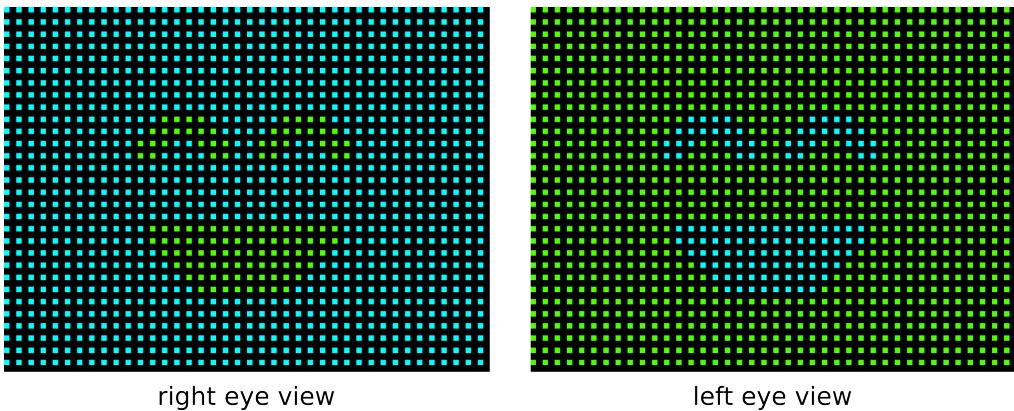
Figure 4.7: Hiding using high-resolution color dot pattern. The two eyes' views are swapped to facilitate crossed-eye stereo viewing.

However, such a technique could not work if there exists a visual contour between the colors in either view. As explained previously in [121], such contours are sensed individually by each eye, thus cannot be eliminated by binocular vision. In order to eliminate this, we convert the shape into a dot grid pattern (figure 4.6 and figure 4.7), so that it is only encoded by the color contrast but not contours. We generated four test image pairs with two levels of grid resolution (low/high) and two color schemes (complementary/similar colors).

Participants reported that they see dots constantly changing color. Although not seeing clearly to be certain, they were able, after intentionally viewing for some time, to describe the correct pattern in the higher resolution image pairs. They

were more confused and uncertain when seeing the lower resolution patterns. The minimum time from the onset of the pattern till the participants voluntarily guessed the correct or similar pattern is 10 seconds in the low resolution and 1 second in the high resolution. This period might be the sweet spot to hide information temporarily.

Hiding using Blurring

According to Fahle [33], higher spatial frequency (sharp features) is more dominant than lower spatial frequency (blur features) when they are presented to the two eyes respectively. To hide information by this principle, we can create image pairs that show different semantic information in corresponding regions but with different levels of sharpness. Contour dominance results in masking of the blurred information by the sharp information when both eyes are open, while the blurred information becomes visible only when the other eye is closed. We can apply this principle to multiple regions of the image pair, so that each image contains regions that either mask the other image or are masked by the other, naturally supporting not one, but two individual views that can be revealed by closing either one of the eyes. Figure 4.8 illustrates one of the image pairs we tested, which shows this technique for both textual and graphical information and in alternate directions between the two eyes.

In general, most participants (5/6) reported seeing the sharper of the text rivalries. With the faces there was more variance between the participants, as 3 of them saw the sharp face, while others saw the alternate or mixed information. We suspect this was because the higher-level perception mechanism involved in recognizing faces interacted with our technique. The averaged baseline image

<div align="center">right eye view   left eye view</div>
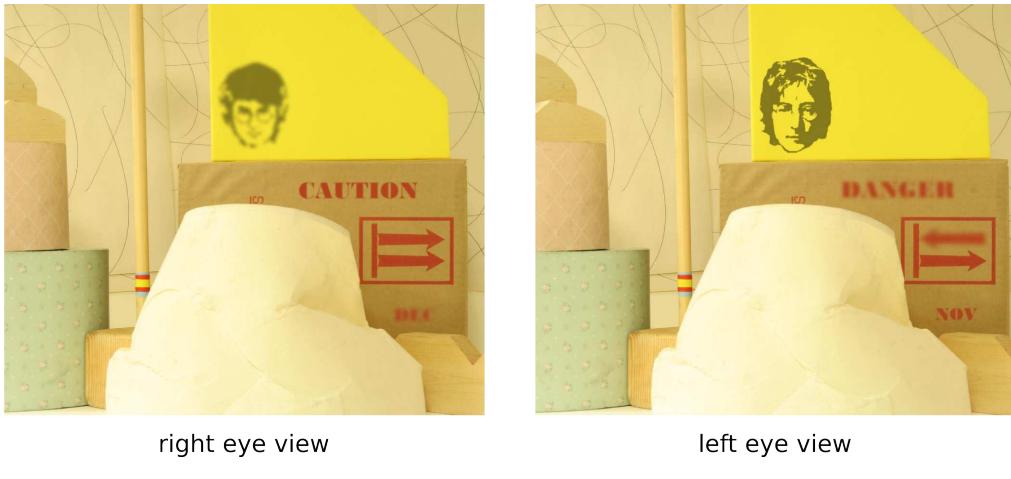
Figure 4.8: Hiding using blurring. The two eyes' views are swapped to facilitate crossed-eye stereo viewing.

appeared confusing and unrecognizable to all participants. When asked to use their single eye to view the images, the participants were able to recognize all information except for the "NOV" / "DEC" texts, which might be due to the small size of the stimuli. After revelation of the effect, all participants found this effect interesting and fun.

Since no excessive attention is paid to the regions with hidden information, this effect might also be used to hide text or simple graphics to uninformed viewers, and only recognizable by informed users.

4.4.4 Wowing

Wowing effects aim at creating surprising sensations that are not necessarily useful for productivity applications but can facilitate compelling experience in applications such as cinema or gaming. The two effects we explored are as follows:

right eye view   left eye view

Figure 4.9: Hyper color effect. The two eyes' views are swapped to facilitate crossed-eye stereo viewing.

Hyper Color

We specifically tried to create the effect of "impossible colors" [14] by showing different colors in each eye, as shown in figure 4.9. However, participants' responses were not the so-called "impossible colors" that are yellowish blue or greenish red. Instead, 3 participants saw inhomogeneous color patches that change smoothly over time. Other responses include "fluorescent light", "jittering color patches", "bright outline" and "shiny and unstable positions". Based on the same principle as color highlighting, here we are addressing a different application context: we name it "hyper color" and see potential enlargement of color vocabulary in binocular visualizations.

Ghosting Effect

We show two image pairs where an object is presented only in one eye's image but not the other, thus giving it a ghostly appearance, as illustrated in figure 4.10. All participants reported the effect to be similar to transparency. Two participants described temporal change in transparency while the same image pair is presented. One participant explicitly used the word "ghost" in the descrip-

right eye view   left eye view

Figure 4.10: Ghosting effect. The two eyes' views are swapped to facilitate crossed-eye stereo viewing.

tion without prompting. All participants reported a difference in transparency between the ghost effect, its left- right swapped version, and the baseline. Further, this effect demonstrates the temporal fluctuation of perceived transparency, which could not be experienced with transparency conventionally rendered in monocular static images.

4.5   Conclusion

In this chapter, we have presented several unconventional binocular presentation techniques to create new visual experiences. These effects are studied in an informal user study with practical usage context in HCI-related applications. We have created a taxonomy of the methods to create these effects and potential applications for them.

Chapter 5

Conclusion and Limitations

In conclusion, this PhD thesis reports a comprehensive research around an emerging topic in human-computer interaction: to leverage on a known but underutilized visual phenomenon known as binocular luster, for novel ways of interacting with computing devices and interfaces. It exemplifies how a perceptual phenomenon previously under-studied in HCI is 'rediscovered' with reference to psychology and neuroscience literature and adapted for potential novel applications in HCI.

Three research works are presented in a 'downstream' fashion, from fundamental knowledge to specific applications.

The first work studied the psychological properties of binocular luster, whose experiment data is used to quantitatively model perceptual characteristics of binocular luster. Psychophysics methods are adapted to measure users' perceptual thresholds to binocular luster, along two dimensions of a binocular luster stimulus, inter-ocular brightness difference, and total energy. To the best of our knowledge, no prior research has addressed the quantitative measure of the

perceptual thresholds of binocular luster, on a commercially available consumer electronics device, with the purpose of direct applicability in Human-Computer Interaction. A 2D space is proposed and used in the study to capture physical parameters of binocular luster stimuli, which also accounts for conventional brightness stimuli without luster. An experiment was carried out to measure the detection and discrimination thresholds for various stimuli in the binocular luster space. Their characteristics are analyzed with statistics tests. Additionally, classic conclusions about brightness perception without luster is also verified.

The statistics tests revealed that the sensitivity to inter-ocular brightness difference increases as its strength increases, which surprisingly contradicts Weber's Law. One possible explanation is that while brightness in one eye overwhelms and saturates the response in that eye, brightness in the other eye becomes smaller, allowing for increased monocular brightness discriminability in that eye, which aligns with classic accounts of Weber's Law. Apart from this curious finding, the sensitivity to inter-ocular brightness difference is found to be reduced by an increase in total energy, and is not statistically affected by sidedness of the stimuli. For sensitivity to total energy change in a binocular luster stimulus, it is found that while sensitivity is reduced by an increase in inter-ocular brightness difference, or an increase in total energy, or both, complete removal of the luster effect (i.e., same brightness in both eyes) would greatly decrease the sensitivity to changes in total energy. We see this as the 'catalyst' effect of binocular luster on total energy discrimination, which is subject to further investigation of future research and applications.

An empirical model is fitted with the experiment data, to describe and predict perceptual responses to stimuli with and without binocular luster, the latter of

163

which is conventional monocular brightness perception. It is further used to calculate approximate perceptual differences between two binocular stimuli. With this model, we developed a generic approach to create binocular images that can appear differently in monocular views, binocular view, and merged view, which is the average of the two monocular views. We also developed computationally tractable methods to create dual-view images in special cases.

We believe that the first research is a solid contribution to psychology and vision research, with quantitative result specifically for perceptual characteristics of binocular luster, and its relationship to brightness perception without luster. Although the results in this study are only empirical, we hope that they could become an inspiration for future research that aims to explain these results from psychological and physiological perspectives.

The second research focused on a specific application of binocular luster, to help color blind people distinguish between colors that appear confusing to them. This is done by first simulating the image perceived by color blind users, then clustering colors that are dissimilar in the original image, but similar in the simulated image. The clusters indicate regions to be annotated with luster, in order to help color blind users distinguish between them. Two annotation methods are proposed. The first is to add different strength of luster for each cluster, a strategy we call 'ColorBless'. The second is to add stripe patterns with different slope to each cluster, then apply a constant luster effect to all patterns, a strategy we call 'PatternBless'.

A study was conducted to investigate three research questions. The first research question concerns the optimal range for luster strength, within which the stimuli would appear noticeable while still comfortable to the users. It is found that while

contrast polarity has a significant effect on the range, all participants reported to be able to distinguish between three different luster levels within the optimal range. The second research question concerns the performance of the two luster-based color blind relief techniques in common information visualization tasks, in comparison with existing solutions. Two existing state-of-the-art color blind relief techniques, based on color substitution and annotation respectively, are included for the comparison. It is found that users are able to process color information with less effort using the ColorBless and PatternBless techniques. In addition, it is found that the ColorBless technique preserves color information better than substitution-based techniques such as recoloring, due to the choice of stereoscopic display technology that blends the left and right views when viewing without stereo glasses. The third research question concerns the subjective preferences of the user when working on information visualization graphs. Through a post-experiment questionnaire, it is found that ColorBless is preferred by the majority of the participants.

Overall, the second research contributes to the human-computer interaction field through the design and evaluation of a novel approach to color blind relief, using binocular luster. It also implies the potential of binocular luster to supplement the visual vocabulary that can be used in visual interfaces and communication.

The third research focuses on exploring other potential applications in HCI of not only binocular luster, but binocular rivalry in general.

By systematically creating differences between the images in the two eyes, several interesting visual effects with binocular rivalry emerged. They are loosely grouped into four categories: highlighting, compositing, hiding, and wowing, for different HCI applications. A user interview was conducted to find out how users

perceive and interpret these effects.

The contribution of the third research is to bridge the gap between binocular rivalry as a visual phenomenon and its potential applications in HCI. It presents concrete examples demonstrating various effects created with binocular rivalry, in practical HCI contexts.

As with every research, the work presented in this thesis is not without limitations. There are mainly three aspects of limitations with this thesis, in terms of methodology, hardware and computation power, and user adoption.

First, methodologically, there are numerous other psychophysical methods and theories that could be used, such as Signal Detection Theory (SDT [99, 22]), and Steven's Power Law. To refrain from complication of the research procedure (e.g., SDT does not scale well, requiring large number of catch trials where the signal/comparison stimulus is absent) and avoid actively discussed theories (e.g., Steven's Power Law and Weber's Law are often disputed [49, 77]), we used the most commonly accepted and the simplest method to interpret our psychophysics result.

Second, in terms of hardware devices, although computation power is getting ever greater, it is not unlimited. The generic approach to multi-view images presented in chapter 2 involves frequent evaluation of high-dimensional functions, therefore is not computationally tractable. Aside from computation power, the stereoscopic display systems introduced in chapter 1 also have various limitations. For the Oculus Rift immersive HMD used in chapter 2, the central pixels are enlarged, suffering from reduced resolution, to the extent that its RGB sub-pixels become apparent to observant participants. For the active shutter glasses used in chapter

3, the cross-talk effect between the two views makes one view partially visible in the other eye, thus interfering with the experimentation. For the previous-generation Vuzix HMD used in chapter 4, the view angle and the brightness range is greatly limited, deteriorating user comfort and perception.

Third, most effects studied in this thesis need to be presented with stereoscopic display devices. Despite the restless marketing from major display manufacturers and cinemas, there is still a long way to go before stereoscopic 3D technology becomes omnipresent, for these effects to have potentially large impact on the users' daily life. The current technologies still require bulky devices and/or special glasses. Imagine that everyone wears contact lenses to enable stereoscopic viewing everywhere, the effects presented in this thesis might receive much more attention and research interest.

It is hoped that future research will benefit from this thesis by designing and evaluating novel applications leveraging on these effects, or augmenting existing applications with binocular rivalry effects, in order to advance the way by which humans interact with computing devices. More ambitiously, this thesis wishes to inspire future research in perception and cognition, to unlock hidden potentials of human brain.

Bibliography

[1] Daltonize. `http://www.vischeck.com/daltonize`. Accessed: 2013-10-06.

[2] Dolby 3D. `http://www.dolby.com/us/en/professional/cinema/products/dolby-3d-cinema-system.html`. Accessed: 2014-05-24.

[3] EyeFly 3D – features. `https://www.eyefly3d.com/features`. Accessed: 2014-06-30.

[4] HP 2311gt 3D LCD monitor – product specifications. `http://h20565.www2.hp.com/portal/site/hpsc/template.PAGE/public/kb/docDisplay?docId=c03077021`. Accessed: 2014-06-30.

[5] iWear VR920 | Vuzix. `http://www.vuzix.com/consumer/products_vr920/`. Accessed: 2014-06-04.

[6] Oculus Rift. `http://www.oculusvr.com/`. Accessed: 2014-06-04.

[7] Sony HMZ-T3W Head-Mounted Display. `http://store.sony.com/wearable-hdtv-2d-3d-virtual-7.1-surround-sound-zid27-HMZT3W/cat-27-catid-3D-Personal-Viewer`. Accessed: 2014-06-04.

[8] Wikipedia – Dolby 3D. `http://en.wikipedia.org/wiki/Dolby_3D`. Accessed: 2014-05-24.

[9] Alpers, G., and Pauli, P. Emotional pictures predominate in binocular rivalry. *Cognition & Emotion 20*, 5 (2006), 596–607.

[10] Anstis, S. M. Monocular lustre from flicker. *Vision Research 40*, 19 (2000), 2551–2556.

[11] Aygül, R., Dane, S., and Ulvi, H. Handedness, eyedness, and crossed hand-eye dominance in male and female patients with migraine with and without aura: A pilot study 1. *Perceptual and Motor Skills 100*, 3c (2005), 1137–1142.

[12] Bailey, J. E., Neitz, M., Tait, D. M., and Neitz, J. Evaluation of an updated HRR color vision test. *Visual Neuroscience 21*, 03 (5 2004), 431–436.

[13] Bal, C., Jain, A. K., and Nguyen, T. Q. Detection and removal of binocular luster in compressed 3D images. In *Acoustics, Speech and Signal Processing (ICASSP), 2011 IEEE International Conference on* (2011), IEEE, pp. 1345–1348.

[14] Billock, V. A., and Tsou, B. H. Seeing forbidden colors. *Scientific American 302*, 2 (2010), 72–77.

[15] Blake, R. A primer on binocular rivalry, including current controversies. *Brain and Mind 2*, 1 (2001), 5–38.

[16] Blake, R., Fox, R., and Westendorf, D. Visual size constancy occurs after binocular rivalry. *Vision Research 14*, 7 (1974), 585–586.

[17] Blake, R., Westendorf, D. H., and Overton, R. What is suppressed during binocular rivalry. *Perception 9*, 2 (1980), 223–231.

[18] BLAKE, R. R., FOX, R., AND MCINTYRE, C. Stochastic properties of stabilized-image binocular rivalry alternations. *Journal of Experimental Psychology 88*, 3 (1971), 327.

[19] CHENG, C.-Y., YEN, M.-Y., LIN, H.-Y., HSIA, W.-W., AND HSU, W.-M. Association of ocular dominance and anisometropic myopia. *Investigative Ophthalmology & Visual Science 45*, 8 (2004), 2856–2860.

[20] COGAN, R., AND GOLDSTEIN, A. G. Reporting of fragmentations in the binocular rivalry of contours. *The American Journal of Psychology 85*, 4 (1972), 569–584.

[21] COMANICIU, D., AND MEER, P. Mean shift: A robust approach toward feature space analysis. *Pattern Analysis and Machine Intelligence, IEEE Transactions on 24*, 5 (2002), 603–619.

[22] COREN, S., WARD, L., AND ENNS, J. *Sensation and perception.* Harcourt Brace College Publishers, 1999.

[23] CORNSWEET, T. N. The staircase-method in psychophysics. *The American Journal of Psychology* (1962), 485–491.

[24] COSSAIRT, O. S., NAPOLI, J., HILL, S. L., DORVAL, R. K., AND FAVALORA, G. E. Occlusion-capable multiview volumetric three-dimensional display. *Applied Optics 46*, 8 (2007), 1244–1250.

[25] COWAN, M. REAL D 3D theatrical system: A technical overview, 2007.

[26] CURCIO, C. A., SLOAN, K. R., KALINA, R. E., AND HENDRICKSON, A. E. Human photoreceptor topography. *Journal of Comparative Neurology 292*, 4 (1990), 497–523.

[27] Dahlman, E., Oestges, C., Bovik, A. C., Fette, B. A., Jack, K., Dowla, F., Parkvall, S., Skold, J., DeCusatis, C., da Silva, E., et al. *Communications engineering desk reference*. Academic Press, 2009.

[28] Deeb, S. The molecular basis of variation in human color vision. *Clinical Genetics 67*, 5 (2005), 369–377.

[29] Dehaene, S. The neural basis of the Weber–Fechner law: a logarithmic mental number line. *Trends in Cognitive Sciences 7*, 4 (2003), 145–147.

[30] Dodgson, N. A. Autostereoscopic 3D displays. *Computer 38*, 8 (2005), 31–36.

[31] Dupač, V. Stochastic approximation. *Handbook of Statistics 4* (1984), 515–529.

[32] Engel, A. K., Fries, P., König, P., Brecht, M., and Singer, W. Temporal binding, binocular rivalry, and consciousness. *Consciousness and Cognition 8*, 2 (1999), 128–151.

[33] Fahle, M. Binocular rivalry: suppression depends on orientation and spatial frequency. *Vision Research 22*, 7 (1982), 787–800.

[34] Favalora, G. E. Volumetric 3D displays and application infrastructure. *IEEE Computer Society 8* (2005), 37–44.

[35] Fechner, G. T., Boring, E. G., Howes, D. H., and Adler, H. E. *Elements of Psychophysics. Translated by Helmut E. Adler. Edited by Davis H. Howes And Edwin G. Boring, With an Introd. by Edwin G. Boring*. Holt, Rinehart and Winston, 1966.

[36] FORMANKIEWICZ, M., AND D MOLLON, J. Binocular lustre as an attribute of surface perception. In *Perception* (2006), vol. 35, ECVP Abstract Supplement, pp. 213–213.

[37] FORMANKIEWICZ, M. A., AND MOLLON, J. The psychophysics of detecting binocular discrepancies of luminance. *Vision Research 49*, 15 (2009), 1929–1938.

[38] FOX, R., AND CHECK, R. Detection of motion during binocular rivalry suppression. *Journal of Experimental Psychology 78*, 3p1 (1968), 388.

[39] FOX, R., AND HERRMANN, J. Stochastic properties of binocular rivalry alternations. *Perception & Psychophysics 2*, 9 (1967), 432–436.

[40] GEGENFURTNER, K. R., AND SHARPE, L. T. *Color vision: From genes to perception.* Cambridge University Press, 2001.

[41] GESCHEIDER, G. A. Psychophysical scaling. *Annual Review of Psychology 39*, 1 (1988), 169–200.

[42] GESCHEIDER, G. A. Psychophysics: The fundamentals.

[43] GOSHTASBY, A., AND NIKOLOV, S. Image fusion: advances in the state of the art. *Information Fusion 8*, 2 (2007), 114–118.

[44] HARDY, L. H., RAND, G., AND RITTLER, M. C. HRR polychromatic plates. *Journal of the Optical Society of America 44*, 7 (1954), 509–523.

[45] HARTENBAUM, N. P., AND STACK, C. M. Color vision deficiency and the X-chrom lens. *Occupational Health & Safety (Waco, Tex.) 66*, 9 (1997), 36–40.

[46] HARTMANN, W., AND HIKSPOORS, H. Three-dimensional TV with cordless FLC spectacles. *Information Display 3*, 9 (1987), 15–17.

[47] HEALEY, C. G., BOOTH, K. S., AND ENNS, J. T. Visualizing real-time multivariate data using preattentive processing. *ACM Transactions on Modeling and Computer Simulation (TOMACS) 5*, 3 (1995), 190–221.

[48] HEER, J., AND STONE, M. Color naming models for color selection, image editing and palette design. In *Proceedings of the SIGCHI Conference on Human Factors in Computing Systems* (2012), ACM, pp. 1007–1016.

[49] HEIDELBERGER, M. *Nature from within: Gustav Theodor Fechner and his psychophysical worldview.* University of Pittsburgh Pre, 2004.

[50] HERRICK, R. M. Psychophysical methodology: Comparison of thresholds of the method of limits and of themethod of constant stimuli. *Perceptual and Motor Skills 24*, 3 (1967), 915–922.

[51] HOLLIMAN, N. S., DODGSON, N. A., FAVALORA, G. E., AND POCKETT, L. Three-dimensional displays: a review and applications analysis. *Broadcasting, IEEE Transactions on 57*, 2 (2011), 362–371.

[52] HOLLINS, M., AND HUDNELL, K. Adaptation of the binocular rivalry mechanism. *Investigative Ophthalmology & Visual Science 19*, 9 (1980), 1117–1120.

[53] HOWARD, I. P. *Seeing in depth, Vol. 1: Basic mechanisms.* University of Toronto Press, 2002.

[54] HUYNH-THU, Q., LE CALLET, P., AND BARKOWSKY, M. Video quality assessment: From 2D to 3D—challenges and future trends. In *Image*

Processing (ICIP), 2010 17th IEEE International Conference on (2010), IEEE, pp. 4025–4028.

[55] IKEDA, M., AND SAGAWA, K. Binocular color fusion limit. *Journal of the Optical Society of America 69*, 2 (1979), 316–321.

[56] JESTEADT, W. An adaptive procedure for subjective judgments. *Attention, Perception, & Psychophysics 28*, 1 (1980), 85–88.

[57] JORKE, H., AND FRITZ, M. Infitec-a new stereoscopic visualisation tool by wavelength multiplex imaging. *Journal of Three Dimensional Images 19*, 3 (2005), 50–56.

[58] JUNG, Y. J., SOHN, H., LEE, S.-I., RO, Y. M., AND PARK, H. W. Quantitative measurement of binocular color fusion limit for non-spectral colors. *Optics Express 19*, 8 (2011), 7325–7338.

[59] KAERNBACH, C. Simple adaptive testing with the weighted up-down method. *Attention, Perception, & Psychophysics 49*, 3 (1991), 227–229.

[60] KESTEN, H. Accelerated stochastic approximation. *The Annals of Mathematical Statistics* (1958), 41–59.

[61] KHAN, A. Z., AND CRAWFORD, J. D. Ocular dominance reverses as a function of horizontal gaze angle. *Vision Research 41*, 14 (2001), 1743–1748.

[62] KOOI, F. L., AND TOET, A. Visual comfort of binocular and 3D displays. *Displays 25*, 2 (2004), 99–108.

[63] KRANTZ, J. *Experiencing sensation and perception.* Pearson Education (US), 2012.

[64] KUHN, G. R., OLIVEIRA, M. M., AND FERNANDES, L. A. An efficient naturalness-preserving image-recoloring method for dichromats. *Visualization and Computer Graphics, IEEE Transactions on 14*, 6 (2008), 1747–1754.

[65] LAGARIAS, J. C., REEDS, J. A., WRIGHT, M. H., AND WRIGHT, P. E. Convergence properties of the Nelder–Mead simplex method in low dimensions. *SIAM Journal on Optimization 9*, 1 (1998), 112–147.

[66] LAMING, D., AND LAMING, J. F. Hegelmaier: On memory for the length of a line. *Psychological Research 54*, 4 (1992), 233–239.

[67] LANMAN, D., HIRSCH, M., KIM, Y., AND RASKAR, R. Content-adaptive parallax barriers for automultiscopic 3D display. In *ACM SIGGRAPH 2010 Posters* (2010), ACM, p. 59.

[68] LEEK, M. R. Adaptive procedures in psychophysical research. *Perception & Psychophysics 63*, 8 (2001), 1279–1292.

[69] LEHKY, S. R. Binocular rivalry is not chaotic. *Proceedings of the Royal Society of London. Series B: Biological Sciences 259*, 1354 (1995), 71–76.

[70] LEVELT, W. J. *On binocular rivalry*, vol. 2. Mouton The Hague, 1968.

[71] LEVISON, M., AND RESTLE, F. Invalid results from the method of constant stimuli. *Perception & Psychophysics 4*, 2 (1968), 121–122.

[72] LEVITT, H. Transformed up-down methods in psychoacoustics. *The Journal of the Acoustical society of America 49*, 2B (1971), 467–477.

[73] LOGOTHETIS, N. K. Single units and conscious vision. *Philosophical Transactions of the Royal Society of London. Series B: Biological Sciences 353*,

1377 (1998), 1801–1818.

[74] LUDWIG, I., PIEPER, W., AND LACHNIT, H. Temporal integration of monocular images separated in time: Stereopsis, stereoacuity, and binocular luster. *Perception & Psychophysics 69*, 1 (2007), 92–102.

[75] MACHADO, G. M., AND OLIVEIRA, M. M. Real-time temporal-coherent color contrast enhancement for dichromats. In *Computer Graphics Forum* (2010), vol. 29, Wiley Online Library, pp. 933–942.

[76] MADIGAN, R., AND WILLIAMS, D. Maximum-likelihood psychometric procedures in two-alternative forced-choice: Evaluation and recommendations. *Perception & Psychophysics 42*, 3 (1987), 240–249.

[77] MASIN, S. C., ZUDINI, V., AND ANTONELLI, M. Early alternative derivations of Fechner's law. *Journal of the History of the Behavioral Sciences 45*, 1 (2009), 56–65.

[78] MEENES, M. A phenomenological description of retinal rivalry. *The American Journal of Psychology* (1930), 260–269.

[79] MEYER, G. W., AND GREENBERG, D. P. Color-defective vision and computer graphics displays. *Computer Graphics and Applications, IEEE 8*, 5 (1988), 28–40.

[80] NEITZ, J., AND BAILEY, J. *H.R.R. Pseudoisochromatic Plates.* Richmond Products, 2002.

[81] NIEDER, A., AND MILLER, E. K. Coding of cognitive magnitude: Compressed scaling of numerical information in the primate prefrontal cortex. *Neuron 37*, 1 (2003), 149–157.

[82] PASTOOR, S., AND WÖPKING, M. 3-d displays: A review of current technologies. *Displays 17*, 2 (1997), 100–110.

[83] PETERKA, T., KOOIMA, R. L., SANDIN, D. J., JOHNSON, A., LEIGH, J., AND DEFANTI, T. A. Advances in the dynallax solid-state dynamic parallax barrier autostereoscopic visualization display system. *Visualization and Computer Graphics, IEEE Transactions on 14*, 3 (2008), 487–499.

[84] PIEPER, W., AND LUDWIG, I. Binocular vision: Rivalry, stereoscopic lustre, and sieve effect. *Perception 30*, Suppl (2001), 75–76.

[85] PIEPER, W., AND LUDWIG, I. The minimum luminance-contrast requirements for stereoscopic lustre. *Perception 31* (2002), 185.

[86] POLONSKY, A., BLAKE, R., BRAUN, J., AND HEEGER, D. J. Neuronal activity in human primary visual cortex correlates with perception during binocular rivalry. *Nature Neuroscience 3*, 11 (2000), 1153–1159.

[87] PORTA, J. B. *De Refractione Optices Parte: Libri Novem.* Carlinum and Pacem, Naples, 1593.

[88] QUARTLEY, J., AND FIRTH, A. Binocular sighting ocular dominance changes with different angles of horizontal gaze. *Binocular Vision & Strabismus Quarterly 19*, 1 (2003), 25–30.

[89] RASCHE, K., GEIST, R., AND WESTALL, J. Detail preserving reproduction of color images for monochromats and dichromats. *Computer Graphics and Applications, IEEE 25*, 3 (2005), 22–30.

[90] ROTH, H. L., LORA, A. N., AND HEILMAN, K. M. Effects of monocular viewing and eye dominance on spatial attention. *Brain 125*, 9 (2002), 2023–

2035.

[91] SAJADI, B., MAJUMDER, A., OLIVEIRA, M. M., SCHNEIDER, R. G., AND RASKAR, R. Using patterns to encode color information for dichromats. *Visualization and Computer Graphics, IEEE Transactions on 19*, 1 (2013), 118–129.

[92] SAMPSON, A. R. Stochastic approximation. *Encyclopedia of Statistical Sciences* (1988).

[93] SCHMIDT, A., AND GRASNICK, A. Multiviewpoint autostereoscopic dispays from 4D-Vision GmbH. In *Electronic Imaging* (2002), International Society for Optics and Photonics, pp. 212–221.

[94] SEXTON, I., AND SURMAN, P. Stereoscopic and autostereoscopic display systems. *Signal Processing Magazine, IEEE 16*, 3 (1999), 85–99.

[95] SHARP, G. D., AND ROBINSON, M. G. Enabling stereoscopic 3D technology. In *Electronic Imaging 2007* (2007), International Society for Optics and Photonics, pp. 64900X–64900X.

[96] SHEEDY, J., AND STOCKER, E. Surrogate color vision by luster discrimination. *American Journal of Optometry and Physiological Optics 61*, 8 (1984), 499–505.

[97] SMITH, T., AND GUILD, J. The CIE colorimetric standards and their use. *Transactions of the Optical Society 33*, 3 (1931), 73.

[98] STEVENS, S. On the theory of scales of measurement. *Science 103*, 2684 (1946), 677–680.

[99] Swets, J. *Signal detection and recognition by human observers: contemporary readings.* Wiley, 1964.

[100] Tong, F., Nakayama, K., Vaughan, J. T., and Kanwisher, N. Binocular rivalry and visual awareness in human extrastriate cortex. *Neuron 21*, 4 (1998), 753–759.

[101] Torgerson, W. S. Theory and methods of scaling.

[102] Treisman, M. Noise and Weber's law: The discrimination of brightness and other dimensions. *Psychological Review 71*, 4 (1964), 314.

[103] Treutwein, B. Adaptive psychophysical procedures. *Vision Research 35*, 17 (1995), 2503–2522.

[104] Tyler, C. W. Sensory processing of binocular disparity. *Vergence Eye Movements: Basic and Clinical Aspects* (1983), 199–295.

[105] Tyler, C. W., and Scott, A. Binocular vision. *Physiology of the Human Eye and Visual System* (1979), 643–74.

[106] Van Berkel, C., and Clarke, J. A. Characterization and optimization of 3D-LCD module design. In *Electronic Imaging* (1997), International Society for Optics and Photonics, pp. 179–186.

[107] Van Strien, J. W., Lagers-Van Haselen, G., Van Hagen, J., De Coo, I., Frens, M., and Van Der Geest, J. Increased prevalences of left-handedness and left-eye sighting dominance in individuals with williams-beuren syndrome. *Journal of Clinical and Experimental Neuropsychology 27*, 8 (2005), 967–976.

[108] Wade, N. *A natural history of vision.* MIT Press, 1998.

[109] WAKITA, K., AND SHIMAMURA, K. SmartColor: disambiguation framework for the colorblind. In *Proceedings of the 7th international ACM SIGACCESS conference on Computers and accessibility* (2005), ACM, pp. 158–165.

[110] WALKER, P. The subliminal perception of movement and the "suppression" in binocular rivalry. *British Journal of Psychology 66*, 3 (1975), 347–356.

[111] WALKER, P., AND POWELL, D. The sensitivity of binocular rivalry to changes in the nondominant stimulus. *Vision Research 19*, 3 (1979), 247–249.

[112] WATSON, A. B., AND PELLI, D. G. QUEST: A bayesian adaptive psychometric method. *Perception & Psychophysics 33*, 2 (1983), 113–120.

[113] WEBER, E. H. *De Pulsu, resorptione, auditu et tactu: Annotationes anatomicae et physiologicae.* CF Koehler, 1834.

[114] WEIBULL, W. A statistical distribution function of wide applicability. *Journal of Applied Mechanics* (1951).

[115] WETZSTEIN, G., LANMAN, D., HIRSCH, M., AND RASKAR, R. Tensor displays: compressive light field synthesis using multilayer displays with directional backlighting. *ACM Transactions on Graphics (TOG) 31*, 4 (2012), 80.

[116] WHEATSTONE, C. Contributions to the physiology of vision.–part the first. on some remarkable, and hitherto unobserved, phenomena of binocular vision. *Philosophical Transactions of the Royal Society of London* (1838), 371–394.

[117] WINNEK, D. F. Composite stereography, Nov. 5 1968. US Patent 3,409,351.

[118] WITT, K. CIE color difference metrics. *Colorimetry: Understanding the CIE System* (2007), 79–100.

[119] WOLFE, J. M., AND FRANZEL, S. L. Binocularity and visual search. *Perception & Psychophysics 44*, 1 (1988), 81–93.

[120] WYSZECKI, G., AND STILES, W. S. *Color Science: Concepts and Methods, Quantitative Data and Formulae.* 1982.

[121] XU, J. P., HE, Z. J., AND OOI, T. L. Surface boundary contour strengthens image dominance in binocular competition. *Vision Research 50*, 2 (2010), 155–170.

[122] YANG, X. S., ZHANG, L., WONG, T.-T., AND HENG, P.-A. Binocular tone mapping. *ACM Transactions on Graphics 31*, 4 (2012), 93.

[123] YOONESSI, A., AND KINGDOM, F. A. A. Dichoptic difference thresholds for uniform color changes applied to natural scenes. *Journal of Vision 9*, 2 (2009), 3.

[124] ZHANG, H., CAO, X., AND ZHAO, S. Beyond stereo: an exploration of unconventional binocular presentation for novel visual experience. In *Proceedings of the SIGCHI Conference on Human Factors in Computing Systems* (2012), ACM, pp. 2523–2526.

Appendix A

Survey Used in ColorBless Study

ColorBless Study Section 3: Post-study questionnaire

Participant # *

[   ]

Color vision *

◯ Normal color vision

◯ Colorblind

General Questions

1. Have you used any colorblind aids in your daily life when looking at digital contents? *

◯ Yes

◯ No

1a. If the answer to question 1 is yes, what kind of colorblind aids you have used?

[   ]

2. Have you encountered difficulties associated with colors in digital contents that impedes your work and daily life? If yes, how do you resolve that problem, and what is the reason that stops you from trying any colorblind aids? *

[   ]

3. Which categories of digital contents confuse you the most? *

[   ]

4. If you encountered such confusing contents frequently in your work and that confusion could impede your work and its efficiency, would you start using colorblind aids? *

○ Yes

○ No

Have you used active-shutter 3D glasses to watch 3D content before in cinema or home television? *

○ Yes

○ No

Do you feel uncomfortable after watching a 3D movie with glasses? *

○ Yes

○ No

Do you wear spectacles? *

○ Yes

○ No

Rate the comfort level of wearing 3D glasses and watching 3D content. *

	1	2	3	4	5	
Not comfortable at all	○	○	○	○	○	Very comfortable

Continue »

25% completed

ColorBless Study Section 3: Post-study questionnaire

Evaluating Different Colorblind Aids (Recoloring, Pattern Applying, and ColorBless)

You have used recoloring, pattern-applying, and ColorBless technique to distinguish confusing colors in the study. Answer the following questions based on your usage experience.

Speed in Distinguishing Colors

Rate the speed of the recoloring technique in distinguishing confusing colours. *

	1	2	3	4	5	
Very slow	○	○	○	○	○	Very fast

Rate the speed of the pattern-applying technique in distinguishing confusing colours. *

	1	2	3	4	5	
Very slow	○	○	○	○	○	Very fast

Rate the speed of the ColorBless technique in distinguishing confusing colours. *

	1	2	3	4	5	
Very slow	○	○	○	○	○	Very fast

Rate the speed of the PatternBless technique in distinguishing confusing colours. *

	1	2	3	4	5	
Very slow	○	○	○	○	○	Very fast

Rate the importance of speed in distinguishing colors in graphs WHEN you are working ALONE. *

1   2   3   4   5

Not important ○ ○ ○ ○ ○ Very important

Rate the importance of speed in distinguishing colors in graphs WHEN you are working WITH normal color vision people.. *

         1   2   3   4   5

Not important ○ ○ ○ ○ ○ Very important

Retaining Original Texture

Rate the retention of the original texture in the recolored image where the technique is applied. *

                              1   2   3   4   5

No retention (Additional texture is   ○ ○ ○ ○ ○   High retention (no change in the texture
applied heavily)   compared to the original image)

Rate the retention of the original texture in the pattern-applied image where the technique is applied. *

                              1   2   3   4   5

No retention (Additional texture is   ○ ○ ○ ○ ○   High retention (no change in the texture
applied heavily)   compared to the original image)

Rate the retention of the original texture in the ColorBless image where the technique is applied. *

                              1   2   3   4   5

No retention (Additional texture is   ○ ○ ○ ○ ○   High retention (no change in the texture
applied heavily)   compared to the original image)

Rate the retention of the original texture in the PatternBless image where the technique is applied. *

                              1   2   3   4   5

No retention (Additional texture is   ○ ○ ○ ○ ○   High retention (no change in the texture
applied heavily)   compared to the original image)

Cognitive effort in distinguishing confusing colors

Rate the cognitive effort required to distinguish colors with recoloring technique. *

	1	2	3	4	5	
Low cognitive effort	○	○	○	○	○	High cognitive effort

Rate the cognitive effort required to distinguish colors with pattern-applying technique. *

	1	2	3	4	5	
Low cognitive effort	○	○	○	○	○	High cognitive effort

Rate the cognitive effort required to distinguish colors with ColorBless technique. *

	1	2	3	4	5	
Low cognitive effort	○	○	○	○	○	High cognitive effort

Rate the cognitive effort required to distinguish colors with PatternBless technique. *

	1	2	3	4	5	
Low cognitive effort	○	○	○	○	○	High cognitive effort

Obviousness of the effects

How easy it is to see (obviousness) the effect produced by the recoloring technique? *

	1	2	3	4	5	
Very difficult to see	○	○	○	○	○	Very easy to see

How easy it is to see (obviousness) the effect produced by the pattern-applying technique? *

	1	2	3	4	5	
Very difficult to see	○	○	○	○	○	Very easy to see

How easy it is to see (obviousness) the effect produced by the ColorBless technique? *

	1	2	3	4	5

Very difficult to see ○ ○ ○ ○ ○ Very easy to see

How easy it is to see (obviousness) the effect produced by the PatternBless technique? *

          1   2   3   4   5

Very difficult to see ○ ○ ○ ○ ○ Very easy to see

Comfort level

Rate the comfort level of using recoloring technique to distinguish confusing colors. *

          1   2   3   4   5

Not comfortable at all ○ ○ ○ ○ ○ Very comfortable

Rate the comfort level of using pattern-applying technique to distinguish confusing colors. *

          1   2   3   4   5

Not comfortable at all ○ ○ ○ ○ ○ Very comfortable

Rate the comfort level of using ColorBless to distinguish confusing colors. *

          1   2   3   4   5

Not comfortable at all ○ ○ ○ ○ ○ Very comfortable

Rate the comfort level of using PatternBless technique to distinguish confusing colors. *

          1   2   3   4   5

Not comfortable at all ○ ○ ○ ○ ○ Very comfortable

Alteration to the original image

Rate the degree of alteration to the original image produced by recoloring technique. *

          1   2   3   4   5

Altered minimumly ○ ○ ○ ○ ○ Altered significantly

Rate the degree of alteration to the original image produced by pattern-applying technique. *

1 2 3 4 5

Altered minimumly ○ ○ ○ ○ ○ Altered significantly

Rate the degree of alteration to the original image produced by ColorBless technique. *

1 2 3 4 5

Altered minimumly ○ ○ ○ ○ ○ Altered significantly

Rate the degree of alteration to the original image produced by PatternBless technique. *

1 2 3 4 5

Altered minimumly ○ ○ ○ ○ ○ Altered significantly

Distraction produced by the techniques

Rate the degree of distraction produced by the effect in recoloring technique. *

1 2 3 4 5

Not distracting at all ○ ○ ○ ○ ○ Very distracting

Rate the degree of distraction produced by the effect in pattern-applying technique. *

1 2 3 4 5

Not distracting at all ○ ○ ○ ○ ○ Very distracting

Rate the degree of distraction produced by the effect in ColorBless technique. *

1 2 3 4 5

Not distracting at all ○ ○ ○ ○ ○ Very distracting

Rate the degree of distraction produced by the effect in PatternBless technique. *

1 2 3 4 5

Not distracting at all ○ ○ ○ ○ ○ Very distracting

« Back   Continue »

50% completed

ColorBless Study Section 3: Post-study questionnaire

Subjective Evaluation of ColorBless & PatternBless

Rate the intuitiveness of using lustre effect to distinguish confusing colors. *

	1	2	3	4	5	
Very unintuitive	○	○	○	○	○	Very intuitive

Rate the learning curve of using ColorBless to distinguish colours *

	1	2	3	4	5	
Very difficult to learn	○	○	○	○	○	Very easy to learn

Rate the learning curve of using PatternBless to distinguish colours *

	1	2	3	4	5	
Very difficult to learn	○	○	○	○	○	Very easy to learn

Is it easy to mistaken the lustre effect produced by ColorBless as some other color? *

	1	2	3	4	5	
Very easily mistaken	○	○	○	○	○	Not easily mistaken

PatternBless is more comfortable to use than ColorBless. *

	1	2	3	4	5	
Strongly disagree	○	○	○	○	○	Strongly agree

PatternBless's luster effect is less distracting than ColorBless's. *

1 2 3 4 5

Strongly disagree ○ ○ ○ ○ ○ Strongly agree

PatternBless's luster effect is less distorting than ColorBless's. *

	1	2	3	4	5	

Strongly disagree ○ ○ ○ ○ ○ Strongly agree

PatternBless's luster effect is more subtle than ColorBless's. *

	1	2	3	4	5	

Strongly disagree ○ ○ ○ ○ ○ Strongly agree

Which one would you prefer to use in distinguishing confusing colors?

○ ColorBless

○ PatternBless

« Back	Continue »

75% completed

ColorBless Study Section 3: Post-study questionnaire

Preferences in Different Scenarios

Based on the scenarios and context given below, choose the technique you will prefer to use.

Non-work scenario, alone, looking at digital content. *

○ Recoloring

○ Pattern-applying

○ ColorBless

○ PatternBless

○ Will not use any technique at all

Non-work scenario, with other people, looking at digital content. *

○ Recoloring

○ Pattern-applying

○ ColorBless

○ PatternBless

○ Will not use any technique at all

Work scenario, alone, looking at digital information with extensive use of colours. *

○ Recoloring

○ Pattern-applying

○ ColorBless

○ PatternBless

○ Will not use any technique at all

Work scenario, alone, looking at digital information with extensive use of colours, and sensitive to the change in original colours. *

i.e. Scientific imagery where colour itself represents a specific information and couldn't be changed, etc.

○ Recoloring

○ Pattern-applying

○ ColorBless

○ PatternBless

○ Will not use any technique at all

Work scenario, alone, looking at digital information with extensive use of colours, and sensitive to the change in original texture. *

i.e. Satellite imagery where terrain information is important, etc.

○ Recoloring

○ Pattern-applying

○ ColorBless

○ PatternBless

○ Will not use any technique at all

Work scenario, alone, looking at digital information with extensive use of colours, and sensitive to the change in both the original color AND texture. *

i.e. Satellite imagery where terrain information is represented by the color and texture.

○ Recoloring

○ Pattern-applying

○ ColorBless

○ PatternBless

○ Will not use any technique at all

Work scenario, with colleagues with normal color vision, looking at digital information with extensive use of colours. *

○ Recoloring

○ Pattern-applying

○ ColorBless

○ PatternBless

○ Will not use any technique at all

Work scenario, with colleagues with normal color vision, looking at digital information with extensive use of colours, and sensitive to the change in original colours. *

i.e. Scientific imagery where colour itself represents a specific information and couldn't be changed, etc.

○ Recoloring

○ Pattern-applying

○ ColorBless

○ PatternBless

○ Will not use any technique at all

Work scenario, with colleagues with normal color vision, looking at digital information with extensive use of colours, and sensitive to the change in original texture. *

i.e. Satellite imagery where terrain information is important, etc.

○ Recoloring

○ Pattern-applying

○ ColorBless

○ PatternBless

○ Will not use any technique at all

Work scenario, with colleagues with normal color vision, looking at digital information with extensive use of colours, and sensitive to the change in both the original color AND texture.
*

i.e. Satellite imagery where terrain information is represented by the color and texture.

○ Recoloring

○ Pattern-applying

○ ColorBless

○ PatternBless

○ Will not use any technique at all

<u>**« Back**</u> **Submit**

Never submit passwords through Google Forms.

100%: You made it.